EVELYN JARDIM DE OLIVEIRA

EMBRIOGÊNESE SOMÁTICA EM *Brachypodium distachyon* (L.) Beauv. (POACEAE): CARACTERIZAÇÃO MORFOANATÔMICA, HISTOQUÍMICA E EXPRESSÃO DE GENES *SERK*

Tese apresentada à Universidade Federal de Viçosa, como parte das exigências do Programa de Pós-Graduação em Botânica, para obtenção do título de *Doctor Scientiae*.

VIÇOSA
MINAS GERAIS – BRASIL
2013

Ficha catalográfica preparada pela Biblioteca Central da Universidade Federal de Viçosa - Câmpus Viçosa

T
O48e
2013

Oliveira, Evelyn Jardim de, 1958-
Embriogênese somática em *Brachypodium distachyon* (L.) Beauv. (Poaceae) : caracterização morfoanatômica, histoquímica e expressão de genes SERK / Evelyn Jardim de Oliveira. – Viçosa, MG, 2013.
ix, 90 f. : il. (algumas color.) ; 29 cm.

Orientador: Wagner Campos Otoni.
Tese (doutorado) - Universidade Federal de Viçosa.
Inclui bibliografia.

1. *Brachypodium distachyon* - Morfogênese. *2.* Histoquímica. 3. Ultraestrutura (Biologia). I. Universidade Federal de Viçosa. Departamento de Biologia Vegetal. Programa Pós-Graduação em Botânica. II. Título.

CDD 22. ed. 584.9

EVELYN JARDIM DE OLIVEIRA

EMBRIOGÊNESE SOMÁTICA EM *Brachypodium distachyon* (L.) Beauv. (POACEAE): CARACTERIZAÇÃO MORFOANATÔMICA, HISTOQUÍMICA E EXPRESSÃO DE GENES *SERK*

Tese apresentada à Universidade Federal de Viçosa, como parte das exigências do Programa de Pós-Graduação em Botânica, para obtenção do título de *Doctor Scientiae*.

APROVADA: 14 de outubro de 2013.

_____
Marcelo de Oliveira Santos

_____
Aristéa Alves Azevedo

_____
Andréa Dias Koehler

_____
Luzimar Campos da Silva
(Coorientadora)

_____
Wagner Campos Otoni
(Orientador)

À minha mãe D. Nice e à memória de meu pai Moacyr.

Às minhas meninas Juliana e Julia.

Dedico

AGRADECIMENTOS

À Universidade Federal de Viçosa (UFV) e ao Programa de Pós-Graduação em Botânica, pela oportunidade de realização do Doutorado.

À Coordenação de Aperfeiçoamento de Pessoal de Ensino Superior (CAPES), pelo apoio financeiro.

Ao CNPq, pela generosa compreensão e apoio.

Ao Prof. Wagner Campos Otoni, pelo apoio incondicional, pela amizade, por ter me pegado pela mão.

À Dra. Ana Claudia Ferreira da Cruz pela grande ajuda, dedicação e otimismo.

À Dra. Andréa Koehler pelo grande auxílio e carinho.

Ao Dr. Elyabe Monteiro de Matos pelo companheirismo desde o começo, pela amizade e disponibilidade.

Ao amigo Diego Rocha pelo apoio, sugestões e críticas dadas ao trabalho.

Aos amigos do LCTII, Cris, Lorena, Marcos, Diego, Marcela e Virgilio por tanta generosidade, companheirismo e boas experiências compartilhadas.

À Dra. Flávia Garcia, pelo apoio, incentivo e amizade sempre presentes.

À Profa. Luzimar pela atenção e sugestões valiosas.

Ao Prof. Francisco Tanaka pelo processamento do material por MET.

Ao Prof. Fábio Tebaldi Silveira Nogueira (ESALQ/USP) pela gentileza em ceder o material vegetal e pelo incentivo e sugestões valiosas.

Aos professores do Departamento de Biologia Vegetal pelos ensinamentos e pelo estimulante convívio acadêmico.

Ao Instituto de Biotecnologia Aplicada à Agropecuária (BIOAGRO) e ao Departamento de Biologia Vegetal (DBV), pelo suporte a este trabalho.

Ao Núcleo de Microscopia e Microanálise (NMM) da UFV e ao Núcleo de Apoio à Pesquisa em Microscopia Eletrônica Aplicada à Agricultura (NAP/MEPA/ESALQ), pelas análises em microscopia eletrônica realizadas.

Ao Paulo Oliveira, pelo apoio e incentivo.

Aos meus queridos irmãos Braulio e Sandra, por uma vida inteira de amor sincero e lealdade.

À minha filha Juliana, por estar sempre ao meu lado e pelas incontáveis trocas de idéias, e à minha neta Julia, por ter nos presenteado com a sua alegria.

MUITO OBRIGADA!

BIOGRAFIA

Evelyn Jardim de Oliveira, filha de Moacyr Augusto de Oliveira e Clenilce Jardim de Oliveira, nasceu em 14 de junho de 1958, na cidade de São Paulo, São Paulo.

Graduou-se em Agronomia na Universidade Federal de Viçosa em 1982.

Concluiu o Mestrado em Genética e Melhoramento na Universidade Federal de Viçosa em 1989 com a dissertação intitulada "Análise multivariada no estudo da divergência genética entre cultivares de feijão (*Phaseolus vulgaris* L.)".

Em 2009 iniciou o doutorado em botânica na Universidade Federal de Viçosa e submeteu à defesa a tese intitulada "Embriogênese somática em *Brachypodium distachyon* (L.) Beauv. (Poaceae): caracterização morfoanatômica, histoquímica e expressão de genes *SERK*" em outubro de 2013.

SUMÁRIO

RESUMO

OLIVEIRA, Evelyn Jardim de, D.Sc., Universidade Federal de Viçosa, outubro de 2013. **Embriogênese somática em *Brachypodium distachyon* (L.) Beauv. (Poaceae): caracterização morfoanatômica, histoquímica e expressão de genes *SERK*.** Orientador: Wagner Campos Otoni. Coorientadora: Luzimar Campos da Silva.

Brachypodium distachyon (L.) P. Beauv. (Poaceae: Poideae) tem se destacado como planta modelo para gramíneas de clima temperado e espécies usadas para a produção de biocombustíveis. A linhagem Bd21 de *Brachypodium distachyon* tem um genoma completamente seqüenciado e montado, além de protocolos de genômica e de transformação bem estabelecidos com base em calos embriogênicos. No entanto, as informações sobre a origem e as alterações celulares que ocorrem durante a diferenciação de embriões somáticos nos estágios iniciais não foi documentada para *B. distachyon*. Também não há relatos sobre o uso de abordagens moleculares para investigar o processo de embriogênese somática nesta espécie. Portanto, os objetivos deste trabalho foram: (1) caracterizar as alterações morfológicas, anatômicas e histoquímicas que ocorrem durante a indução de embriogênese somática a partir de embriões zigóticos imaturos (EZI) da *B. distachyon* linhagem de referência Bd21 usando microscopia de luz e de varredura em associação com testes histoquímicos e, (2), realizar a clonagem e caracterização de genes *SERK* (*SOMATIC EMBRYOGENESIS RECEPTOR-LIKE KINASE*) e analisar sua expressão na indução de embriogênese somática utilizando hibridização *in situ* para monitorar os processos morfogenéticos *in vitro*. Culturas embriogênicas de *B. distachyon* (BD21) foram estabelecidas usando EZI 15 dias após a antese, em meio Murashige e Skoog (1962) contendo ácido 2,4- diclorofenoxiacético. A regeneração *in vitro* de plântulas derivadas de embriões somáticos ocorreu pela embriogênese somática através da via indireta. Os embriões somáticos tiveram uma origem multicelular e originaram-se de calo embriogênico formado a partir de células da epiderme na região do nó escutelar que se estenderam para a periferia do EZI. A ordem de acumulação de reservas nos embriões somáticos foi semelhante a dos embriões zigóticos. Nas culturas embriogênicas, proteínas e lipídios foram utilizados nos primeiros 2 dias em meio de indução. O teor de amido aumentou nos primeiros 2 dias em meio de indução e diminuiu em seguida em número de grânulos que se tornaram maiores e apareceram principalmente nas células vacuoladas adjacentes às massas pró-embriogênicas. Pequenos grânulos de amido

começaram a acumular nos pró-embrioides após 4 dias em meio de indução e tornaram-se maior e mais abundantes em células do escutelo aos 12 dias em meio de indução. A diferenciação do embrião somático seguiu a mesma sequência de desenvolvimento verificado em outros membros da família Poaceae, ou seja, a passagem pelos estádios globular, escutelar e coleoptilar. O gene *SERK* tem sido usado como um marcador para as células competentes na embriogênese somática de várias espécies. Neste estudo, utilizando iniciadores degenerados, uma sequência específica homóloga de um fragmento do gene *SERK* foi amplificada de *B. distachyon* Bd21. A análise da sequência do fragmento de *SERK* (766 bp) revelou altos níveis de similaridade com genes *SERK* relatados em outras espécies. A análise de hibridização *in situ* mostrou que o gene *SERK* estava presente nos tecidos embriogênicos de *B. distachyon* antes do desenvolvimento de embriões somáticos e continuou sendo expresso nos estágios globular e escutelar. Estes resultados sugerem que a expressão do gene *SERK* de *B. distachyon* pode estar associada com a indução da embriogênese somática. Este estudo faz a primeira descrição de mudanças morfoanatômicas e histoquímicas durante o processo de embriogênese somática em *B. distachyon* linhagem Bd21. Este é também o primeiro relato sobre a clonagem e expressão de um gene *SERK* para a espécie e sugere que este gene pode servir como um marcador molecular para monitorar a transição de células somáticas em células competentes e embriogênicas também em *B. distachyon*.

ABSTRACT

OLIVEIRA, Evelyn Jardim de, D. Sc., Universidade Federal de Viçosa, October, 2013. **Somatic embryogenesis in *Brachypodium distachyon* (L.) Beauv. (Poaceae): morphoanatomical and histochemical characterization and analysis of *SERK* gene expression.** Adviser: Wagner Campos Otoni. Co-adviser: Luzimar Campos da Silva.

Brachypodium distachyon (L.) P. Beauv. (Poaceae: Poideae) has been proposed as a new model for temperate and biofuel grasses. *Brachypodium distachyon* inbred line Bd21 has a fully sequenced and assembled genome, a series of genomics resources, and well-established somatic embryogenesis-based transformation protocols. However, information about origin and cellular changes occurring during the early differentiation of somatic embryos has not been documented for *B. distachyon*. There are also no reports on the use of molecular approaches to investigate somatic embryogenesis in *B. distachyon*. Therefore, the objectives of this study were (1) to characterize the morphological, anatomical and histochemical changes occurring during the induction of somatic embryogenesis from immature zygotic embryos (IZE) of *B. distachyon* community standard line Bd21 using light and scanning electron microscopy in association with histochemical tests and, (2), to carry out the cloning and characterization of *SOMATIC EMBRYOGENESIS RECEPTOR-LIKE KINASE* (*SERK*) genes and analysis of its expression in somatic embryogenesis induction using *in situ* hybridization for monitoring the morphogenetic processes in vitro. Somatic embryogenic cultures of *B. distachyon* (Bd21) were established following culture of IZE, 15 days post anthesis, on Murashige and Skoog (1962) medium containing 2,4-dichlorophenoxyacetic acid. *In vitro* regeneration of plantlets derived from somatic embryos occurred by the indirect somatic embryogenesis pathway. Somatic embryos had a multicellular origin and originated from embryogenic callus formed from cells of the epidermis in the region of the scutellar node and extended to the periphery of IZE. The order in accumulation of storage reserves in somatic embryos was similar to that of zygotic embryos. In the embryogenic cultures, storage proteins and lipids were used up in the first 2 days after culture (DAC). The levels of starch increased in the first 2 DAC and then decreased in number of granules that became larger and appeared mainly in the vacuolated cells subtending the proembryonic masses. Small starch granules started accumulating in proembryoids after 4 DAC and became larger and abundant in scutellar cells 12 DAC. Somatic embryo differentiation in *B. distachyon* proceeded through

globular, scutellar and coleoptilar stages, following the morphological pattern of development of that reported in other members of the Poaceae. The *SERK* gene has been used successfully as a marker for competent cells in somatic embryogenesis of several species. In this study, using degenerate primers, it was possible to amplify a specific homologous sequence of a *SERK* gene fragment from *B. distachyon* Bd21. Sequence analysis of the *SERK* fragment (766 bp) revealed high levels of similarity to other reported *SERKs*. *In situ* hybridization analysis showed that the *SERK* gene was present in embryogenic tissues of *B. distachyon* before somatic embryo development and continued expressing through globular and scutellar stages. These results suggest that the expression of the *B. distachyon SERK* gene was associated with induction of somatic embryogenesis. This study provides the first description of morphoanatomical and histochemical changes underlying the embryogenic process in *B. distachyon* reference line Bd21. It is also the first report on the cloning and expression of a *SERK* gene for the species, suggesting that it could serve as a molecular marker to monitor the transition of IZE cells into competent and embryogenic cells also in *B. distachyon* line Bd21.

GENERAL INTRODUCTION

Brachypodium distachyon (L.) P. Beauv. is a temperate wild grass native to the Mediterranean region (Vogel et al., 2009; Catalán et al., 2012) and has successfully invaded disturbed areas of central Europe, Australia, New Zealand, South Africa and North and South America (Garvin et al., 2008; Bakker et al., 2009). It has little agricultural importance and is of no major economic value except for its invasive habit and some varieties that have been used to protect soils of olive orchards from erosion in Spain (Bakker et al., 2009; Hammami et al., 2011).

Brachypodium distachyon is a member of the large grass family Poaceae that provides most of human and domestic animal nutrition (Kellogg, 2001). Members of the Poaceae subfamilies Ehrhartoideae (rice), Panicoideae (maize, sorghum) and Pooideae (wheat, barley) are the main grain crops throughout the world (Febrer et al., 2010). Furthermore, highly productive grasses of the Panicoideae subfamily (sugarcane, switchgrass, *Miscanthus sinensis*) are promising sources of sustainable energy (Vogel et al., 2009).

The *Brachypodium* genus comprises 12 to 15 species with most of them being wide-spread in Mediterranean and Eurosiberian areas (Catalán and Olmstead, 2000). The diploid *B. distachyon* is the only annual member within the genus, a self-compatible species with chromosome base number x = 5 (Catalán and Olmstead, 2000). Phylogenetic analyses based on plastid and nuclear genes from different *Brachypodium* lineages indicated a close relationship of *B. distachyon* to the rhizomatous perennials *B. arbuscula, B. retusum, B. rupestre, B. phoenicoides, B. pinnatum*, and *B. sylvaticum* (Catalán and Olmstead, 2000; Wolny et al., 2011; Catalán et al., 2012). Most of the perennial species are self-incompatible (except for *B. sylvaticum*) and have chromosome base numbers ranging from 7 to 9 (Robertson, 1981; Khan and Stace, 1999; Catalán and Olmstead, 2000).

Brachypodium distachyon was first characterized as having three different ploidy levels (2n = 10, 20 and 30) that have been considered as part of a single species or single autopolyploid series (Robertson, 1981). However, modern cytogenetic analyses using fluorescence in situ hybridization (FISH) with total genomic DNA (GISH) and multiple DNA sequences as probes, as well as comparative chromosome painting (CCP) indicated that the 2n = 10 and 2n = 20 cytotypes actually represent two

different taxa, and the 2n = 30 cytotype represents their derived allotetraploid (Hasterok et al., 2006; Idziak et al., 2011; Catalán et al., 2012). The name *B. distachyon* was kept for the 2n = 10 cytotype and two novel species were described as *B. stacei* and *B. hybridum* for, respectively, the 2n = 20 and 2n = 30 cytotypes (Catalán et al., 2012).

The phylogenetic relationship between the genus *Brachypodium* and the other grasses has been firmly established (Vogel and Bragg, 2009). The genus *Brachypodium* belongs to the Brachypodieae tribe, which has consistently been shown to be sister group to the four economically important tribes Triticeae, Aveneae, Poeae, and Bromeae and closely related to rice (Draper et al. 2001; Kellogg 2001; Vogel et al. 2006) (Fig. 1).

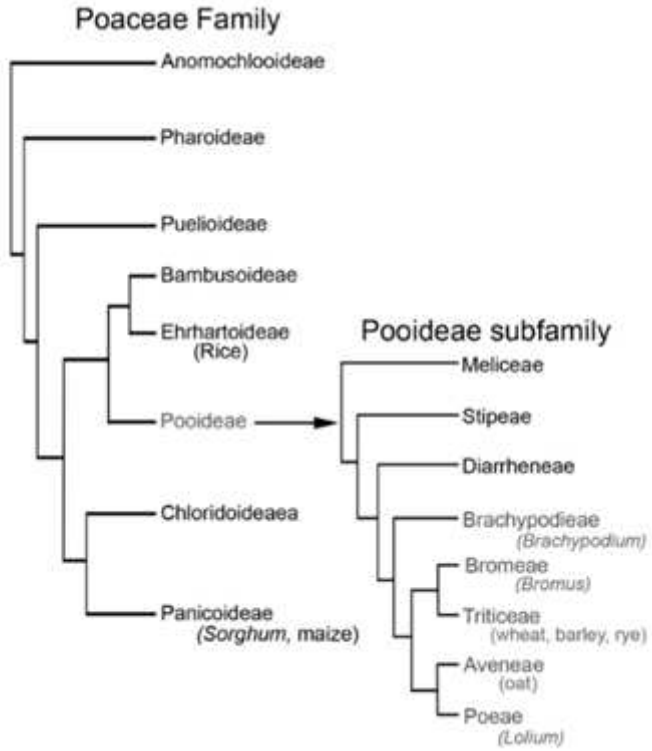

Figure 1. Phylogenetic relationship of *Brachypodium distachyon* to other Poaceae. Figure derived from Hands and Drea (2012).

Brachypodium distachyon has been developed as a model system for the genomic analysis of the grasses of temperate climates and biofuel grass crops since 2001 (Draper et al., 2001; Opanowicz et al., 2008). A comparison with other plants shows that *B. distachyon* has the physical and genomic attributes (small stature, fast generation time, simple growth conditions, small genome, self-fertile, diploid, annual

lifecycle) necessary to a model system (Table I). A model grass is needed to answer questions that are specific of the grass biology such as cell wall composition, plant architecture, grain properties, yield, stress tolerance, intercalary meristems, root architecture, development, and plant-pathogen interactions (Vogel and Bragg, 2009; Brkljacic et al., 2011).

Many Pooideae species have large and complex genomes, which makes genome comparisons and biotechnological approaches for crop improvement very difficult in these crops (Shang et al., 2011). *B. distachyon* has a genome size smaller than that of rice and is closely related to wheat, barley, and oat, thus it can serve as a structural genomic tool to assist the exploration of the large genomes of these crops (Huo et al., 2009).

Table 1. Comparison of *Brachypodium distachyon* with other models and crops

	B. distachyon	***Arabidopsis***	**Wheat**	**Maize**	**Rice**	**Barley**	**Switchgrass**	**Sorgum**	***M. sinensis***
Chromosome Number	10 (2n)	10 (2n)	42 (2n)	20 (2n)	24 (2n)	14 (2n)	18-108 (2n)	20 (2n)	48 (2n)
Genome size (Mb)	272	119	16,000	2,300	382	5,000	2,400	700	5,000
Reproduction	Selfing	Selfing	Selfing	Outcrossing	Selfing	Selfing	Outcrossing	Selfing	Outcrossing
Life cycle (weeks)	8-12	8-12	10-20	8-15	12-24	10-20	26	13-18	12
Height (m)	0.3	0.2	Up to 1	Up to 2	1.2	Up to 1.2	Up to 3	Up to 2.5	Up to 3
Growth Requirements	Very simple	Very simple	Simple	Demanding	Demanding	Simple	Demanding	Demanding	Demanding
Density (plants m^{-2})	1,000	2,000	50	4	36	80-120	6	50	3-4
Assembled genome Sequence	Draft genome	Finished genome sequence	Sequencing in progress	Draft genome	Finished genome sequence	Draft genome in progress	Sequencing in progress	Draft genome	No
T-DNA resources	10,000 lines available	Extensive	None	Transposon mutants available	Extensive	None	None	None	None
Transformation	Highly efficient	Extremely easy	Inefficient	Efficient, but laborious	Highly efficient	Efficient, but laborious	Efficient, but slow	Inefficient	Inefficient
Cell wall type	Type 2	Type 1	Type 2	Type 2	Type 2	Type 2	Type 2	Type 2	Type 2
Photosynthesis	C3	C3	C3	C4	C3	C3	C4	C4	C4

Adapted from Opanowicz et al. (2008) and Brkljacic et al. (2011).

Brachypodium distachyon can also be used as a model system for the emerging energy crops like maize, sugarcane, switchgrass and *Miscanthus sinensis* with which it shares the typical cell wall of grasses (Opanowicz et al., 2008; Vogel et al., 2009). The large size, large genomes and outcrossing breeding system of these species hinder their use in experimental conditions. In addition, the close relationship within the genus of *B. distachyon* with the core of perennial species can be explored to study the perennial life cycle and self-incompatibility that are also common traits to wild grasses (e.g. *Miscanthus* and switchgrass) that are being developed into biofuel crops (Vogel and Bragg, 2009). However, *B. distachyon* uses the C3 photosynthetic pathway, while many

of the energy crops use a C4 photosynthetic pathway, which is more efficient under hot, dry conditions. But even though *B. distachyon* alone is not suitable to study C4 photosynthesis, it can be used as a model system to study the feasibility of engineering the C4 mechanism into C3 crops such as rice and wheat (Brkljacic et al., 2011).

A remarkable progress has been made in the development of genomic resources for *B. distachyon*, which include the whole nuclear and chloroplast genome sequences (Bortiri et al., 2008; IBI, 2010); germplasm collections (Garvin et al., 2008; Filiz et al., 2009; Vogel et al., 2009) , genetic markers (Vogel et al., 2009), a genetic linkage map (Garvin et al., 2010), bacterial artificial chromosome (BAC) libraries (Huo et al., 2006; Farrar and Donnison, 2007; Huo et al., 2008), physical maps (Gu et al., 2009; Febrer et al., 2010), mutant collections (Thole et al., 2012), microarrays and databases (comprehensive lists of Internet *B. distachyon* resources are found in Brkljacic et al., 2011 and Vain, 2011).

Another important aspect considered a key technology for a model plant species is the availability of an easy and efficient transformation system and *B. distachyon* has proven to be very responsive to *in vitro* culture and current transformation techniques. Methods for transformation using particle gun (Draper et al., 2001; Christiansen et al., 2005) and *Agrobacterium*-mediated (Vogel et al., 2006; Păcurar et al., 2008; Vain et al., 2008) have been developed for several genotypes of *B. distachyon*. Average transformation efficiencies have been reported to range from 30–80% (Păcurar et al., 2008; Vain et al., 2008; Vogel and Hill, 2008; Alves et al., 2009). The highly efficient transformation procedures established for *B. distachyon* allow the generation of large collections of T-DNA mutant lines (http://www.brachytag.org/services.htm), the characterization of gene function through over-expression or gene silencing (Olsen et al., 2006; Pacak et al., 2010), and recently, a T-DNA mutation in *B. distachyon* has been complemented with an *Arabidopsis* ortholog, bridging dicotyledonous and monocotyledonous models (Vain et al., 2011). In all cases, embryogenic calli were used as the target tissue for transformation.

Bablak et al. (1995) developed, for the first time, a protocol for the induction of embryogenic callus from mature seeds of *B. distachyon* and the regeneration of fertile plants, making a breakthrough toward developing *B. distachyon* transformation. In this study, optimum development of embryogenic callus of three diploid accessions of *B. distachyon* (B200, B373, and B377) occurred on LS (Linsmaier and Skoog, 1965) and N6 (Chu et al., 1975) media containing 3.0% w/v sucrose and 2.5 mg L^{-1} of 2,4-

dichlorophenoxyacetic acid (2,4-D). Plant regeneration occurred on several common media and the incidence of albino plantlets was around 10%.

However, the regeneration ability of mature seeds/embryos of most Poaceae species, such as wheat, maize, sorghum and barley, is poor (Schulze, 2007), and the success of the transformation techniques relies on the culture of highly embryogenic callus (Hansen and Wright, 1999). The morphogenetic competence of immature embryos in monocotyledonous species was first described in maize by Green and Philipps (1975). Since then, for most of the important cereals and grasses, plant regeneration systems have been developed based on immature embryos (Eudes et al., 2003; Schulze, 2007).

A considerable improvement in embryogenic callus production and plant regeneration of *B. distachyon* was achieved by using immature embryos as initial explant. Draper et al. (2001) cultured immature embryos of the diploid ecotype ABR1 to induce callus. They observed that the immature embryos with the greatest potential for plant regeneration via somatic embryogenesis were in the size range of 0.3 to 0.7 mm. When cultured on LS or N6 containing 2.5 mg L^{-1} 2,4-D the immature embryos formed a mass of embryogenic callus around the edge and on the surface of the scutellum, in general after 10 to 15 d. The level of albinism in plantlets regenerated from the embryonic calli induced on LS medium (7%) was much lower than from calli formed on N6 medium (45%).

The induction and control of somatic embryogenesis are largely dependent upon plant genotype, tissue-type, physiological conditions of the donor plant, type and level of growth regulators supplemented to culture medium and varied cultural regimes (Toonen and De Vries, 1996). Differences in response of *B. distachyon* genotypes to *in vitro* culture have been reported indicating that the interaction between the genotype explant source and the culture medium influences the development of *B. distachyon* in terms of the callus induction and regeneration response (Bablak et al., 1995; Draper et al., 2001; Vogel et al., 2006; Hammami et al., 2011).

Christiansen et al. (2005) tested the ability of immature embryos of diploid and tetraploid *B. distachyon* accessions to form embryogenic callus on LS with 2.5 mg L^{-1} 2,4-D, 3% maltose. The two tetraploid accessions investigated, BDR017 and BDR030, had higher percentage of embryos producing embryogenic callus (67% and 91%, respectively) than the two diploid BDR001 and BDR018 (51% and 46%, respectively). All four accessions showed 90–100% of regeneration in 3–6 week-old calli, but lower

than 80% when cultured for 8 weeks. They found that longer duration of callus culture resulted in lower regeneration efficiency, with regeneration percentages dropping to 30% and 55% in the accessions BDR017 and BDR030, respectively, when kept for 16 weeks in culture.

The tissue culture capacity of the community standard line Bd21 and its variation line Bd21-3 for the production of embryogenic callus was compared by culturing immature embryos (less than or equal to 0.3 mm in length) on an optimized callus induction medium (Vain et al., 2008). The medium was based on MS salts (Murashige and Skoog, 1962), M5 vitamins, 3% sucrose, 0.2% phytagel and supplemented with 0.6 mgL^{-1} $CuSO_4$. Embryogenic callus production for the diploid lines Bd21 (68%) and Bd21-3 (94%) was higher than that of tetraploid genotypes (67% for BRD017 and 91% for BRD030) reported by Christiansen et al. (2005). The addition of $CuSO_4$ to the tissue culture medium promoted efficient callus induction and higher-frequency plant regeneration from Bd21 calli (Vain et al., 2008). $CuSO_4$ was also reported to decrease the regeneration of albino plants and increase the number of regenerated shoots per embryo in barley (Dahleen, 1995; Bartlett et al., 2008). It has been suggested that some copper enzymes might play important role in regeneration since copper ions are components or activators of many important enzymes involved in electron transport, protein, carbohydrate biosynthesis and polyphenol metabolism (Purnhauser and Gyulai, 1993).

The variability of the *in vitro* culture response was studied in representatives of the three *Brachypodium distachyon* cytotypes. Hammami et al. (2011) cultured immature embryos of two commercial lines of *B. distachyon*, with 10 and 30 chromosomes, and 23 wild populations (2n=10, 2n=20 and 2n=30) on Murashige and Skoog medium containing 1 mgL^{-1} 2,4-D with 30 gL^{-1} of sucrose or maltose. Callus induction was not affected by the different media and plant regeneration was very variable depending on the induction medium. The diploid plants with 2n=10 showed the greatest callus-forming ability, but the 2n=20 plants produced significantly more compact embryogenic calli. The proportion of albinism was low in all cases, but the plants with 20 or 30 chromosomes generated the higher proportions of albino plants than plants with 10 chromosomes. It seems that callus induction, plant regeneration, and green plantlet formation are probably differently controlled in the plants with different chromosome numbers, which supports the idea that the three *B. distachyon* cytotypes represent different species (Hammami et al., 2011).

Somatic embryogenesis *in vitro* is an excellent model for studying the theory of plant embryogenesis, determining gene expression and measure substance accumulation at different stages of embryogenesis (Brukhin and Morozova, 2011).

In general, the process of somatic embryogenesis can be divided into two phases: induction and expression. The induction of somatic embryogenesis consists of the end of the current gene expression pattern in the explant tissue, and its replacement with an embryogenic gene expression program, where the somatic cells regain their totipotency (Pasternak et al., 2002; von Arnold et al. 2002). This process involves changes in the morphology, physiology, metabolism and gene expression of the cells, in which the cell must dedifferentiate, acquire embryonic competence, become embryogenically induced and become determined (Namasivayam et al., 2007; Rose et al., 2010). Plant growth regulators (PGRs) and stress factors (e.g. culture conditions and culture medium) are recognized inducers that allow differentiated cells to develop into competent dedifferentiated cells (Fehér, 2005; Potters et al., 2009; Zavattieri et al., 2010). Morphological and anatomical observations indicate that somatic embryos may arise from one cell or a group of embryogenic cells which, in turn, come from cytoplasm-rich, meristematic cells (Kurczynska et al., 2012). However, the events involved in the transition of a somatic cell to an embryogenic-competent cell capable of forming an embryo are still unclear (Verdeil et al., 2007).

Analysis of histological and ultrastructural changes during SE has contributed to a better understanding of the embryogenic process in dicot and monocot systems (Taylor and Vasil, 1996; Verdeil et al., 2001; Namasivayam et al., 2006; Rocha et al., 2012). During somatic embryogenesis, cells involved in proembryoid formation share distinct features such as dense cytoplasm, increased endoplasmic reticulum, ribosomes and dictyosomes, deep invaginations of the nuclear envelope, increase in cell wall thickness, decreased vacuole size, few amyloplasts and numerous mitochondria, evidencing increased metabolic activity (Fransz and Schel, 1991; Taylor and Vasil, 1996; Verdeil et al., 2001, 2007).

In the literature, there is a general agreement that reserves are essential to morphogenetic processes. The histodifferentiation of somatic embryos is normally associated with changes in the synthesis and mobilization of proteins, carbohydrates, and lipids and histochemical tests have been used to monitor the levels of these substances during the developmental stages of the embryogenic tissue (Cangahuala-Inocente et al., 2009; Moura et al., 2010; Pinto et al., 2010; Correia et al., 2012; Rocha

et al., 2012). Therefore, a change in the pattern of storage product metabolism can be a good indicator of the acquisition of the embryogenic potential of the tissues (Puigderrajols et al., 2001; Griga et al., 2007).

The morphological, physiological and biochemical changes which occur during the vegetative-to-embryogenic transition in the embryogenic pathway involves differential gene expression and various signal transduction pathways (Santos et al., 2009). Studies have been conducted to identify the genes that have some role in the acquisition of embryogenic competence. Most of the identified genes were structural genes, early or late embryogenesis genes, hormone responsive genes and wound or stress induced genes (Namasivayam and Hanke, 2008). Among the genes expressed in early embryogenesis, Schmidt et al. (1997) identified, in carrot cell suspension cultures, the *SOMATIC EMBRYOGENESIS RECEPTOR KINASE* (*SERK*) gene, which was specifically expressed in cells that developed into somatic embryos. This gene encodes a leucine-rich transmembrane receptor-like kinase that belongs to the large family of plant receptor kinase genes with roles in signal transduction pathways in plant development, metabolism and defense pathways (Hecht et al., 2001; Nolan et al., 2009).

The *SERK* gene was also found to be a good molecular marker of cells competent to form somatic embryos in *Dactylis glomerata* (Somleva et al. 2000) and *Arabidopsis thaliana* (Hecht et al. 2001). Since then, in several plant species the acquisition of embryogenic competence have been correlated with an increase in *SERK1* expression, including *Medicago truncatula* (Nolan et al., 2003), *Ocotea catharinensis* (Santa-Catarina et al., 2004), *Theobroma cacao* (de Oliveira Santos et al., 2005), *Triticum aestivum* (Singla et al., 2008), *Musa acuminata* (Huang et al., 2009) and *Brachiaria* spp (Koehler, 2010).

Cytological, physiological, biochemical and molecular changes associated with the transition of somatic cells into embryos have been widely studied in the carrot system (Raghavan, 2006). Other model plants such as *Arabidopsis thaliana* and the legume *Medicago truncatula* have also been used to investigate the molecular basis of somatic embryogenesis using mutants and functional genomics (Rose and Nolan, 2006). *Brachypodium distachyon* with its sequenced genome database and its large number of mutant strains could also provide valuable insights into processes underlying morphogenesis in the grass family.

The use of specific markers to distinguish between competent and non-competent cells and/or between embryogenic and non-embryogenic cells or tissues, can help to elucidate the mechanism involved in the determination of cell type. Likewise, an understanding of the origin of somatic embryogenesis, uni- or multicellular, is critical to scientific and biotechnological applications (Quiroz-Figueroa et al., 2006).

Today, embryogenic callus is the most widely used target tissue for the genetic transformation of *B. distachyon* (Brkljacic et al., 2011; Vain, 2011). Nevertheless, information about origin and cellular changes occurring during the early differentiation of somatic embryos has not been documented for *B. distachyon*. Similarly, molecular studies to investigate the *SERK* gene expression as a potential marker for distinguishing competent cells in early somatic embryogenesis have not been approached in *B. distachyon*.

Therefore, the objectives of this study are: (1) the morphological, anatomical and histochemical characterization of changes occurring during the induction of somatic embryogenesis from immature zygotic embryos of *B. distachyon* community standard line Bd21 using light and scanning electron microscopy in association with histochemical tests; and (2) cloning and characterization of SERK genes and analysis of its expression in somatic embryogenesis induction using *in situ* hybridization for monitoring the morphogenetic processes in vitro.

REFERENCES

ALVES S. C., WORLAND B., THOLE V., SNAPE J. W., BEVAN M. W., VAIN P. A protocol for *Agrobacterium*-mediated transformation of *Brachypodium distachyon* community standard line Bd21. **Nature Protocols**, v. 4, n. 5, p. 638-649, 2009.

BABLAK P., DRAPER J., DAVEY M. R., LYNCH P. T. Plant regeneration and micropropagation of *Brachypodium distachyon*. **Plant Cell Tissue Organ Culture**, v. 42, p. 97–107, 1995.

BAKKER E.G., MONTGOMERY B., NGUYEN T., EIDE K., CHANG J., MOCKLER T.C., LISTON A., SEABLOOM E.W., BORER E.T. Strong population structure characterizes weediness gene evolution in the invasive grass species *Brachypodium distachyon*. **Molecular Ecology**, v. 18, p. 2588–2601, 2009.

BARTLETT J.C., ALVES S.A., SMEDLEY M., SNAPE J.W., HARWOOD W.A. High-throughput *Agrobacterium*-mediated barley transformation. **Plant Methods**, v. 4, n. 22, 2008.

BORTIRI E., COLEMAN-DERR D., LAZO G.R., ANDERSON O.D., GU Y.Q. The complete chloroplast genome sequence of *Brachypodium distachyon*: sequence comparison and phylogenetic analysis of eight grass plastomes. **BMC Research Notes**, v. 1, p. 61, 2008.

BRKLJACIC J., GROTEWOLD E., SCHOLL R., MOCKLER T., GARVIN D.F., VAIN P., BRUTNELL T., SIBOUT R., BEVAN M., BUDAK H., CAICEDO A. L., GAO C., GU Y., HAZEN S.P., HOLT III B.F., HONG S.-Y., JORDAN M., MANZANEDA A.J., MITCHELL-OLDS T., MOCHIDA K., MUR L.A.J., PARK C.-M., SEDBROOK J., WATT M., ZHENG S.J., VOGEL J.P. *Brachypodium* as a Model for the Grasses: Today and the Future. **Plant Physiology**, v. 157, p. 3–13, 2011.

BRUKHIN V., MOROZOVA N. Plant Growth and Development - Basic Knowledge and Current Views. **Mathematical Modelling of Natural Phenomena**, v. 6, n. 2, p. 1-53, 2011.

CANGAHUALA-INOCENTE G.C., STEINER N., MALDONADO S.B., GUERRA M.P. Patterns of protein and carbohydrate accumulation during somatic embryogenesis of *Acca sellowiana*. **Pesquisa Agropecuária Brasileira**, v. 44, p. 217–224, 2009.

CATALÁN P., OLMSTEAD R.G. Phylogenetic reconstruction of the genus *Brachypodium* P-Beauv. (Poaceae) from combined sequences of chloroplast *ndhF* gene and nuclear ITS. **Plant Systematics and Evolution**, v. 220, p.1–19, 2000..

CATALÁN P., MŰLLER J., HASTEROK R., JENKINS G., MUR L.A.J., LANGDON T., BETEKHTIN A., SIWINSKA D., PIMENTEL M., LÓPEZ-ALVAREZ D. Evolution and taxonomic split of the model grass *Brachypodium distachyon*. **Annals of Botany**, v. 109, p. 385–405, 2012.

CHRISTIANSEN P., DIDION T., ANDERSEN C. H., FOLLING M., NIELSEN K. K. A rapid and efficient transformation protocol for the grass *Brachypodium distachyon*. **Plant Cell Reports**, v. 23, p. 751–758, 2005.

CHU C.C., WANG C.C., SUN C.S., HSU C., YIN K.C., CHU C.Y., BI F.Y. Establishment of an efficient medium for anther culture office through comparative experiments on the nitrogen sources. **Scientia Sinica**, v. 18, p. 659—668, 1975.

CORREIA S., ESTEFANIA CUNHA A. E., SALGUEIRO L., CANHOTO J. M. Somatic embryogenesis in tamarillo (*Cyphomandra betacea*): approaches to increase efficiency of embryo formation and plant development. **Plant Cell Tissue and Organ Culture**, v. 109, p. 143–152, 2012.

DAHLEEN, L. S. Improved plant regeneration from barley callus cultures by increased copper levels. **Plant Cell Tissue Organ Culture**, v. 43, p. 267–269, 1995.

DRAPER J., MUR L. A. J., JENKINS G., GHOSH-BISWAS G. C., BABLAK P., HASTEROK R., ROUTLEDGE A. P. M. *Brachypodium distachyon*. A new model system for functional genomics in grasses. **Plant Physiology**, v. 127, p. 1539–1555, 2001.

EUDES, F., ACHARYA, S., LAROCHE, A., SELINGER, L.B., CHENG, K.J. A novel method to induce direct somatic embryogenesis, secondary embryogenesis and regeneration of fertile green cereal plants. **Plant Cell Tissue Organ Culture**, v.73, p. 147-157, 2003.

FARRAR, K., DONNISON, I.S. Construction and screening of BAC libraries made from *Brachypodium* genomic DNA. **Nature Protocols**, v. 2, p. 1661-1674, 2007.

FEBRER M, GOICOECHEA J.L., WRIGHT J., MCKENZIE N., SONG X., LIN J., COLLURA K., WISSOTSKI M., YU Y., AMMIRAJU J.S.S., et al An integrated physical, genetic and cytogenetic map of *Brachypodium distachyon*, a model system for grass research. **PLoS ONE**, v. 5, n. 10, e13461, 2010.

FEHÉR A. Why somatic plant cells start to form embryos? In: MUJID, A.; SAMAJ, J. (Eds). **Somatic Embryogenesis. Plant Cell Monographs**. Springer: Berlin/Heidelberg, 2:85-101, 2005.

FILIZ E., OZDEMIR B. S., BUDAK F., VOGEL J. P., TUNA M., BUDAK H. Molecular, morphological and cytological analysis of diverse *Brachypodium distachyon* inbred lines. **Genome,** v. 52, p. 876–890, 2009.

FRANSZ P. F, SCHEL J. H. N. 1991. Cytodifferentiation during the development of friable embryogenic callus of maize (*Zea mays*). **Canadian Journal of Botany**, v. 69, p. 26-33, 1991.

GARVIN D.F., GU Y.Q., HASTEROK R., HAZEN S.P., JENKINS G., et al. Development of Genetic and Genomic Research Resources for *Brachypodium distachyon*, a new model system for Grass Crop Research. **Plant Genome**, v. 48, p. 69–84, 2008.

GARVIN D. F., MCKENZIE N., VOGEL J. P., MOCKLER T. C., BLANKENHEIM Z. J., WRIGHT J., CHEEMA J. J., DICKS J., HUO N., HAYDEN D. M., GU Y., TOBIAS C., CHANG J. H., CHU A., TRICK M., MICHAEL T. P., BEVAN M.

W., SNAPE J. W. An SSR-based genetic linkage map of the model grass *Brachypodium distachyon*. **Genome**, v. 53, p. 1–13, 2010.

GREEN C. E., PHILLIPS R. L. Plant regeneration from tissue cultures of maize. **Crop Science**, v. 15, p. 417-421, 1975.

GRIGA M., HORÁČEK J., KLENOTIČOVÁ H. Protein patterns associated with *Pisum sativum* somatic embryogenesis. **Biologia Plantarum**, v. 51, n. 2, p. 201-211, 2007.

GU Y. Q., MA Y., HUO N., VOGEL J. P., YOU F. M., LAZO G. R., NELSON W. M., SODERLUND C., DVORAK J., ANDERSON O. D., LUO M-C. A BAC-based physical map of *Brachypodium distachyon* and its comparative analysis with rice and wheat. **BMC Genomics,** v. 10, p. 496, 2009.

HAMMAMI R., CUADRADO A., FRIERO E., JOUVE N., SOLER C., GONZÁLEZ J.M. Callus induction and plant regeneration from immature embryos of *Brachypodium distachyon* with different chromosome numbers. **Biologia Plantarum**, v. 55, n. 4, p. 797-800, 2011.

HANDS P., DREA S. A comparative view of grain development in *Brachypodium distachyon*. **Journal of Cereal Science**, v. 56, p. 2-8, 2012.

HANSEN G., WRIGHT M. S. Recent advances in the transformation of plants. **Trends in Plant Science**, v. 4, p. 226–231, 1999.

HASTEROK R., MARASEK A., DONNISON I.S., et al. Alignment of the genomes of *Brachypodium distachyon* and temperate cereals and grasses using bacterial artificial chromosome landing with fluorescence *in situ* hybridization. **Genetics** 173: 349–62, 2006.

HECHT V., VIELLE-CALZADA J. P., HARTOG M. V., SCHMIDT E. D., BOUTILIER K., GROSSNIKLAUS U. The *Arabidopsis* SOMATIC EMBRYOGENESIS RECEPTOR KINASE 1 gene is expressed in developing ovules

and embryos and enhances embryogenic competence in culture. **Plant Physiology**, v. 127, p. 803–816, 2001.

HUANG X., LU X. Y., ZHAO J. T., CHEN J. K., DAI X. M., XIAO W., CHEN Y. P., CHEN Y. F., HUANG X. L. *MaSERK1* gene expression associated with somatic embryogenic competence and disease resistance response in banana (*Musa* spp.). **Plant Molecular Biology Reports**, v. 28, p. 309–316, 2009.

HUO N., GU Y., LAZO G., VOGEL J., COLEMAN-DERR D., LUO M. C., THILMONY R., GARVIN D., ANDERSON O. Construction and characterization of two BAC libraries from *Brachypodium distachyon*, a new model for grass genomics. **Genome**, v. 49, p. 1099–1108, 2006.

HUO N., LAZO G. R., VOGEL J. P., YOU F. M., MA Y., HAYDEN D. M., COLEMAN-DERR D., HILL T. A., DVORAK J., ANDERSON O. D., LUO M. C., GU Y. Q. The nuclear genome of *Brachypodium distachyon*: analysis of BAC end sequences. **Functional and Integrative Genomics**, v. 8, p.135–147, 2008.

HUO N., VOGEL J.P., LAZO G.R., YOU F.M., MA Y., MCMAHON S., DVORAK J., ANDERSON O.D., LUO M-C., GU Y.Q. Structural characterization of *Brachypodium* genome and its syntenic relationship with rice and wheat. **Plant Molecular Biology**, **v.** 70, p. 47–61, 2009.

IBI – THE INTERNATIONAL *BRACHYPODIUM* INITIATIVE. Genome sequencing and analysis of the model grass *Brachypodium distachyon.* **Nature**, v. 463, p. 763-768, 2010.

IDZIAK D., BETEKHTIN A., WOLNY E., et al.. Painting the chromosomes of *Brachypodium* – current status and future prospects. **Chromosoma**, v. 120, p. 469–479, 2011.

KHAN A., STACE C.A. Breeding relationships in the genus *Brachypodium* (Poaceae: Pooideae). **Nordic Journal of Botany**, v. 19, p. 3, 1999.

KELLOGG E. A. Evolutionary History of the Grasses. **Plant Physiology**, v. 125, p. 1198–1205, 2001.

KOEHLER A. D., **Reprodução em *Brachiaria* spp.: *SERK* (Somatic Embryogenesis Receptor-Like Kinase) no desenvolvimento da antera, do ovário e na embriogênese.** Tese (Doutorado), CENA, USP. 2010, 108 P.

KURCZYNSKA E. U., POTOCKA I., DOBROWOLSKA I., KULINSKA-LUKASZEK K., SALA K., WROBEL J.. Cellular Markers for Somatic Embryogenesis, Embryogenesis, Dr. Ken-Ichi Sato (Ed.), 2012 InTech, Available from: http://www.intechopen.com/books/embryogenesis/cellularmarkers-for-somatic-embryogenesis

LINSMAIER E.M., SKOOG F. Organic growth factor requirements of tobacco tissue cultures. **Physiologia Plantarum**, v. 18, p. 100-127, 1965.

MOURA E. F., VENTRELLA M. C., MOTOIKE S. Y. Anatomy, histochemistry and ultrastructure of seed and somatic embryo of *Acrocomia aculeata* (Arecaceae). **Scientia Agricola**, v. 67, p. 399–407, 2010.

MURASHIGE T., SKOOG F. A revised medium for rapid growth and bio assays with tobacco tissue cultures. **Physiologia Plantarum,** v. 15, p. 473–497, 1962.

NAMASIVAYAM, P. Acquisition of embryogenic competence during somatic embryogenesis. **Plant Cell, Tissue and Organ Culture**, v. 90, n. 1, p. 1-8, 2007.

NAMASIVAYAM P., HANKE D.E. Molecular characterization of *Dg3*, a cDNA that encodes a novel lipid transfer protein in *Brassica napus*. **Journal of Biological Sciences**, v. 8, n. 5, p. 846-856, 2008.

NAMASIVAYAM, P., SKEPPER, J. HANKE, D. Identification of a potential structural marker for embryogenic competency in the *Brassica napus* ssp. *Oleifera* embryogenic tissue. **Plant Cell Reports**, v. 25, n. 9, p. 887-895, 2006.

NOLAN K. E., IRWANTO R. R., ROSE R. J. Auxin upregulates *MtSERK1* expression in both *Medicago truncatula* root-forming and embryogenic cultures. **Plant Physioology**, v. 133, p. 218–230, 2003.

NOLAN K. E., KURDYUKOV S., ROSE R. J. Expression of the *SOMATIC EMBRYOGENESIS RECEPTOR-LIKE KINASE1* (*SERK1*) gene is associated with developmental change in the life cycle of the model legume *Medicago truncatula*. **Journal of Experimental Botany**, v. 60, p.1759–1771, 2009.

OLSEN P., LENK I., JENSEN C. S., PETERSEN K., ANDERSEN C. H., DIDION T., NIELSEN K. K. Analysis of two heterologous flowering genes in *Brachypodium distachyon* demonstrates its potential as a grass model plan. **Plant Science**, v. 170, p. 1020–1025, 2006.

OPANOWICZ, M., VAIN, P., DRAPER, J., PARKER, D., DOONAN, J.H. *Brachypodium distachyon*: making hay with a wild grass. **Trends in Plant Science**, v. 13, p. 172–177, 2008.

PACAK A., GEISLER K., JORGENSEN B., BARCISZEWSKA-PACAK M., NILSSON L., NIELSEN T.H., JOHANSEN E., GRONLUND M., JAKOBSEN I., ALBRECHTSEN M. Investigations of barley stripe mosaic virus as a gene silencing vector in barley roots and in *Brachypodium distachyon* and oat. **Plant Methods**, v.6, p. 26, 2010.

PASTERNAK T.P., PRINSEN E., AYAYDIN F., MISKOLCZI P., POTTERS G., ASARD H., VANONCKELEN H.A., DUDITS D., FEHÉR A. The role of auxin, pH, and stress in the activation of embryogenic cell division in leaf protoplast- derived cells of alfalfa. **Plant Physiology**, v. 129, n. 4, p. 1807-1819, 2002.

PĂCURAR, D.I., THORDAL-CHRISTENSEN, H., NIELSEN, K.K., LENK, I**.** A high-throughput *Agrobacterium*-mediated transformation system for the grass model species *Brachypodium distachyon* L. **Transgenic Research**, v. 17, p. 955–963, 2008.

PINTO G., SILVA S., ARAÚJO C., NEVES L., SANTOS C. Histocytological changes and reserves accumulation during somatic embryogenesis in *Eucalyptus globulus*. **Trees**, v. 24, p. 763–769, 2010.

POTTERS G., PASTERNAK T.P., GUISEZ Y., JANSEN M.A.K. Different stresses, similar morphogenic responses: integrating a plethora of pathways. **Plant, Cell and Environment**, v. 32, p. 158–169, 2009.

PUIGDERRAJOLS P., MIR G., MOLINAS M. Ultrastructure of early secondary embryogenesis by multicellular and unicellular pathways in cork oak (*Quercus suber* L.). **Annals of Botany**, v. 87, p. 179–189, 2001.

PURNHAUSER L., GYULAI G. Effect of copper on shoot and root regeneration in wheat, triticale, rape and tobacco tissue cultures. **Plant Cell Tissue and Organ Culture**, v. 35, p.131–139, 1993.

QUIROZ-FIGUEROA F.R., ROJAS-HERRERA R., GALAZ-AVALOS R.M., LOYOLA-VARGAS V.M. Embryo production through somatic embryogenesis can be used to study cell differentiation in plants. **Plant Cell Tissue Organ Culture**, v. 86, p. 285–301, 2006.

RAGHAVAN V. Can carrot and *Arabidopsis* serve as model systems to study the molecular biology of somatic embryogenesis? **Current Science**, v. 90, n. 10 (25), p. 1336-1343, 2006.

ROBERTSON I.H. Chromosome numbers in *Brachypodium* Beauv. (Gramineae). **Genetica**, v. 56: p. 55–60, 1981.

ROCHA D.I., VIEIRA L.M., TANAKA F.A.O., DA SILVA L.C., OTONI W.C. Somatic embryogenesis of a wild passion fruit species *Passiflora Cincinnata* Masters: histocytological and histochemical evidences. **Protoplasma**, v. 249, n. 3, p. 747-758, 2012.

ROSE R.J., NOLAN K.E. Invited review: genetic regulation of somatic embryogenesis with particular reference to *Arabidopsis thaliana* and *Medicago truncatula*. **In Vitro Cellular and Developmental Biology—Plant**, v. 42, p. 473–481, 2006.

ROSE R.J., MANTIRI F.R., KURDYUKOV S., CHEN S.-K., WANG X.-D., NOLAN K.E., SHEAHAN M.B. Developmental biology of somatic embryogenesis. In: PUA E.-C., DAVEY M.R. (Eds.) **Plant developmental biology-biotechnological perspectives**, vol 2. Springer:Heidelberg, pp 3-26, 2010.

SANTA-CATARINA C., HANAI L. R., DORNELAS M.C., VIANA A. M., FLOH E. I. S. *SERK* gene homolog expression, polyamines and amino acids associated with somatic embryogenic competence of *Ocotea catharinensis* Mez. (Lauraceae). **Plant Cell, Tissue and Organ Culture**, v. 79, p. 53–61, 2004.

SANTOS M.O., ARAGÃO F.J.L. Role of *SERK* genes in plant environmental response. **Plant Signaling and Behavior**, v. 4, n. 12, p. 1111–1113, 2009.

SANTOS M. O., ROMANO E., YOTOKO K. S. C., TINOCO M. L. P., DIAS B. B. A., ARAGÃO F. J. L. Characterization of the cacao somatic embryogenesis receptor-like kinase (*SERK*) gene expressed during somatic embryogenesis. **Plant Science**, v. 168, p. 723–729, 2005.

SHANG Y., MA L., WANG H., FENG W., CHEN P., CAO X., LIU D., WANG X. The evolutionary history of PDR in *Brachypodium distachyon* polyploids. **Molecular Biology Reports**, v. 38, p. 2211–2217, 2011.

SCHMIDT E. D., GUZZO F., TOONEN M. A., DE VRIES S. C. A leucine-rich repeat containing receptor-like kinase marks somatic plant cells competent to form embryos. **Development**, v. 124, p. 2049–2062, 1997.

SCHULZE J. Improvements in Cereal Tissue Culture by Thidiazuron: A Review. In: **Fruit Vegetable and Cereal Science and Biotechnology.** GSB Publisher, Isleworth, UK, p. 64-79, 2007.

SINGLA B., KHURANA J.P., KHURANA P. Characterization of three somatic embryogenesis receptor kinase genes from wheat, *Triticum aestivum*. **Plant Cell Reports**, v. 27, p.833–843, 2008.

SOMLEVA M. N., SCHMIDT E. D. L., DE VRIES S. C. Embryogenic cells in *Dactylis glomerata* L. (Poaceae) explants identified by cell tracking and by *SERK* expression. **Plant Cell Reports**, v. 19, p.718–726, 2000.

TAYLOR M.G., VASIL I.K. The ultrastructure of somatic embryo development in pearl millet (*Pennisetum glaucum*; Poaceae). **American Journal of Botany,** v. 83, n. 1, p. 28-44, 1996.

THOLE V., PERALDI A., WORLAND B., NICHOLSON P., DOONAN J.H., VAIN P. T-DNA mutagenesis in *Brachypodium distachyon*. **Journal of Experimental Botany**, v. 63, n. 2, p. 567–576, 2012.

TOONEN M. A. J., DE VRIES S. C. Initiation of somatic embryos from single cells. In: Wang T. L., Cuming A. (Eds.) **Embryogenesis: The Generation of a Plant**, Bios Scientific Publishers, Oxford, UK, pp. 173–189, 1996.

VAIN P. *Brachypodium* as a model system for grass research. **Journal of Cereal science**, v. 54, p. 1-7, 2011.

VAIN P., THOLE V., WORLAND B., OPANOWICZ M., BUSH M.S., DOONAN J.H. A T-DNA mutation in the RNA helicase, eIF4A, confers a dose-dependent dwarfing phenotype in *Brachypodium distachyon*. **The Plant Journal**, v. 66, p. 929–940, 2011.

VAIN P., WORLAND B., THOLE V., MCKENZIE N., ALVES S. C., OPANOWICZ M., FISH L. J., BEVAN M. W. SNAPE J. W. *Agrobacterium*-mediated transformation of the temperate grass *Brachypodium distachyon* (genotype Bd21) for T-DNA insertional mutagenesis. **Plant Biotechnology**, v. 6, p. 236–245, 2008.

VERDEIL, J.L., HOCHER, V., HUET, C., GROSDEMANGE, F., ESCOUTE, J, FERRIERE, N., NICOLE, M. Ultrastructural changes in coconut calli associated with

the acquisition of embryogenic competence. **Annals of Botany**, v. 88, n. 1, p. 9-18, 2001.

VERDEIL, J.L., ALEMANNO, L., NIEMENAK, N., TRAMBARGER, T.J. Pluripotent versus totipotent plant stem cells: dependence versus autonomy? **Trends in Plant Science**, v. 12, n. 6, p. 245-252, 2007.

VOGEL J., BRAGG J. *Brachypodium distachyon*, a New Model for the Triticeae. In: FEUILLET C., MUEHLBAUER G. (eds.) **Genetics and Genomics of the Triticeae**. Springer. vol. 7, p. 427-449, 2009.

VOGEL J. P., M., BUDAK H., HUO N., GU Y. Q., STEINWAND M. A. Development of SSR markers and analysis of diversity in Turkish populations of *Brachypodium distachyon.* **BMC Plant Biology**, v. 9, p. 88, 2009.

VOGEL J. P., GARVIN, D. F., LEONG, O. M., HAYDEN, D. M. *Agrobacterium*-mediated transformation and inbred line development in the model grass *Brachypodium distachyon*. **Plant Cell, Tissue and Organ Culture**, v. 84, p. 199–211, 2006.

VOGEL J., HILL, T. High-efficiency *Agrobacterium*-mediated transformation of *Brachypodium distachyon* inbred line Bd21–3. **Plant Cell Reports**, v. 27, p. 471–478, 2008.

VON ARNOLD S., SABALA I., BOZHKOV P., DYACHOK J., FILONOVA L. Developmental pathways of somatic embryogenesis. **Plant Cell, Tissue and Organ Culture**, v. 69, p. 233–249, 2002.

WOLNY E., LESNIEWSKA K., HASTEROK R., LANGDON T. Compact genomes and complex evolution in the genus *Brachypodium*. **Chromosoma**, v. 120, p. 199–212, 2011.

ZAVATTIERI M.A., FREDERICO A.M., LIMA M., SABINO R., ARNHOLDT-SCHMITT B. Induction of somatic embryogenesis as an example of stress-related plant reactions. **Electronic Journal of Biotechnology**, v. 13, n. 1, 2010.

CHAPTER 1

SOMATIC EMBRYOGENESIS FROM IMMATURE ZYGOTIC EMBRYOS OF *Brachypodium distachyon* (POACEAE): MORPHOLOGICAL, HISTOLOGICAL AND HISTOCHEMICAL INVESTIGATIONS

ABSTRACT

This study provides the first description of morphological, histological and histochemical changes underlying the embryogenic process in *B. distachyon* reference line Bd21 using light and electron microscopic techniques. *In vitro* regeneration of plantlets derived from somatic embryos occurred by indirect somatic embryogenesis pathway. This process was initiated from zygotic embryo explants cultured 15 days post anthesis. Embryogenic callus and somatic embryos originated from cells of the scutellar epidermis and extended to the periphery of immature zygotic embryos of *B. distachyon* Somatic embryo had a multicellular origin. The order in accumulation of storage reserves in somatic embryos was similar to that of zygotic embryos. In the embryogenic cultures, storage proteins and lipids were used up in the first 2 days after culture (DAC). The levels of starch increased in the first 2 DAC and then decreased in number of granules that became larger and appeared mainly in the vacuolated cells subtending the proembryonic masses. Small starch granules started accumulating in proembryoids after 4 DAC and became larger and abundant in scutellar cells 12 DAC. Somatic embryo differentiation in *B. distachyon* proceeded through globular, scutellar and coleoptilar stages, following the morphological pattern of development of that reported in other members of the Poaceae. These results provide important information for the understanding of the developmental processes and the mechanisms that lead to cell differentiation and transition from the somatic to the embryogenic stage that has been lacking in *B. distachyon*.

Key words: *Brachypodium distachyon*, somatic embryogenesis, histology, histochemistry, reserve mobilization

EMBRIOGÊNESE SOMÁTICA A PARTIR DE EMBRIÕES ZIGÓTICOS DE SEMENTES IMATURAS DE *Brachypodium distachyon* (POACEAE): INVESTIGAÇÕES MORFOLÓGICAS, HISTOLÓGICAS E HISTOQUÍMICAS.

RESUMO

Este estudo fornece a primeira descrição de alterações morfológicas, histológicas e histoquímicas associadas ao processo de embriogenese somática em *B. distachyon* linhagem BD21 usando técnicas de microscopia de luz e eletrônica. A regeneração in vitro de plântulas derivadas de embriões somáticos ocorreu por embriogênese somática através da via indireta. Os embriões somáticos tiveram uma origem multicelular e originaram-se de calo embriogênico formado a partir de células da epiderme na região do nó escutelar que se estenderam para a periferia do IZE. A ordem de acúmulo de reservas nos embriões somáticos foi semelhante a dos embriões zigóticos. Nas culturas embriogênicas, proteínas e lipídios de armazenamento foram mobilizados nos primeiros 2 dias em meio de indução (DAC). O teor de amido aumentou nos primeiros 2 DAC e diminuiu em seguida em número de grânulos que se tornaram maiores e apareceram principalmente nas células vacuoladas adjacentes às massas pró-embriogênicas. Pequenos grânulos de amido começaram a acumular nos pró-embrióides após 4 DAC e tornaram-se maior e mais abundantes em células do escutelo aos 12 DAC. A diferenciação do embrião somático seguiu a mesma sequência de desenvolvimento verificado em outros membros da família Poaceae, ou seja, a passagem pelos estádios globular, escutelar e coleoptilar. Estes resultados fornecem informações importantes para a compreensão dos processos de desenvolvimento, e os mecanismos que conduzem à diferenciação celular e da transição das células somáticas para o estágio embriogênico que ainda não foram relatados em *B. distachyon*.

Palavras-chave: *Brachypodium distachyon*, embriogênese somática, histologia, histoquímica, mobilização de reservas.

INTRODUCTION

Over the past decade, *Brachypodium distachyon* has been proposed as a model species for temperate grasses and cereals (Draper et al., 2001; Vogel and Bragg, 2009). *B. distachyon* is an ideal system for functional genomic studies, because of its easy growth requirements, small stature, and rapid life cycle, small genome and self-pollination (Opanowicz et al., 2008). In addition, important genomic resources have been developed for using *B. distachyon* as a model for grass crops: transformation protocols, large expressed sequence tag (EST) databases, tools for forward and reverse genetic screens, highly refined cytogenetic probes, germplasm collections and, recently, a complete genome sequence has been generated (Vain, 2011; Brkljacic et al., 2011).

Functional genomics studies require from any model plant efficient transformation and regeneration systems. Efficient tissue culture protocols have been established for *B. distachyon* (Ye and Tao, 2008), but there have been no reports on the literature of basic histological and histochemical studies of the events taking place in the explant cells during the regeneration process. This fundamental knowledge for the understanding of the developmental processes occurring during plant growth and development as well as the mechanisms that lead to cell differentiation and passage from the somatic to the competent stage to form organs or embryos is lacking in *B. distachyon*.

Somatic embryogenesis (SE) is the process by which somatic cells differentiate into somatic embryos (von Arnold, 2002). SE plays a very important role in *in vitro* plant regeneration of various cereal and grass species (Ozias-Akins and Vasil, 1982; Vasil et al., 1985; Brisibe et al., 1993; Taylor and Vasil, 1996; Mariani et al., 1998; Wrobel et al., 2011). When integrated with conventional breeding programs and molecular and genetic engineering techniques, SE provides a valuable tool to enhance genetic improvement of crop species (Quiroz-Figueroa et al., 2006). However, genetic engineering or mutagenesis techniques cannot be successfully achieved if the processes underlying morphogenesis are not well understood (Fortes and Pais, 2000).

The transition and induction of embryogenic competence is the most important, step during SE, but, in spite of the accumulation of experimental data, the key events underlying the transition of differentiated somatic cells to the totipotent and embryogenic cell state is still not elucidated (Fehér et al., 2003). During this step, competent cells are those which are in a transitional state and which still require some

stimuli to become embryogenic (Namasivayam, 2007). It is not clear how the embryogenic cells originate within the explants and what mechanisms control this process. Cells will change fate and the direction of differentiation by erasing the genetic developmental program and starting a new one. It is unknown how the explant cells do so. Studies indicate that changes in the developmental program occur through the physical isolation of a cell or a group of cells from the surroundings. It has been shown that there are some features of the transition from the somatic to the embryogenic state on the cellular and histological level which allows the recognition of this developmental stage (Kurczynska et al., 2012).

In most embryogenic systems described until now, embryogenic cells show characteristics common to meristematic cells, including a high nucleus:cytoplasm ratio, a dense cytoplasm, and small fragmented vacuoles (Williams and Maheswaran 1986; Fehér et al., 2003). However, meristematic cells have spherically shaped nuclei with several small nucleoli and most of the chromatin exists as heterochromatin, whereas embryogenic cells have irregularly shaped nuclei with invaginations of the nuclear membrane, contain one large nucleolus and thick cell walls (Verdeil et al., 2007).

The morphological, histological and cytological analysis of SE is also an object of studies leading to an understanding of the basis of the totipotency, differentiation, dedifferentiation, transdifferentiation and changes in cell fate and can help in the understanding of the developmental processes taking place during plant growth and development (Quiroz-Figueroa et al., 2006; Sugimoto et al., 2011).

Descriptions of the changes occurring during the transition of somatic cells into embryogenically competent cells and histodifferentiation of somatic embryos were reported for *Acrocomia aculeata* (Moura et al., 2010), *Hordeum vulgari* (Wrobel et al., 2011), *Musa* spp. (Pan et al., 2011) and *Passiflora* (Rocha et al.,2012). Histochemical tests and ultrastructure analysis have also been used to monitor the synthesis and mobilization of reserves during the embryogenic process (Taylor and Vasil, 1996; Moura et al., 2010; Rocha et al., 2012).

Somatic embryogenesis of *Brachypodium distachyon* has not been characterized. Particularly, early stages of embryogenic callus development have not been examined by light and scanning electron microscopy to confirm somatic embryogenesis and to understand the mechanisms underlying the changes occurring in the transition from the somatic to the embryogenic stage. Therefore, the objectives of this study were to characterize the morphological and anatomical changes involved in somatic embryo

formation and monitor, using histochemical methods, reserve mobilization during the induction of somatic embryogenesis from immature zygotic embryos (IZE) of *B. distachyon* community standard line Bd21.

MATERIALS AND METHODS

Plant material

Selfed seeds of *Brachipodium distachyon* (L.) P.Beauv line Bd21 (2n = 10), Poaceae, were provided by Prof. Fabio Tebaldi Silveira Nogueira, Dept of Genetics, Unesp – Botucatu, Brazil, and stored at 4 ^{o}C (dark, low humidity), prior to use.

Seeds were sown in 8 cm plastic pots with a mixture (2:1) of compost and vermiculite and fertilized every week with fertilizer containing micronutrients. To encourage synchronous germination during growth-chamber experiments, seeds were stratified at 4 ºC for 1 week after sowing. Plants were grown for 6 weeks in growth chambers 20 h light:4 h dark photoperiod, 23 ºC with cool-white fluorescent lighting at a level of 150 µE m^{-2} s^{-1}.

Zygotic embryo morphology

The immature zygotic embryo, dissected 15 days post anthesis, is about 0.5 mm wide with a large scutellum. The scutellar node or mesocotyl is the region between the coleorhiza and the coleoptile where the scutellum is attached to the embryo axis (Fig. 1A). The coleoptile initiates from the adaxial surface of the scutellum at the mesocotyl just below the plumule and surrounds the first two leaves (Figs. 1A, B). The coleorhiza, a conical sheath-like structure, is formed at the proximal end of the primary root. Two epiblasts arise just below the scutellar node, each at the two opposite sides of the coleoptile base, and are continuous with the scutellar parenchyma (Fig. 1A).

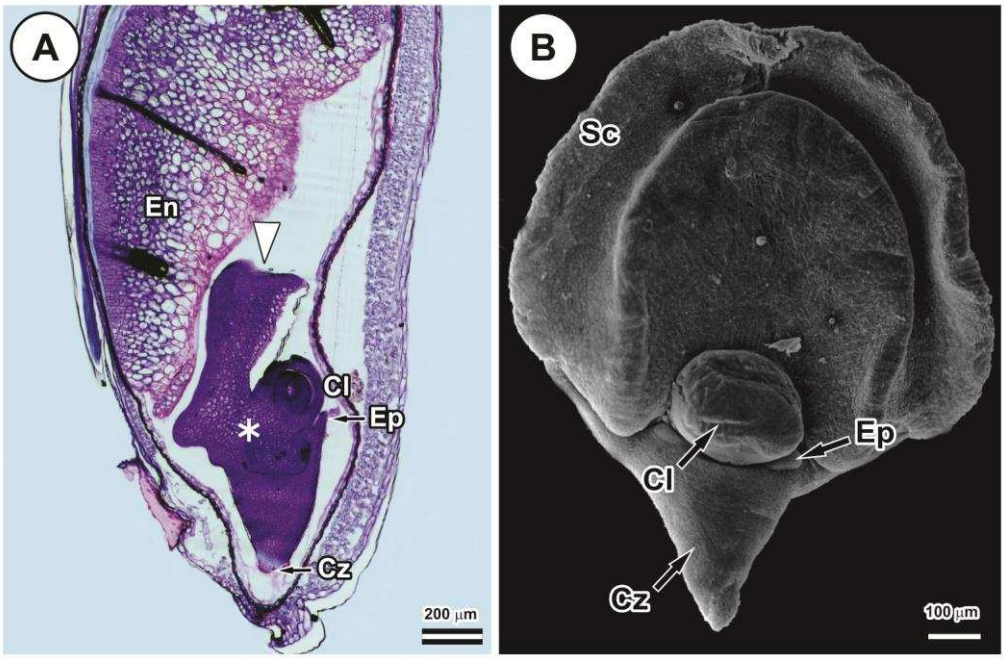

Figure 1. *Brachypodium distachyon* immature embryo 15 d post anthesis. (**A**) Light micrograph of longitudinal section of immature seed showing the scutellum (white arrow), scutellar node (asterisk), coleoptile enclosing the plumule (Cl), coleorhiza enclosing the primary root (Cz), epiblast (Ep) and endosperm (En). (**B**) Scanning electron micrograph of immature embryo showing the scutellum (Sc), coleoptile (Cl), coleorhiza (Cz) and epiblast (Ep).

Production of compact embryogenic callus (CEC) and plant regeneration

Immature seeds obtained around 8–12 weeks after potting were sterilized for 30 s with 20 ml of 70% ethanol in a sterile Petri dish with a lid. Ethanol was drained and seeds rinsed with sterile deionized water. Seeds were placed in 20 ml of 1.3% sodium hypochlorite solution for 4 min and then rinsed three times with sterile deionized water. Lamea (upper glume) was removed from immature seeds and immature embryos removed from seeds with watery to milky endosperm, with a fine forceps under a laminar flow hood using a stereo microscope. Twenty immature embryos were cultured with the scutellum facing up in 9 cm Petri dishes containing 25 mL of induction medium [Murashige andSkoog (MS) salts (Murashige and Skoog, 1962), 4 g L^{-1} Fe-ethylenediaminetetraacetate (Fe-EDTA), 30 g L^{-1} sucrose, 2.5 mg L^{-1} 2,4-Dichlorophenoxyacetic acid, 0.6 mg L^{-1} $CuSO_4$ and 2 g L^{-1} Phytagel (Sigma), pH 5.8] at 25 °C in the dark. Filter-sterilized vitamin M5 [2 mg L^{-1} glycine, 0.4 mg L^{-1} nicotinic acid, 0.4 mg L^{-1} pyridoxine-HCl, 0.5 mg L^{-1} thiamine-HCl, 40 mg L^{-1} cysteine] was added after autoclaving. The elongated coleoptiles were excised when they appeared, during the first 2-3 days of culture. After 3-4 weeks, CECs with a creamy color and

pearly surface were fragmented in 2-4 pieces and transferred (20 callus pieces per plate) onto regeneration medium (MS salts, Fe-EDTA, 30 g L^{-1} sucrose, 0.2 mg L^{-1} kinetin, vitamins M5, 2 g L^{-1} Phytagel - pH 5.8) for 2-3 weeks at 25 ºC under 16-h photoperiod. Shoots (rooted or not) were transferred to jars containing germination medium (40% MS salts, Fe-EDTA, 10 g L^{-1} sucrose, vitamins B5, 2 g L^{-1} l Phytagel, 6 g L^{-1} agar - pH 5.8). Shoots were cultured for 2-3 weeks at 23ºC under 16-h photoperiod. Regenerated plantlets were potted in plastic pots containing a wet compost mixture (3:1 Plantmax®:vermiculite). Plants were grown in a Controlled Environment Room (CER) at 23 °C with a 20-hour photoperiod for 5-6 weeks.

Microscopy sample preparation

For anatomical and histochemical characterization of the process of somatic embryogenesis, immature seeds obtained around 15 days post anthesis (DPA), Day 0, and immature embryos were collected every day from 1 to 6 days after culture in induction medium (DAC), then at days 8, 12 and 21 DAC. The samples were fixed in Karnovsky (1965) solution (glutaraldehyde [2.5%] and paraformaldehyde [4%] in 0.1-M monobasic potassium phosphate buffer [pH 7.2], plus 5 mM of calcium chloride). Mature seeds (35 DPA) were also prepared for histological and histochemical analyses.

Light microscopy and histochemical characterization

Pro-embryonic masses were stained with Evan's blue (0.5%) for 3 min and acetocarmine (0.1%) for 3 min, according to Durzan (1988). For the anatomical studies, fixed samples of immature embryos collected from day 0 to day 21 were dehydrated in a graded ethanol series and embedded in methacrylate (Historesin, Leica Instruments, Germany). Longitudinal sections (7 μm thick) were obtained with an automated advance rotary microtome (RM2155, Leica Microsystems Inc., USA) and stained with toluidine blue at pH 4.4 (O'Brien and McCully, 1981) for structural characterization, xylidine Ponceau for total protein (Vidal, 1977), periodic acid–Schiff's reagent (PAS) for polysaccharides with vicinal glycol groups (Feder and O'Brien, 1968) and Sudan black B (Pearse, 1980) for total lipids. Sections of mature seeds at 35 days post-anthesis (DPA) were also examined by light microscopy and the same histochemical tests used for the immature embryos were used to provide a picture of whether the analyzed store reserves are present in the mature embryo and seed.

Image capture was performed with a light and fluorescence microscope (Olympus AX70TRF, Olympus Optical, Japan) coupled with a digital camera (AxioCam HR, Zeiss).

Scanning electron microscopy

Fixed samples were dehydrated with an increasing acetone series, subjected to critical point drying (CPD 030, Bal-Tec, Balzers, Germany), and coated with gold (SCD 050, Bal-Tec, Balzers, Germany). The analyses were conducted using a scanning electron microscope (LEO 435-VP, Cambridge, England) at the Center for the Support of Research in Electron Microscopy (NAP/MEPA) of the Luiz de Queiroz School of Agriculture (ESALQ/USP) and all images were processed digitally.

RESULTS

General morphology

After 24 h in culture, the coleorhiza and coleoptile had begun to elongate and epidermal hairs had grown on the coleorhiza. During the first 2-3 days in culture, a progressive swelling of the scutellum was observed and the surface of the periphery and scutellar node started to bulge (Figs. 2A, B). At day 4, nodular structures started to develop on the surface of the scutellar node (Figs. 2C, D). After 6-8 days, embryos had formed a mass of callus on the surface of the scutellum with areas of creamy-white embryogenic tissue (denser, with a pale, translucent, nodular appearance, fast growing) (Fig. 2E). The nonembryogenic callus was friable, pale yellow, soft, translucent and slower growing (tissue indicated by arrow in Fig. 2E).

The embryogenic potential of the nodular calli produced in induction medium was confirmed by the double staining technique with Evan's blue and acetocarmine. The embryogenic cells of the nodular structures at Day 8 (Fig. 2F) with large nuclei and dense cytoplasms stained intense bright red with acetocarmine. The large and vacuolated cells, with small nuclei, of the nonembryogenic callus stained blue with Evan's blue. At day 21 (Fig. 2G), these calli showed a deeply folded appearance with formation of scutellar embryos.

After 21-28 days, the compact embryogenic calli (CEC) were transferred onto the regeneration medium in the light and developed into well-formed creamy-white

scutella (Figs. 3A, C, D). Localized chlorophyll also occurred in some zones of the callus (Fig. 3D). Coleoptiles emerged from the coleoptilar pore in the scutellum of fully developed somatic embryos (Figs. 3B, C, D). Coleoptiles were also creamy-white but more translucent and had trichome hairs on the surface (Fig. 3D). Development of coleorhiza and coleoptile was observed by SEM examination (Fig. 3E), indicating a bi-polarity of somatic embryo development. Somatic embryos germinated (Fig. 4A) and shoot-root axis growth occurred in regeneration medium and developed green plantlets (Fig. 4B). Occasionally, root development was delayed and the plantlet remained connected to the callus or produced small roots. These plantlets further developed following subculture for 2-3 weeks on the germination medium (Fig. 4C). Rooted plants were established successfully in compost mixture, produced fertile flowers and set viable seeds (Fig. 4D).

Histological examination

Sections through immature embryos, at day 1 DAC, showed that the scutellar tissue is composed of a single epidermal layer, consisting of richly cytoplasmic cells, and the ground tissue consists of relatively large, compact parenchyma cells (Fig. 5A). The abaxial epidermal scutellar cells were densely stained and markedly distinguishable from scutellar ground cells (Fig. 5A). At day 3 DAC, after several mitotic divisions, there was the differentiation of a region with embryogenic cells initiating nodular callus (Fig. 5B). The cells in the scutellar ground layers increased in size (Figs. 5B, C).

From days 4-5 onwards, mitotic divisions were also observed in the ground tissue, in cells associated with the vascular bundle in the mesocotyl of the zygotic embryo (Fig. 5C). Meristematic cells were produced adjacent to the scutellar vascular bundle, which is connected to the embryo provascular tissue in the scutellar node and extend to the scutellum parenchyma (Fig. 5D). No proembryoids were observed arising from these cells. Cells of the shoot and root meristems in the embryo axis remained without modifications.

From 6-8 days, organized proembryonic cell masses (proembryoids) further developed through a continued series of organized divisions (Fig. 5E), corresponding to the nodular callus observed macroscopically (Fig. 2E. The proembryoids presented a well-defined protodermis with a smooth surface and showed a fold or lateral notch that marked the beginning of the new scutellum (Fig. 5E). They were attached to the callus by a broad multicellular base (Figs. 5E, H). At this stage, the adaxial/abaxial polarity of

the somatic embryo is established by the formation of the scutellum and zones of cytoplasm-rich cells are clearly visible (Figs. 5F, G). Later (28 days in culture), in regeneration medium, these zones developed into shoot and root meristems and formed the shoot-root axis that established the apical/basal polarity of the somatic embryo (Fig. 3E).

While embryogenic cells were being produced in the surface layer, cells of the scutellar ground tissue, coleorhiza, embryo axis and coleoptile became enlarged, highly vacuolated and with small nucleus (Figs. 5B, C, F). The progressive vacuolation of these cells and the formation of large inter-cellular spaces led to their degradation and fragmentation, and the consequent detachment of the inner layers of the callus and, from 8 to 21 days of culture, the embryogenic tissue was separated from the original explant (Figs. 5 F, G).

Embryogenic callus maintained in culture showed progressive growth and the cells of the inner parts of these calli increased in size and also became vacuolated, restarting the process of proembryoid separation. Staining with Lugol's iodine solution indicated the presence of starch in these cells (Fig. 5H).

Histochemical analysis of storage compounds

The histochemical tests confirmed the presence of storage reserves in the scutellum of the immature zygotic embryos used to initiate the embryogenic cultures.

The scutellum of the immature embryo (15 DPA) used to initiate the embryogenic callus (Day 0) showed positive reaction to xylidine Ponceau, though rather less intense (Fig. 6A). However, after 2 days in culture on somatic embryogenesis induction medium, cells of the immature scutellum did not react to xylidine Ponceau and the test was unable to detect storage proteins as the embryogenic callus developed and the epidermal cells were actively dividing to form the proembryonic cell masses (Figs. 6D, G, J, M, P).

The PAS staining revealed that scutellar cells of immature zygotic embryos at Day 0 contained numerous starch granules (Fig. 6B), indicating that they are accumulated as storage starch in the amyloplasts, while none were observed in cells of the embryo axis. By Day 2 of culture on induction medium, the cells had enlarged and there was a striking increase in accumulation of starch granules (Fig. 6E) in the layers of the scutellum nearest to the embryo axis and coleorhiza. At this time, small starch

granules were also present in the epidermal cells that were actively dividing. From Day 4, starch granules had increased in size and appeared more localized, but in smaller numbers, in the vacuolated cells near the proembryonic cell masses (Figs. 6H, K, N). This pattern of starch accumulation was observed until Day 21. From Day 4 to 8 in culture, small starch granules became apparent scattered through the cells of the proembryoids (Figs. 6H, K). From Day 12-21, these small granules enlarged and became abundant in the cells of the proembryoids (Fig. 6Q).

The embryonic and scutellar cells of the dissected immature zygotic embryo (15 DPA) at Day 0 showed negative reaction with Sudan black for lipid bodies (Fig. 6C). From 2-21 days of culture on somatic embryogenesis induction medium, there was also no reaction of cells of the immature scutellum and embryo axis with Sudan black B (Figs. 6F, I, L, O, R).

The histochemical tests confirmed the presence of protein, starch and lipids in the mature seeds.

The storage endosperm of mature seeds of *B. distachyon* consists of vacuolated cells with thick cell walls (Figs. 7B, D, F). At 35 days post-anthesis (DPA), small protein bodies deeply stained with xylidine Ponceau appeared in large amounts in the scutellar parenchyma cells, but none were found in embryo axis cells (Fig. 7A). In endosperm cells, protein appeared coalesced into a single mass surrounded by small starch granules (Fig. 7B).

Starch accumulation in the endosperm of mature seeds of *B. distachyon* was confirmed by light microscopy using PAS staining (Fig. 7D). At 30 DPA, the endosperm cells were mainly occupied by large vacuoles filled with proteins (Fig. 7B) and small even-sized starch granules concentrated in the free spaces (Fig. 7D). No starch granules were detected with PAS staining in the embryonic and scutellar cells of mature seeds (Fig. 7C).

The staining of the very small oil bodies of embryonic cells (e.g. the embryo radicle) was darker than in the scutellum in mature seeds of *B. distachyon* (Fig. 7E), using Sudan black B stain. The aleurone layer showed rich quantity of lipid bodies and some groups of cells in the endosperm contained abundant oil bodies, but the central part of the endosperm contained no lipids (Fig. 7F).

Figure 2. Embryogenic callus initiation from *Brachypodium distachyon* immature zygotic embryos. (**A**) Immature embryos on induction medium with scutellum facing up. (**B**) At 3 days after culture (DAC) bulges started to form on the surface of the periphery of the scutellum and scutellar node. (**C**) At 4 DAC nodular callus (Nc) developed in the region of the scutellar node and trichome hairs on the coleorhiza. (**D**) Scanning electron micrograph showing nodular callus (Nc) in the region of the scutellar node at 4 DAC on induction medium. (**E**) At 8 DAC a mass of non-embryogenic callus (Ne) with areas of proembryonic tissue (proembryoids) formed on the surface of the scutellum (Ec). (**F**) Cells reacting both to acetocarmine and Evan's blue at 8 DAC. A large portion of the embryogenic callus stained red and the non-embryogenic callus stained blue. (**G**) Scanning electron micrograph showing scutellar embryos formed in compact embryogenic callus at 21 DAC. Bars= A, B = 100 µm; C = 125 µm; D = 125 µm; E = 250 µm; F = 50 µm; G = 250µm.

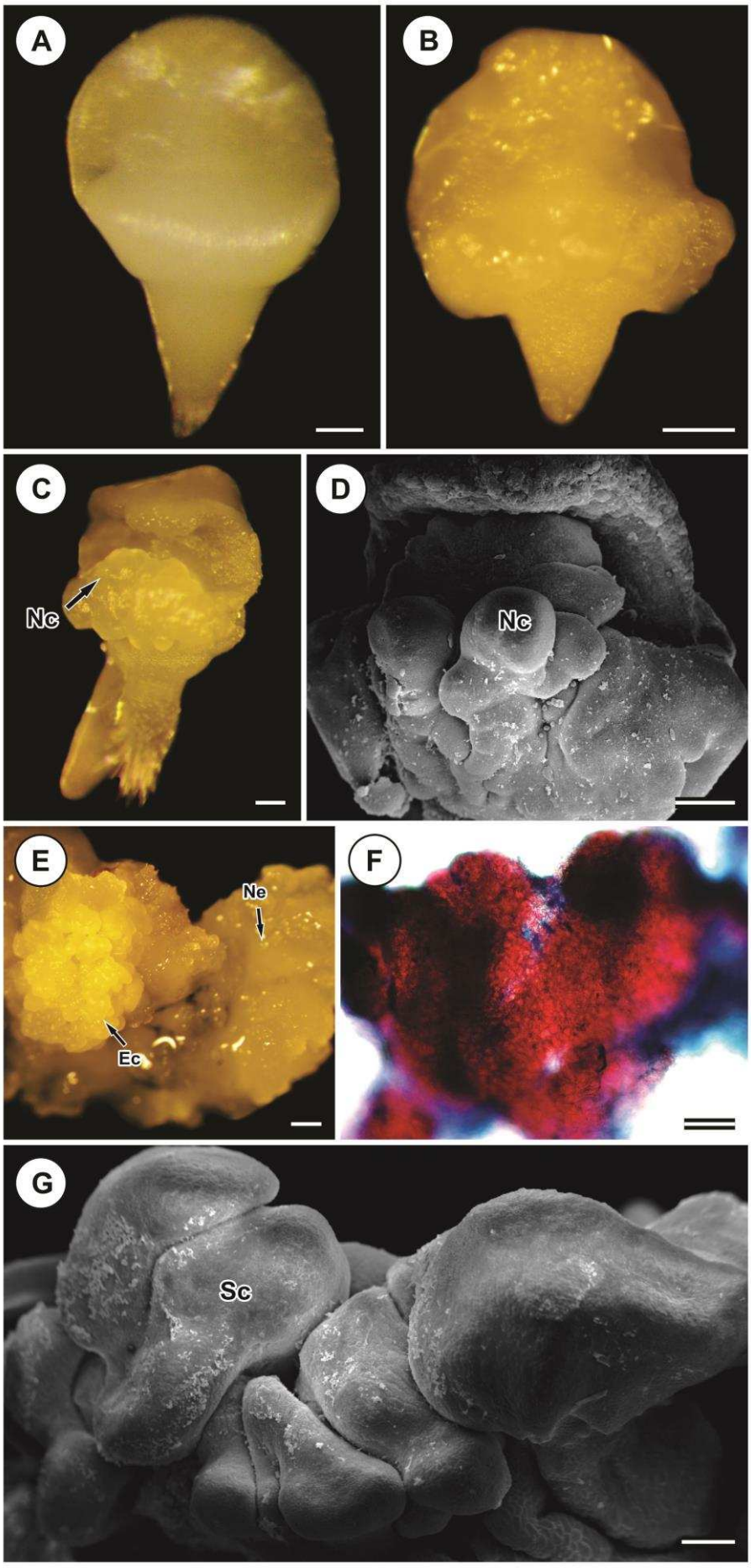
A
B
C
Nc
D
Nc
E
Ne
Ec
F
G
Sc

Figure 3. Development of embryogenic callus from cultured *Brachypodium distachyon* immature zygotic embryos. (**A**) CEC with early scutellar somatic embryos 1 week after transfer to regeneration medium. Arrow indicates scutellar notch. (**B**) Scanning electron micrograph showing somatic embryo at the coleoptilar stage showing the coleoptilar pore (Cp) and scutellum (Sc). (**C**) CEC after 10-15 days on regeneration medium showing somatic embryos at different stages of development. Arrow indicates scutellar embryo with emerging coleoptile. White circles indicate semicircular scutella. (**D**) CEC after 15 days on regeneration medium. Somatic embryo at the coleoptilar stage initiates germination (white arrow). Somatic embryo at the early coleoptilar stage (black arrow). Callus with localized chlorophyll (white circle). (**E**) Scanning electron micrograph showing well-developed somatic embryo attached to the subtending callus after 2 weeks on regeneration medium. Coleorhiza (Cz); Coleoptile (Cl); Scutellum (Sc). Bars: A = 250 µm; B = 100 µm; C, D = 250 µm; E = 100 µm.

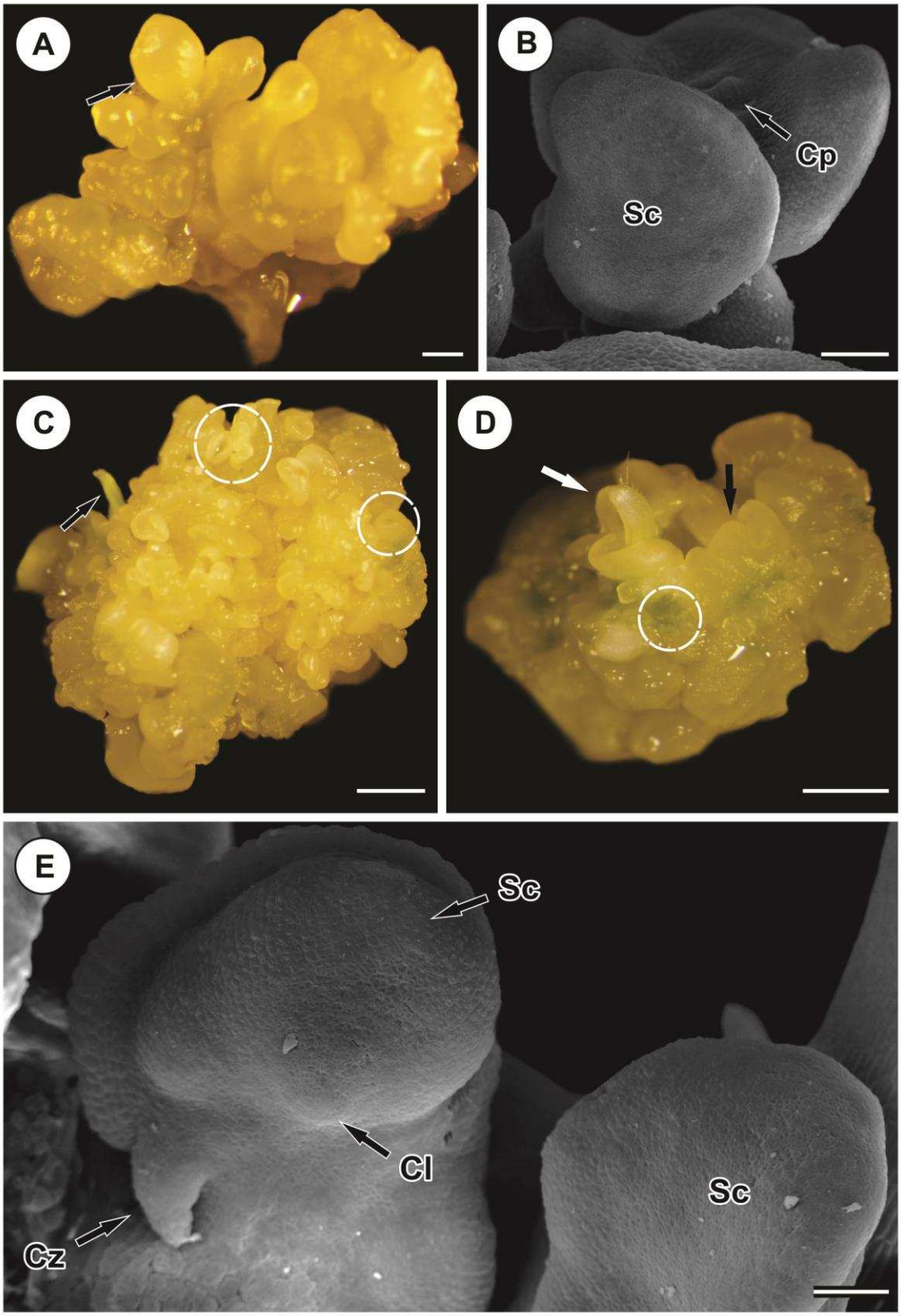
A
B
Cp
Sc
C
D
E
Sc
Cl
Sc
Cz

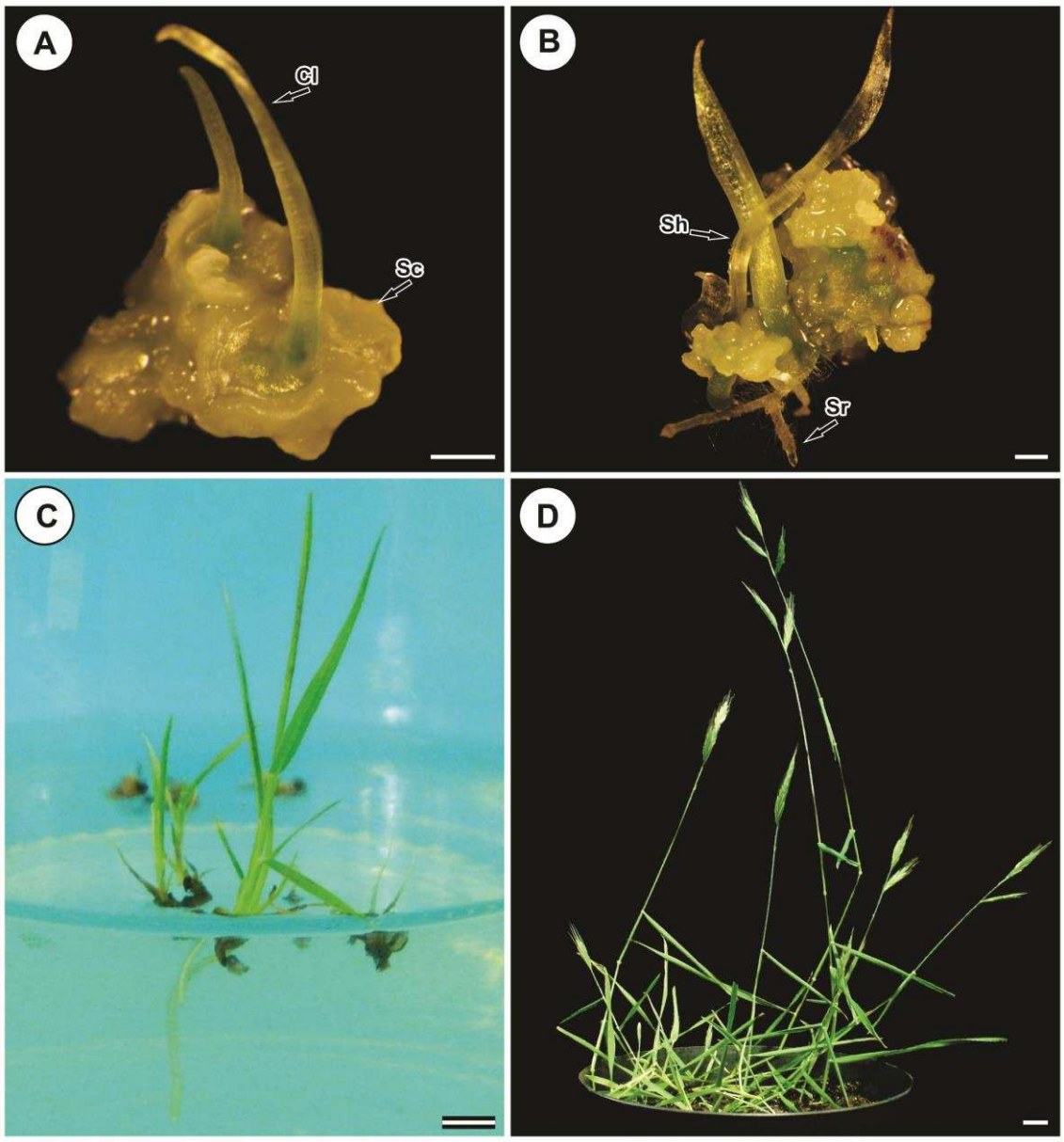

Figure 4. Plant regeneration from cultured *Brachypodium distachyon* immature zygotic embryos. (**A**) Regenerating embryos with coleoptiles (Cl) directly coming from scutella (Sc) after 15-21 days on regeneration medium. (**B**) Plantlet with well-defined shoot (Sh) and root (Sr) bipolar structure at 21 days on regeneration medium. (**C**) Regenerated plantlet developing roots 2 weeks after transfer to germination medium. (**D**) Regenerated plants after 6 weeks in compost mixture producing viable seeds. Bars: plastic pot = 10 mm; jar = 5 mm; A, B = 500 µm.

Figure 5. Induction of embryogenic culture from immature zygotic embryos of *Brachypodium distachyon*. Light micrographs of longitudinal sections. (**A**) Immature embryo 1 day after culture (DAC). Actively dividing cells of the protodermis of the scutellum were densely stained. (**B**) Numerous divisions of protodermal cells 3 DAC give rise to the site of somatic embryo origin (*black arrow*) initiating the nodular callus. (**C**) Mitotic divisions of cells adjacent to the vascular bundle (Vb) in the ground tissue 5 DAC (white square). Cells of the abaxial side of the vascular bundle become enlarged and vacuolated. Scutellum (Sc); embryo axis (Ea); coleoptile (CL); coleorhiza (Cz). (**D**) The area covered is designated by the white square on picture (C). The enlargement here shows densely stained mitotically active small cells with large nuclei close to the vascular bundle (**E**) Proembryoids at 6 DAC with well-defined protodermis (Pt) and smooth surface. The lateral notch is visible (*black arrow*). Proembryoids attached to the callus by a broad multicellular base without vascular connection with the explant tissue (*asterisk*). Large subepidermal cells divide slowly (*white arrow*). (**F**) Densely stained compact embryogenic callus (Ec) deriving from the scutellum, whereas the region of embryo axis (Ea), coleoptile (Cl) and coleorhiza (Cz) produce friable nonembryogenic callus. (**G**) Densely stained compact embryogenic callus (Ec) completely separated from the original explant at 12 DAC. (**H**) From 12 to 21 DAC, the embryogenic callus continues to sector into embryogenic (Ec) and nonembryogenic callus-types. Staining with Lugol's iodine solution shows starch granules (St) accumulated in the large vacuolated cells of the subtending callus. Bars: A, E, F, G, H = 25 µm; B = 10 µm; C = 250 µm; D = 50 µm.

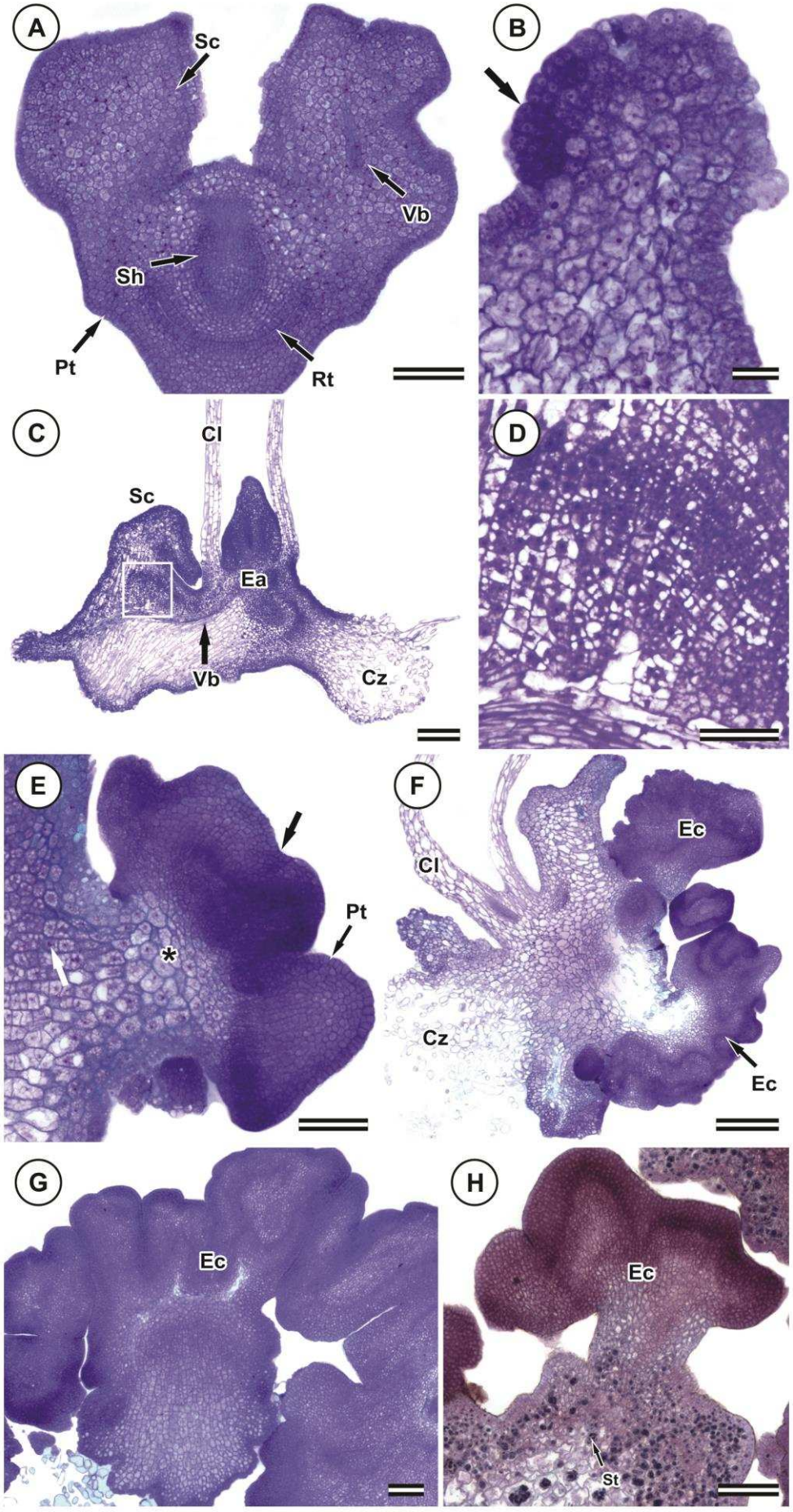
A
Sc
Vb
Sh
Pt
Rt
B
C
Cl
Sc
Ea
Vb
Cz
D
E
Pt
*
F
Ec
Cl
Cz
Ec
G
Ec
H
Ec
St

Figure 6. Histochemical analysis of *Brachypodium distachyon* immature embryos (15 days post anthesis) cultured on somatic embryogenesis induction medium. Longitudinal sections of immature scutellum from 0 to 21 days after culture (DAC) were subjected to staining with xylidine Ponceau (A, D, G, J, M, P), PAS (B, E, H, K, N, Q) and Sudan black (C, F, I, L, O, R). (**A**) Protein bodies stained red in cells of the immature scutellum at Day 0. (**B**) A positive reaction for starch at Day 0. (**C**) A negative reaction for lipids at Day 0. (**D, G, J, M, P**) Negative reaction for protein from 2-21 DAC. (**E)** Increased accumulation of starch granules at Day 2. (**H, K**) Large starch granules within vacuolated cells and deposition of small starch granules in cells of the proembryoids. (**N,** Q) Large starch granules accumulate in cells of the proembryoids. (**F, I, L, O, R**) Negative reaction for lipids from 2-21 DAC. (All bars = 25 μm).

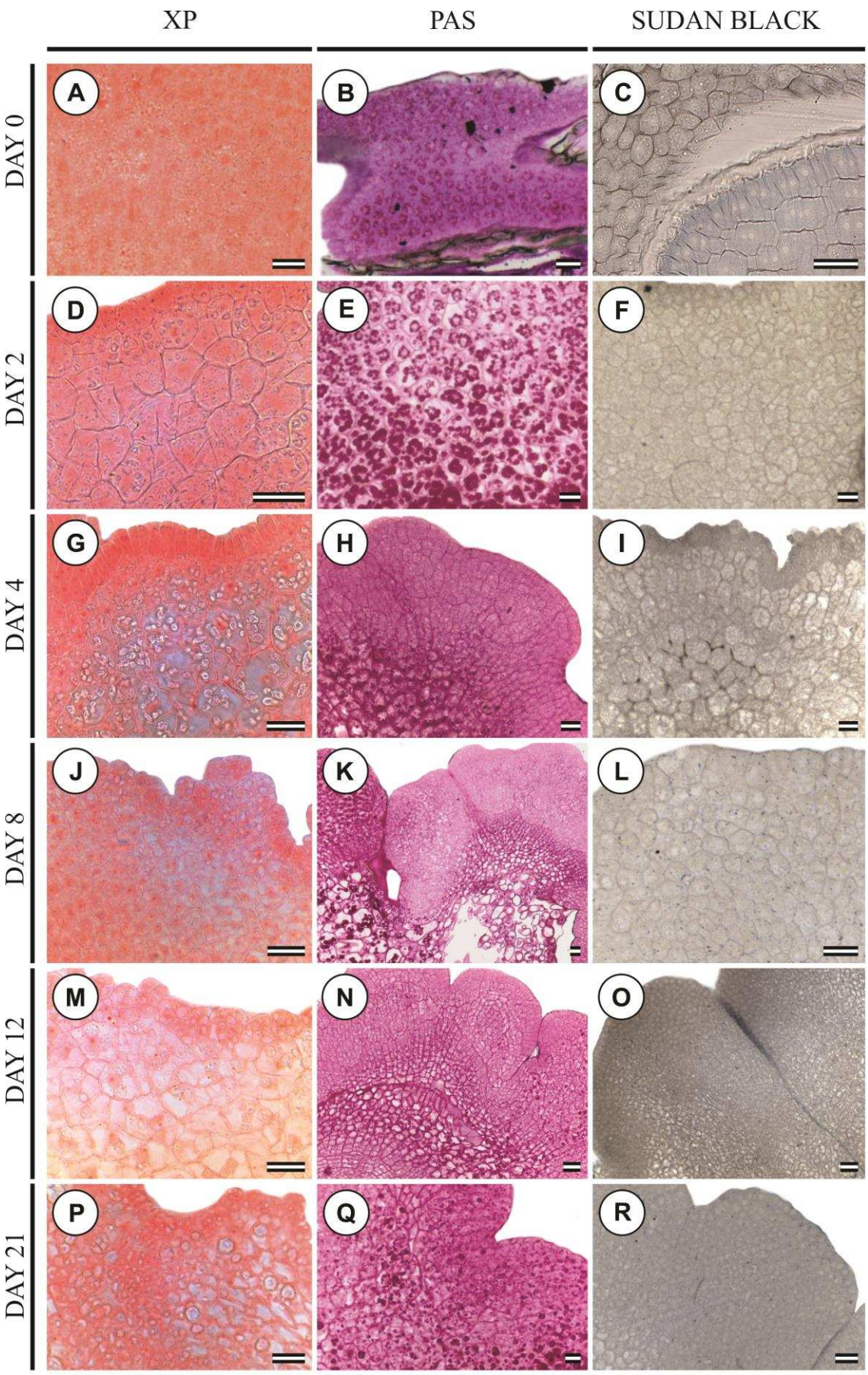
XP
PAS
SUDAN BLACK
DAY 0
DAY 2
DAY 4
DAY 8
DAY 12
DAY 21
A
B
C
D
E
F
G
H
I
J
K
L
M
N
O
P
Q
R

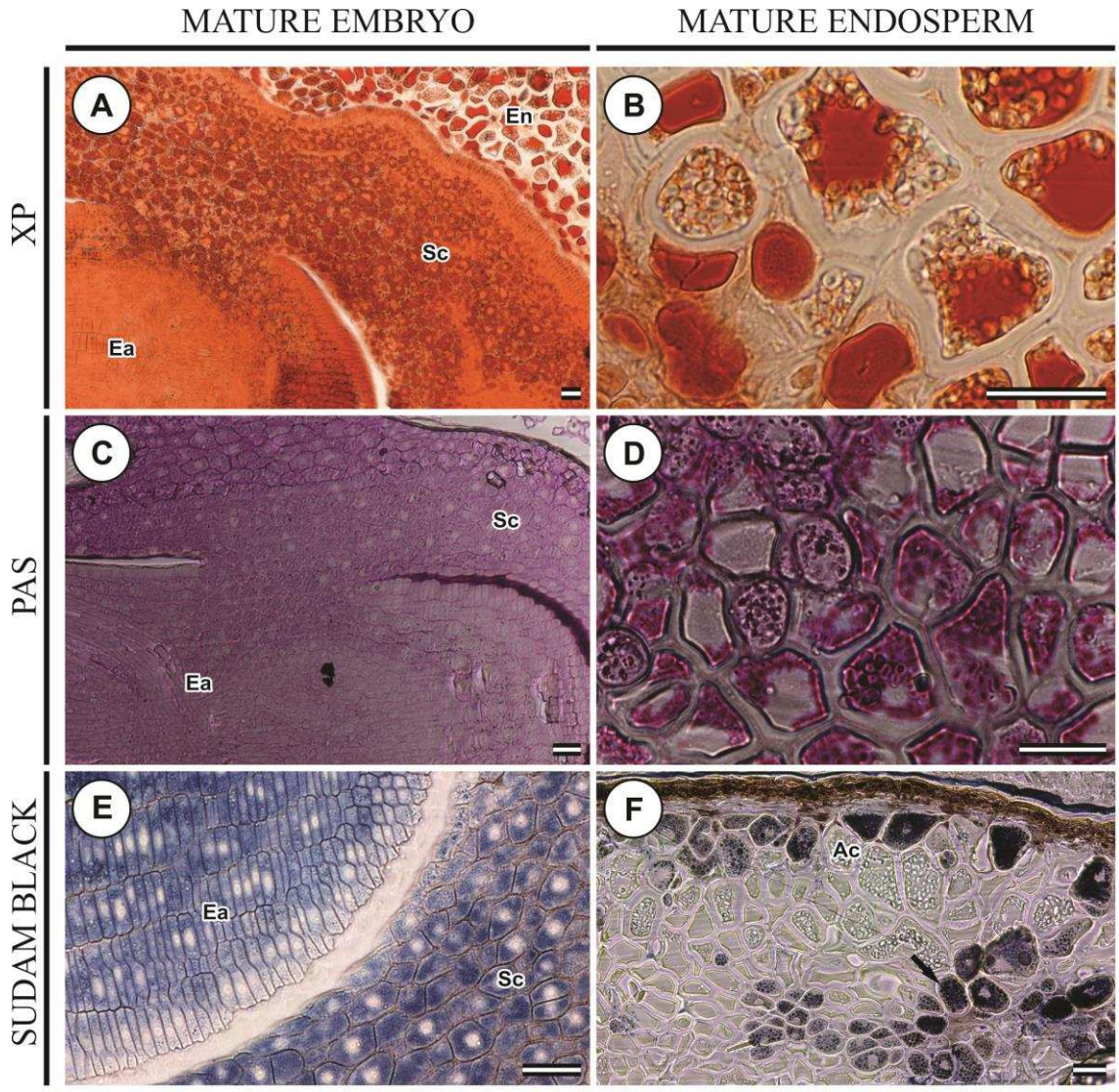

Figure 7. Histochemical analysis of *Brachypodium distachyon* mature seeds (35 days post anthesis). Longitudinal sections subjected to xylidine Ponceau (A, B), PAS (C, D) and Sudan black (E, F). (**A**) Small protein bodies stained deeply red in cells of the scutellar parenchyma, protodermal layer and coleoptile, but none in the embryo axis. (**B**) Protein is coalesced into a single mass surrounded by small starch granules in endosperm cells. (**C**) Negative reaction for starch PAS staining in the embryonic and scutellar cells. (**D**) Small even-sized starch granules concentrated around large vacuoles. (**E)** Few small oil bodies in embryonic and scutellum cells. (**F**) A positive reaction to Sudan black in aleurone cells (Ac) and some cells of the basal but not the central endosperm. (All bars = 25 μm).

DISCUSSION

This study provides morphological, histological and histochemical insights into somatic embryogenesis from immature zygotic embryos of the model plant *Brachypodium distachyon* line Bd21.

Proembryonic cells in *B. distachyon* initiated divisions at the scutellar node of immature embryos cultured in induction medium containing 2.5 mg L^{-1} of 2,4-Dichlorophenoxyacetic acid. Similarly, somatic embryos of several grass and cereal species were also obtained directly or indirectly through the proliferation of cells in the nodal region of immature embryo scutella, as reported on wheat, barley, pearl millet, maize and palisade grass (Ozias-Akins and Vasil, 1982; Oka et al., 1995; Taylor and Vasil, 1996; Al-Abed et al., 2006; Lenis-Manzano et al., 2010). The cell growth in the nodal region of *B. distachyon* immature embryo may be due to the presence of growth regulators in this region, which is in proximity to the root meristem and the procambium of the embryo axis, as it has also been suggested for pearl millet (Vasil and Vasil, 1982). In this study, the positive effect of 2,4-D in inducing meristematic cells in the scutellar node of *B. distachyon* immature embryos to proliferate and form proembryonic masses has been extensively reported for *B. distachyon* and other grass species (Vasil et al., 1985; Maeda and Radi, 1991; Bablak et al., 1995; Draper et al., 2001; Vogel et al., 2006; Hammami et al., 2011). In grasses, the scutellar epidermis functions as a haustorium for sugars and plant growth regulators dissolved in the endosperm and this could be the reason for the high metabolic activity of these cells in *B. distachyon* and the facility to dedifferentiate and give rise to embryogenic calli, as suggested by Maeda and Radi (1991) for rice.

Proembryonic cells were clearly distinguished by the double staining technique. The double staining technique was also successfully used to distinguish embryogenic cells from nonembryogenic cells in passionfruit (*Passiflora cincinnata*), sainfoin (*Onobrychis sativa*), mangosteen (*Garcinia mangostana* L.) and *Byrsonima intermedia* A. Juss. (Silva et al., 2009; Mohajer et al., 2012; Rineksane et al., 2012; Silva et al., 2012).

In the present study, somatic embryos were observed to develop from groups of embryogenic cells in the proliferating protodermal layers in the abaxial side of the *B. distachyon* immature scutellum. The proliferation of cell divisions and spread of a continuous meristematic tissue throughout the abaxial scutellar epidermis were similar

to previous reports for embryos of wheat, pearl millet, barley and durum wheat (Magnusson and Bornman, 1985; Taylor and Vasil, 1996; Nonohay et al., 1999; Fernandez et al., 1999). Williams and Maheswaran (1986) discussed the question of single- or multiple-cell origin for somatic embryos. According to these authors, in indirect somatic embryogenesis, embryoids develop from a compact clump of embryogenic cells, the proembryonal complex. The authors also stated that, in general, a unicellular origin produces embryoids attached to the parent tissue by a suspensor-like structure, whereas a multicellular origin gives rise to embryoids fused with the parent tissue over a broad area of the root pole or axis region. In this study, the *B. distachyon* somatic embryos observed were attached to the subtending callus by a broad multicellular base. The broad multicellular base connecting cells between somatic embryos and callus has been reported in several grass species (Dunstan et al., 1979; Vasil and Vasil, 1982; McCain and Hodges, 1986; Taylor and Vasil, 1996). Embryos arising directly from single cells, indicating unicellular origin, were not observed. Nevetheless, reports have shown that somatic embryos, in pearl millet for example, can arise both from multiple cells of the scutellum and also from single cells (Vasil and Vasil, 1982; Taylor and Vasil, 1996). Nonohay et al. (1999) also observed that in barley, somatic embryo could originate from a superficial callus cell, possibly indicating a unicellular origin, or from epidermal and subepidermal callus cells, representing a multicellular origin. Because the response of *B. distachyon* immature embryos to the stimulus provided by the conditions of the in vitro culture is very fast, it is possible that the first events of cell division in the scutellar node taking place during the first hours in culture have not been documented. The first divisions of single cells might also have led to formation of proembryoids. If it is the case, samples should be taken for fixation in smaller time intervals (e.g., 4-6 h) during the first 3 days of culture.

The pattern of somatic embryogenesis observed in this study such that an embryogenic callus is formed across the tissue and subsequently proembryoids are formed after the callus had developed into a typical compact callus can be considered indirect somatic embryogenesis. The number of cells involved in the formation of the nodular structures and the broad multicellular base connecting somatic embryos and callus observed in the conditions of this study possibly indicate a multicellular origin of the somatic embryos.

The chronology of the immature zygotic embryo response was similar to that previously described in barley, durum wheat (*Triticum durum* Desf.) and maize (Oka et

al., 1995; Fernandez et al., 1999; Jakubeková et al., 2011; Ślesak et al., 2013). *B. distachyon* somatic embryos had the same morphological and histological features as those of zygotic embryos described by Guillon et al. (2012). In monocots, both types of embryos develop through typical developmental stages, such as globular, scutellar and coleoptilar stages (Raghavan, 1986; Brisibe et al., 1993; Taylor and Vasil, 1996; Mariani et al., 1998; Wrobel et al., 2011). The scutellar notch that was observed in the initial scutellar stage of *B. distachyon* proembryoids was also described in pearl millet, sugarcane, barley and rice (Vasil and Vasil, 1982; Rodriguez et al., 1995; Nonohay et al., 1999; Mariani et al., 2002) as a marker of the beginning of proembryoid differentiation.

The slow division rate of the large subepidermal cells and the vacuolated scutellar ground cells indicates that region was developing into nonembryogenic callus. It has been suggested that these nonembryogenic cells may serve as a suspensor, which functions to provide nutrients to the proembryonic cell masses (Emons and Kieft, 1991; Fransz and Schel, 1991). The presence of starch detected by staining with Lugol's iodine solution and PAS reagent in these cells is in line with this hypothesis. High starch accumulation in nonembryogenic cells later in culture possibly supports the continued embryogenic callus growth and proembryoid differentiation in *B. distachyon*. Taylor and Vasil (1996) reported that nonembryogenic cells formed in pearl millet immature scutellum were ultrastructurally similar to zygotic suspensor cells and had a slower division rate than embryogenic cells.

Guillon et al. (2012) reported that protein accumulation during grain development of *B. distachyon,* Bd21-3 accession, was visible by 13 days after fertilization (DAF) reflecting the beginning of grain maturation, together with the initial differentiation of the embryo epidermis and acquisition of apico-basal symmetry. They observed storage proteins, both globulins and prolamins, by 15 days after fertilization (DAF) and considered this stage as a change in direction in protein synthesis and function from high metabolic activity to storage. Protein accumulation continue until grain maturity in the form of small protein bodies mostly located at the periphery of the endosperm cells and close to starch granules and, also, as large vacuoles filling the endosperm cell lumen. In this study, storage protein appeared coalesced, probably within the vacuole, and surrounded by starch granules in the storage endosperm of mature seeds of *B. distachyon*, corroborating the results of Guillon et al. (2012). It was also demonstrated that cells of the scutellar parenchyma of mature seeds were packed

with small protein bodies that were also present in the epithelial layer of the scutellum and the coleoptile, but in smaller amounts.

In *B. distachyon,* the weak reaction of cells of immature embryo scutellum (15 DPA) to xylidine Ponceau is in conformity with the findings of Guillon et al. (2012), where it was found that storage protein deposition increases from this stage of grain development until grain maturity. However, from 2 to 21 days of culture on induction medium, when epidermal cells of the immature scutellum were actively dividing to form the proembryonic cell masses, the test with xylidine Ponceau did not detect storage proteins. In sugarcane, Brisibe et al. (1993) reported that embryonic cells at early stages of somatic embryo differentiation also lacked storage proteins which began to accumulate only at later stages of differentiation, in the coleoptilar stage and prior to maturation. In both cases, it seems that rather than a failure of embryonic cells to synthesize and accumulate storage proteins, it could be a result of their high synthetic metabolism before maturation. This conclusion is in line with Müntz's (1987) finding that, in zygotic embryogenesis, 'the tissue-specific formation of storage proteins is under developmental control, since they are only synthesized and deposited after the mitotic activity of the respective cells ceased'.

Storage proteins were also not detected during the early phases of proembryoid formation in pearl millet, but proembryoid cells formed from the epidermal scutellar cells had abundant Golgi bodies and endoplasmic reticulum (ER), demonstrating their increased metabolic activity (Taylor and Vasil, 1996). Similarly, in maize, cells adjacent to embryogenic masses developed large amounts of ER (Fransz and Schel, 1991). Interestingly, in developing seeds of a number of cereal species, storage proteins are known to accumulate within the ER lumen of endosperm cells (Herman and Larkins, 1999; Vitale and Ceriotti, 2004). Ultrastructural studies of embryogenic callus formation in *B. distachyon* have already been initiated and will provide information on cytological features of these tissues.

Lipid storage in embryo cells, during the maturation stage of zygotic embryo development, is common in many species (Bewley and Black 1994). In *B. distachyon*, the total fatty acid content and composition were measured in dry mature grains (Guillon et al., 2012), but there is no available information on timing of oil deposition.

In this study, histochemical staining with Sudan black B confirmed lipid accumulation in cells of the embryo and scutellum of mature seeds of *B. distachyon*. Small oil bodies were also observed the aleurone layer and scattered groups of cells in

the endosperm. This result is in consonance with the finding of Neuberger et al. (2008), who used magnetic resonance-based lipid mapping to quantify lipid in barley grain. During development of barley seed, lipid deposition occurred mainly in the embryo and aleurone layer and, within the embryo, the scutellum and nodal region had a high lipid concentration. Lipids of oat grains also accumulated in the embryo and scutellum and in a lower percentage in the endosperm and the aleurone layer (Banas et al., 2007).

Light microscopic observations of sections of immature *B. distachyon* embryos stained with Sudan black B showed that at Day 0 embryonic and scutellar cells did not stain for lipids, probably because of their low concentrations. At 15 DPA, immature *B. distachyon* seeds have only reached half of their final size and content was watery to milk, which represents the first phase of grain development (Hong et al., 2011). At this stage of development, it is likely that storage lipid accumulation was still very low. Staining with Sudan black B did not detect storage lipids during the early stages of induction phase, when actively dividing cells of the scutellar epidermis were forming proembryonic masses, or later, when proembryoids were differentiating. It seems that the storage lipids in the embryogenic tissue, probably at very low concentration in the initial explant, were used up when the metabolic programs of the pro-embryogenic cells switched to support the many divisions needed to form the globular structures. Decrease in lipid content in metabolically active cells in early embryogenic callus development has been reported in other species (Brisibe et al., 1993; Taylor and Vasil, 1996; Rocha et al., 2012; Correia et al., 2012).

In seeds, lipids stored in oil bodies are converted to starch during germination. This process involves the conversion of triacylglycerides into glycerol and free fatty acids that are moved to the glyoxysome and converted into succinate and malate in the glyoxylate cycle, and then reverse glycolysis to produce sucrose for use by the developing embryo (Graham, 2008). The histochemical findings described in this study seem to indicate that embryonic cells at early stages of somatic embryo differentiation in *B. distachyon* lack storage lipids, which presumably begin to accumulate later in embryoid development. Nevertheless, ultrastructural studies on embryogenic callus cells of *B. distachyon* are in progress to give insight on the subcellular organization of these tissues.

Starch is the most important storage material for energy and carbon source in plants (Asatsuma et al., 2005). Guillon et al. (2012) reported that during grain development of *B. distachyon* starch accumulation in the endosperm started about 14

DAF and increased slowly until the completion of maturation. By contrast, in the embryo, the concentration of starch decreased sharply between 10 and 14 DAF and then slowly decreased to almost non-detectable levels at maturation. In this study, sections of mature seeds of *B. distachyon* stained with periodic acid-Schiff (PAS) confirmed the presence of starch granules in vacuolated cells of the storage endosperm and the lack of starch in the embryonic tissues. The light microscopy examinations also showed that cells of the mature endosperm have very thick cell walls. Recent reports have shown that (1-3)(1-4)-b-D glucan, a cell wall polysaccharide, accumulates in the endosperm of *B. distachyon* mature grains, accounting for most of the increase in cell wall thickness (Opanowicz et al., 2011; Guillon et al., 2011).

Staining with PAS reagent revealed numerous starch granules in scutellar cells of immature zygotic embryos at Day 0. This result is also in agreement with the report of Guillon et al. (2012), in which starch grains were observed in zygotic embryo cells at the early stages of grain development.

In the endosperm of germinating cereal seeds, α-amylases secreted from the scutellar epithelium and the aleurone layer degrade reserve starch by hydrolysis producing glucose, maltose and limited dextrin (Smith et al., 2005). Embryogenesis is a high-energy-requiring process and the catabolism of glycolytic intermediates produced in the starch degradation yield high amounts of ATP (Martin et al., 2000) that can be used by cellular metabolism during proembryoid development. The high accumulation of starch in scutellar cells of *B. distachyon* observed in the first 2 days of culture was followed by a decrease in number of granules in the vacuolated cells subtending the proembryonic masses and, then, a subsequent de novo accumulation in the inner parts of these masses later in culture. This repetitive cycle of starch accumulation/mobilization reflected the continued growth of the embryogenic callus and proembryoid differentiation in the induction medium. It also suggests that starch is used both during embryogenic callus initiation and later in its development into proembryoids. The starch deposition observed in proembryoids of *B. distachyon* has also been reported for maize, orchardgrass, sugarcane and pearl millet (Gray *et al.*, 1984; Vasil et al., 1985; Fransz and Schel, 1991; Brisibe et al., 1993; Taylor and Vasil, 1996).

Based on ultrastructural evidence, Rocha et al. (2012) proposed that the synthesis of starch in the initial stages of somatic embryogenesis of *Passiflora cincinnata* from mature zygotic embryos was directly linked to lipid mobilization via the glyoxilate cycle because the appearance of starch granules coincided with the

reduction in lipids, as well as the presence of lipid bodies close to glyoxysomes. Otherwise, it has also been suggested that high levels of carbohydrate accumulation in somatic embryos is due to the uptake and metabolism of carbon supplied in the culture medium (Hara et al., 1985; Horbowicz et al., 1995; Santa Catarina et al., 2003; Pinto et al., 2010). In this study, lipids were not detected during the stages of induction and proembryoid formation, probably because of their low concentration, however, ultrastructural examination will help identify if there is such an association occurring in *B. distachyon* embryogenic cultures.

Brachypodium distachyon has a high potential as a small rapid cycling model for investigating numerous aspects of grass biology. According to information available in the literature, this study is the first to provide a morphological, histological and histochemical description of *Brachypodium distachyon* somatic embryogenesis from immature zygotic embryos in the reference line Bd21. The morphohistochemical analysis presented in this study makes important contribution to the understanding of the process of acquisition of embryogenic competence and development of somatic embryos in *B. distachyon*.

REFERENCES

AL-ABED D., RUDRABHATLA S., TALLA R., GOLDMAN S. Split-seed: a new tool for maize researchers. **Planta**, v. 223, p. 1355–1360, 2006.

ASATSUMA S., SAWADA C., ITOH K., OKITO M., KITAJIMA A., MITSUI T. Involvement of α-amylase I-1 in starch degradation in rice chloroplasts. **Plant Cell Physiology**, v. 46, n. 6, p. 858–869, 2005.

BABLAK P., DRAPER J., DAVEY M. R., LYNCH P. T. Plant regeneration and micropropagation of *Brachypodium distachyon*. **Plant Cell Tissue Organ Culture**, v. 42, p. 97–107, 1995.

BANAS A., DEBSKI H., BANAS W., HENEEN W. K., DAHLQVIST A., BAFOR M., GUMMESON P-O., MARTTILA S., EKMAN A., ANDERS S. CARLSSON A. S., STYMNE S. Lipids in grain tissues of oat (Avena sativa): differences in content, time of deposition, and fatty acid composition. **Journal of Experimental Botany**, v. 58, n. 10, p. 2463-2470, 2007.

BEWLEY J. D., BLACK M. Seeds: physiology of development and germination. Plenum, London, 1994.

BRISIBE, E. A., NISHIOKA D., H. MIYAKE H., TANIGUCHI T., MAEDA E. Developmental electron microscopy and histochemistry of somatic embryo differentiation in sugarcane. **Plant Science**, v. 89, p. 85- 92, 1993.

BRKLJACIC J., GROTEWOLD E., SCHOLL R., MOCKLER T., GARVIN D.F., VAIN P., BRUTNELL T., SIBOUT R., BEVAN M., BUDAK H., CAICEDO A. L., GAO C., GU Y., HAZEN S.P., HOLT III B.F., HONG S.-Y., JORDAN M., MANZANEDA A.J., MITCHELL-OLDS T., MOCHIDA K., MUR L.A.J., PARK C.-M., SEDBROOK J., WATT M., ZHENG S.J., VOGEL J.P. *Brachypodium* as a model for the grasses: today and the future. **Plant Physiology**, v. 157, p. 3–13, 2011.

CORREIA S., ESTEFANIA CUNHA A. E., SALGUEIRO L., CANHOTO J. M. Somatic embryogenesis in tamarillo (*Cyphomandra betacea*): approaches to increase efficiency of embryo formation and plant development. **Plant Cell Tissue and Organ Culture**, v. 109, p. 143–152, 2012.

DRAPER J., MUR L. A. J., JENKINS G., GHOSH-BISWAS G. C., BABLAK P., HASTEROK R., ROUTLEDGE A. P. M. *Brachypodium distachyon*. A new model system for functional genomics in grasses. **Plant Physiology**, v. 127, p. 1539–1555, 2001.

DUNSTAN D. I., SHORT K. C., DHALIWAL H., THOMAS E. Further studies on plantlet production from cultured tissues of *Sorghum bicolor*. **Protoplasma**, v. 101, p. 355-361, 1979.

DURZAN D. J. **Process control in somatic polyembryogenesis**, in J.E. Hallgren, Proceeding of Frans Symposium Department of Forest Genetics and Plant Physiology. Swedish University of Agricultural Sciences, v. 8, p. 147-186, 1988.

EMONS A. M. C., KIEF H. 1991. Histological comparison of single somatic embryos of maize from suspension culture with somatic embryos attached to callus cells. **Plant Cell Reports**, v. 10, p. 485- 488, 1991.

FERNANDEZ F., MICHAUX-FERRIÈRE N., COUMANS M. The embryogenic response of immature embryo cultures of durum wheat (*Triticum durum* Desf.): histology and improvement by $AgNO_3$. **Plant Growth Regulation**, v. 28, p. 147–155, 1999.

FEHÉR A., PASTERNAK T. P., DUDITS D. Transition of somatic plant cells to an embryogenic state. **Plant Cell, Tissue and Organ Culture**, v. 74, p. 201–228, 2003.

FEDER N., O'BRIEN T. P. Plant microtechnique: some principles and new methods. **American Journal of Botany**, v. 55, p.123–142, 1968.

FORTES A. M., PAIS M. S. Organogenesis from internode-derived nodules of *Humulus lupulus* var. Nugget (Cannabinaceae): histological studies and changes in the starch content. **American Journal of Botany**, v. 87, n.7, p. 971–979, 2000.

FRANSZ P. F, SCHEL J. H. N. 1991. Cytodifferentiation during the development of friable embryogenic callus of maize (*Zea mays*). **Canadian Journal of Botany**, v. 69, p. 26-33, 1991.

GRAHAM I. A. Seed storage oil mobilization. **Annual Review of Plant Biology**, v. 59, p. 115 -142, 2008.

GRAY D. J., CONGER B. V, HANNING, G.F. Somatic embryogenesis in suspension and suspension-derived callus cultures of *Dactylis glomerata*. **Protoplasma**, v. 122, p. 196-202, 1984.

GUILLON F., BOUCHET B., JAMME F., ROBERT P., QUEMENER B., BARRON C., LARRE C., DUMAS P., SAULNIER L. *Brachypodium distachyon* grain: characterization of endosperm cell walls. **Journal of Experimental Botany**, v. 62, p. 1001–1015, 2011.

GUILLON F., LARRE C., PETIPAS F., BERGER A., MOUSSAWI J., ROGNIAUX H. A comprehensive overview of grain development in *Brachypodium distachyon* variety Bd21. **Journal of Experimental Botany**, v. 63, p. 739–755, 2012.

HAMMAMI R., CUADRADO A., FRIERO E., JOUVE N., SOLER C., GONZÁLEZ J.M. Callus induction and plant regeneration from immature embryos of *Brachypodium distachyon* with different chromosome numbers. **Biologia Plantarum**, v. 55, n. 4, p. 797-800, 2011.

HARA S., FALK H., KLEINIG H. Starch and triacylglycerol metabolism related to somatic embryogenesis in *Papaver orientale* tissue cultures . **Planta**, v. 164, p. 303-307, 1985.

HERMAN E.M., LARKINS B.A. Protein storage bodies and vacuoles. **Plant Cell**, v. 11, p. 601–614, 1999.

HONG S.Y., PARK J.H., CHO S.H., YANG M.S., PARK C.M. Phenological growth stages of *Brachypodium distachyon*: codification and description. **Weed Research**, v. 51, p. 612–620, 2011.

HORBOWICZ M., OBENDORF R.L., MCKERSIE D., VIANDS D.R. Soluble saccharides and cyclitols in alfafa (*Medicago sativa* L.) somatic embryos, leaflets and mature seeds. **Plant Scence**, v. 109, p. 191-198, 1995.

JAIN S.M., GUPTA P.K. **Protocol for Somatic Embryogenesis in Woody Plants.** Springer, Netherland. p. 585, 2005.

JAKUBEKOVÁ M., PREŤOVÁ A., OBERT B. Somatic embryogenesis and plant regeneration from immature embryo induced callus of maize (*Zea mays* L.) **Journal of Microbiology, Biotechnology and Food Sciences**, v. 1, n. 4, p. 478-487, 2011.

KARNOVSKY M. J. A formaldehyde-glutaraldehyde fixative of high osmolality for use in electron microscopy. **Journal of Cell Biology**, v. 27, p. 137–138, 1965.

KURCZYNSKA E. U., POTOCKA I., DOBROWOLSKA I., KULINSKA-LUKASZEK K., SALA K., WROBEL J. Cellular Markers for Somatic Embryogenesis, Embryogenesis. SATO, K.-I. (Eds.), 2012 InTech, Available from: http://www.intechopen.com/books/embryogenesis/cellularmarkers-for-somatic-embryogenesis

LARRÉ C., PENNINCK S., BOUCHET B., LOLLIER V., TRANQUET O., DENERY-PAPINI S., GUILLON F., ROGNIAUX H. *Brachypodium distachyon* grain: identification and subcellular localization of storage proteins. **Journal of Experimental Botany**, v. 61, p. 1771–1783, 2010.

LENIS-MANZANO S.J., ARAUJO A.C.G., VALLE C.B., SANTANA E.F., CARNEIRO V.T.C. Histologia da embriogênese somática induzida em embriões de

sementes maduras de *Urochloa brizantha* apomítica. **Pesquisa Agropecuária Brasileira**, v. 45, n. 5, p. 435-441, 2010.

MAEDA E., RADI S.H. Ultrastructural aspects of rice scutellum as related to seminal root cultures. **Biotechnology in Agriculture and Forestry (Rice)**, v. 14, p. 78-91, 1991.

MAGNUSSON, I., BORNMAN C. H. Anatomical observations on somatic embryogenesis from scutellar tissues of immature zygotic embryos of *Triticum aestivum*. **Physiologia Plantarum**, v. 63, p. 137-145, 1985.

MARIANI T.S., MIYAKE H., TAKEOKA Y. Changes in surface structure during direct somatic embryogenesis in rice scutellum observed by scanning electron microscopy. **Plant Production Science**, v. 1, n. 3, p. 223-231, 1998.

MARIANI T.S., MIYAKE H., TAKEOKA Y. Direct somatic embryogenesis in rice (*Oryza sativa* L.): Structural and developmental patterns. **Journal Matematika dan Sains** v. 7, n. 2, p. 53 – 56, 2002.

MARTIN A. B., CUADRADO Y., GUERRA H., GALLEGO P., HITA O., MARTIN L., DORADO A., VILLALOBOS N. Differences in the contents of total sugars, reducing sugars, starch and sucrose in embryogenic and non-embryogenic calli from *Medicago arborea* L. **Plant Science**, v. 29, n. 154(2), p. 143-151, 2000.

McCAIN, J. W., HODGES T. K. Anatomy of somatic embryos from maize embryo cultures. **Botanical Gazette,** v. 147, p. 453-460, 1986.

MOHAJER S., TAHA R. M., KHORASANI A., YAACOB J. S. Induction of different types of callus and somatic embryogenesis in various explants of Sainfoin (*Onobrychis sativa*). **Australian Journal of Crop Science**, v. 6, n. 8, p. 1305-1313, 2012.

MOURA E. F., VENTRELLA M. C., MOTOIKE S. Y. Anatomy, histochemistry and ultrastructure of seed and somatic embryo of *Acrocomia aculeata* (Arecaceae). **Scientia Agricola**, v. 67, p. 399–407, 2010.

MÜNTZ K. Developmental control of storage protein formation and its modulation by some internal and external factors during embryogenesis in plant seeds. **Biochemie und Physiologie der Pflanzen**, v. 182, p. 93-116, 1987.

MURASHIGE T., SKOOG F. A revised medium for rapid growth and bio assays with tobacco tissue cultures. **Physiologia Plantarum**, v. 15, p. 473–497, 1962.

NAMASIVAYAM, P. Acquisition of embryogenic competence during somatic embryogenesis. **Plant Cell, Tissue and Organ Culture**, v. 90, n. 1, p. 1-8, 2007.

NEUBERGER T, SREENIVASULU N, ROKITTA M, ROLLETSCHEK H, GOBEL C, RUTTEN T, RADCHUK V, FEUSSNER I, WOBUS U, JAKOB P. Quantitative imaging of oil storage in developing crop seeds. **Plant Biotechnology Journal**, v. 6, p. 31–45, 2008.

NONOHAY J.S., MARIATH J.E.A., WINGE H. Histological analysis of somatic embryogenesis in Brazilian cultivars of barley, *Hordeum vulgare vulgare*, Poaceae. **Plant Cell Reports**, v. 18, p. 929–934, 1999.

O'BRIEN T. P., McCULLY M. E. **The study of plant structure principles and selected methods**. Termarcarphi Pty, Melbourne, 1981.

OKA S., SAITO N., KAWAGUCHI H., Histological observations on initiation and morphogenesis in immature and mature embryo derived callu of barley (*Hordeum vulgare L.*). **Annals of Botany**, v. 76, p. 487-492, 1995.

OPANOWICZ M., VAIN P., DRAPER J., PARKER D., DOONAN J.H., DREA S. *Brachypodium distachyon*: making hay with a wild grass. **Trends in Plant Science**, v. 13, p. 172–177, 2008.

OPANOWICZ M. HANDS P., BETTS D., PARKER M. L., TOOLE G. A., CLARE MILLS E. N., DOONAN J. H., SINE'AD D. Endosperm development in *Brachypodium distachyon*. **Journal of Experimental Botany**, v. 62, p. 735–748, 2011.

OZIAS-AKINS P., VASIL I.K.. Plant regeneration from cultured immature embryos and inflorescences of *Triticum aestivum* L. (wheat): evidence for somatic embryogenesis. **Protoplasma**, v. 110, p. 95–105, 1982.

PAN X., YANG X., LIN G., ZOU R., CHEN H., SAMAJ J., XU C. Ultrastructural changes and the distribution of arabinogalactan proteins during somatic embryogenesis of banana (*Musa* spp. AAA cv. 'Yueyoukang 1'). **Physiologia Plantarum**, v. 142, p. 372–389, 2011.

PINTO G., SILVA S., ARAÚJO C., NEVES L., SANTOS C. Histocytological changes and reserves accumulation during somatic embryogenesis in *Eucalyptus globulus*. **Trees**, v. 24, p. 763–769, 2010.

QUIROZ-FIGUEROA F.R., ROJAS-HERRERA R., GALAZ-AVALOS R.M., LOYOLA-VARGAS V.M. Embryo production through somatic embryogenesis can be used to study cell differentiation in plants. **Plant Cell, Tissue Organ Culture**, v. 86, p. 285–301, 2006.

RAGHAVAN V. **Embryogenesis in angiosperms: a developmental and experimental study.** Cambridge University Press, Cambridge, p. 15–35, 1986.

RINEKSANE I.A., KADIR M.A., KADZIMIN S., ZAMAN F.Q. In vitro development of embryogenic calli and embryogenic stages in suspension cultures of mangosteen (*Garcinia mangostana* L.). **Journal of Medicinal Plants Research**, v. 6, n. 13, p. 2549-2559, 2012.

ROCHA D.I., VIEIRA L.M., TANAKA F.A.O., DA SILVA L.C., OTONI W.C. Somatic embryogenesis of a wild passion fruit species *Passiflora cincinnata* Masters: histocytological and histochemical evidences. **Protoplasma**, v. 249, n. 3, p. 747-758, 2012.

RODRIGUEZ S., MONDEJAR C., RAMOS M.E., DIAZ E., MARIBONA R., ANCHETA O., Sugarcane somatic embryogenesis: a scanning electron microscopy study. **Tissue and Cell**, v. 28, p. 149-154, 1995.

SANTA CATARINA C., RANDI, A. M., VIANA, A. M. Growth and accumulation of storage reserves by somatic embryos of *Ocotea catharinensis* Mez. (Lauraceae). **Plant Cell, Tissue and Organ Culture**, v. 74: p.67–71, 2003.

ŚLESAK H., GÓRALSKI G., PAWŁOWSKA H., SKUCIŃSKA B., POPIELARSKA–KONIECZNA M., JOACHIMIAK A.J. The effect of genotype on a barley scutella culture. Histological aspects. **Central European Journal of Biology**, v. 8, n. 1, p. 30-37, 2013.

SILVA M.L., PAIM-PINTO D.L., GUERRA M.P, FLOH E.I.S., BRUCKNER C.H., OTONI W.C. A novel regeneration system for wild passion fruit species (*Passiflora cincinnata* Mast.) based on somatic embryogenesis from mature zygotic embryos. **Plant Cell, Tissue and Organ Culture**, v. 99, p. 47-54, 2009.

SILVA L.C., PAIVA R., SILVA D.P.C., BARBOSA S., HERRERA R.C., DAVIDE L.C., PAIVA P.D.O. Characterization of pro-embryogenic calli and somatic embryogenesis of *Byrsonima intermedia* A. Juss. **Journal of Agricultural Science and Technology**, v. A 2, p. 962-970, 2012.

SMITH A. M., ZEEMAN S. C., SMITH S. M. Starch degradation. **Annual Review of Plant Biology**, v. 56, p. 73–98, 2005.

SUGIMOTO K., GORDON S. P., MEYEROWITZ E.M. Regeneration in plants and animals: dedifferentiation, transdifferentiation, or just differentiation? **Trends in Cell Biology**, v. 21, n. 4, p. 213-218, 2011.

TAYLOR M.G., VASIL I.K. The ultrastructure of somatic embryo development in pearl millet (*Pennisetum glaucum*; Poaceae). **American Journal of Botany**, v. 83, n. 1, p. 28-44, 1996.

VAIN P. *Brachypodium* as a model system for grass research. **Journal of Cereal science**, v. 54, p. 1-7, 2011.

VASIL V., LU C., VASIL I. K. Histology of somatic embryogenesis in cultured immature embryos of maize (*Zea mays* L.). **Protoplasma**, v. 127, p. 1-8, 1985.

VASIL V., VASIL I.K. The ontogeny of somatic embryos of *Pennisetum americanum* (L.) K. Schum. I. In cultured immature embryos. **Botanical Gazette**, v. 143, n. 4, p. 454-465, 1982.

VEGA R., VÁSQUEZ N., ESPINOZA A.M., GATICA A.M., VALDEZ-MELARA M. Histology of somatic embryogenesis in rice (*Oryza sativa* cv. 5272) **Revista de Biología Tropical**, v. 57 (Suppl. 1), p. 141-150, 2009.

VERDEIL, J.L., ALEMANNO, L., NIEMENAK, N., TRAMBARGER, T.J. Pluripotent versus totipotent plant stem cells: dependence versus autonomy? **Trends in Plant Science**, v. 12, n. 6, p. 245-252, 2007.

VIDAL B. C. Acid glycosaminoglycans and endochondral ossification microespectrophotometric evaluation and macromolecular orientation. **Cellular and Molecular Biology**, v. 22, p. 45–64, 1977.

VITALE A., CERIOTTI A. Protein quality control mechanisms and Potein storage in the endoplasmic reticulum. A conflict of interests? **Plant Physiology**, v. 136, p. 3420–3426, 2004.

VOGEL J. P., GARVIN, D. F., LEONG, O. M., HAYDEN, D. M. *Agrobacterium*-mediated transformation and inbred line development in the model grass *Brachypodium distachyon*. **Plant Cell, Tissue and Organ Culture**, v. 84, p. 199–211, 2006.

VOGEL J., BRAGG J. *Brachypodium distachyon*, a New Model for the Triticeae. Genetics and Genomics of the Triticeae. **Plant Genetics and Genomics: Crops and Models**, v. 7, p. 427-449, 2009.

VON ARNOLD S., SABALA I., BOZHKOV P., DYACHOK J., FILONOVA L. Developmental pathways of somatic embryogenesis. **Plant Cell, Tissue and Organ Culture**, v. 69, p. 233–249, 2002.

WILLIAMS E. G., MAHESWARAN G. Somatic embryogenesis: factors influencing coordinated behavior of cell as an embryogenic group. **Annals of Botany**, v. 57: p. 443–462, 1986.

WROBEL J., BARLOW P.W., GORKA K., NABIALKOWSKA D., KURCZYNSKA E.U. Histology and symplasmic tracer distribution during development of barley androgenic embryos. **Planta**, v. 233, p. 873–881, 2011.

YE X.-G., TAO L.-L. Research outline on some characteristics of *Brachypodium distachyon* as a new model plant species. **Acta Agronomica Sinica**, v. 34, n. 6, p. 919–925, 2008.

CHAPTER 2

SOMATIC EMBRYOGENESIS IN *Brachypodium distachyon*: DYNAMICS OF *SERK* GENE EXPRESSION.

ABSTRACT

The wild grass species *Brachypodium distachyon* (L.) P. Beauv. has been proposed as a new model for temperate grasses because of its small genome and its phylogenetic position close to economically important cereal crops and several potential biofuel grasses. It also has important attributes for a model plant such as a short life cycle, self-fertility, many diploid accessions, and simple growth requirements. Increasing interest in *Brachypodium distachyon* inbred line Bd21 has led to the development of a series of genomics resources, including a fully sequenced and assembled genome and somatic embryogenesis-based transformation protocols. Somatic embryogenesis plays a primary role in plant regeneration, involving differential gene expression and various signal transduction pathways. One of the genes identified in early somatic embryogenesis is *SOMATIC EMBRYOGENESIS RECEPTOR-LIKE KINASE* (*SERK*). In this study, using degenerate primers, it was possible to amplify a specific homologous sequence of a *SERK* gene fragment from *B. distachyon* Bd21. Sequence analysis of this fragment (766 bp) revealed high levels of similarity to other reported *SERK*s. Somatic embryogenic cultures of *B. distachyon* (Bd21) were established following culture of immature zygotic embryos (IZE) on Murashige and Skoog (1962) medium containing 2,4-dichlorophenoxyacetic acid. In situ hybridization analysis showed that the amplified *SERK* fragment was present in tissues of the endosperm and embryo axis of the immature seed, in embryogenic tissues before somatic embryo development and continued expressing through globular and scutellar stages. These results suggest that *SERK* expression was associated with induction of somatic embryogenesis and could serve as a molecular marker to monitor the transition of IZE tissues into competent and embryogenic cells in *B. distachyon* line Bd21.

Key words: *Brachypodium distachyon*. *SOMATIC EMBRYOGENESIS RECEPTOR-LIKE KINASE* (*SERK*). *In situ* hybridization.

EMBRIOGÊNESE SOMÁTICA EM *Brachypodium distachyon*: DINÂMICA DA EXPRESSÃO DO GENE *SERK*.

RESUMO

A espécie *Brachypodium distachyon* (L.) P. Beauv. foi proposta como uma planta modelo para gramíneas de clima temperado devido ao seu pequeno genoma e a sua proximidade filogenética de cereais economicamente importantes e várias gramíneas com potencial biocombustível. Além disso, *B. distachyon* tem um ciclo de vida curto, autogamia, muitos acessos diplóides e requisitos de crescimento simples. O interesse crescente na linhagem *B. distachyon* BD21 levou ao desenvolvimento de uma série de recursos da genômica, incluindo um genoma completamente sequenciado e montado e eficientes protocolos de transformação baseados em embriogénese somática. A embriogênese somática desempenha um papel fundamental na regeneração de plantas, envolvendo a expressão diferencial de genes e várias vias de transdução de sinal. Um dos genes identificados no início de embriogênese somática é o gene *SERK* (*Somatic Embryogenesis Receptor-Like Kinase*). Neste estudo, utilizando iniciadores degenerados, uma sequência específica homóloga de um fragmento do gene *SERK* foi amplificada de *B. distachyon* Bd21. A análise da seqüência do fragmento de *SERK* (766 bp) revelou altos níveis de similaridade com *SERKs* relatados em outras espécies. Culturas embriogênicas de *B. distachyon* (BD21) foram estabelecidas usando IZE 15 dias após a antese, em meio Murashige e Skoog (1962) contendo ácido 2,4-diclorofenoxiacético. A análise de hibridização *in situ* mostrou que o fragmento *SERK* de *B. distachyon* estava presente nos tecidos embriogênicos antes do desenvolvimento de embriões somáticos e continuou sendo expresso através dos estágios globular e escutelar. Estes resultados sugerem que a expressão do fragmento *SERK* de *B. distachyon* pode estar associada com a indução da embriogênese somática, podendo servir como um marcador molecular para monitorar a transição de células somáticas em células competentes e embriogênicas em *B. distachyon* linhagem BD21.

Palavras-chave: *Brachypodium distachyon*, gene *Somatic Embryogenesis Receptor-Like Kinase*, hibridação *in situ*.

INTRODUCTION

Brachypodium distachyon (L.) Beauv is an annual temperate grass native to the Mediterranean and Middle East and is a member of the Pooideae subfamily (Catalán et al., 2012)**.** This group also contains cereal and forage grasses including the economically important species *Triticum aestivum* (bread wheat), *Hordeum vulgare* (barley), and *Avena sativa* (oats).

Brachypodium distachyon is self-fertile and has a short generation time, small size and simple growth requirements (Draper et al., 2001; Bevan et al., 2010). *B. distachyon* line Bd21 is the first member of the Pooideae subfamily to have its genome sequenced and assembled, a compact 272 Mbp diploid genome (2n = 10) (Bevan et al., 2010; IBI, 2010). These attributes and similarities in gene content and gene family structure between *B.distachyon*, wheat, rice and sorghum have led to the rapid adoption of *B.distachyon* as a model system to study functional genomics and specific traits for crop improvement in all grasses, cereals, and biofuel monocotyledonous crops (Draper et al., 2001; Brkljacic et al., 2011).

In the last decade, *B. distachyon* research programs have gathered an extensive core of highly sophisticated genomic resources such as efficient transformation methods, EST collections, BAC libraries, genetic linkage maps, and segregating populations (Bevan et al., 2010). However, despite these considerable advances, there is a surprising lack of studies on the molecular mechanisms that underlie the transition of cells from somatic to embryogenic state and regeneration of plants.

During somatic embryogenesis, biochemical and morphological changes occur throughout the development of induced tissues, which is closely related to alterations in gene expression (Fehér, 2003). The *Somatic Embryogenesis Receptor Kinase* (*SERK*) gene is among the genes involved in the induction of somatic embryogenesis and has been used as a molecular marker to monitor the transition from tissue to callus and embryogenic cells (Schmidt et al., 1997; Somleva et al., 2000). SERK is a leucine-rich repeat (LRR) transmembrane protein kinase that enhances the ability of the apical meristem in *Arabidopsis* to form somatic embryos (Hecht et al., 2001). LRR kinases transmit their signal by forming homodimers or heterodimers with other receptor-like kinases (RLKs), in response to binding by a ligand. This ligand-induced dimerization causes phosphorylation of the intracellular kinase domains of the RLKs, which activates the next stages of the signal transduction pathway (Nolan et al., 2009).

Of all the genes that have been isolated during somatic embryogenesis, only *SERK* has successfully been shown to be a specific marker distinguishing individual embryo-forming cells in carrot suspension cultures (Schmidt et al. 1997). The *SERK* gene was found to be expressed during proembryogenic mass formation and up to the globular stage during carrot somatic embryogenesis (Schmidt et al. 1997). It could also be detected in zygotic embryos up to the early globular stage, but not in unpollinated flowers or any other tissue. Cell tracking experiments using a *SERK* promoter::luciferase reporter construct verified that somatic embryos were indeed derived from *SERK* expressing cells (Schmidt et al. 1997).

Later, an *Arabidopsis thaliana* homologue (*AtSERK1*) of the carrot *SERK*, cDNA was cloned as one of the five members of a small gene family (Hecht et al. 2001). The *AtSERK1* was shown to be expressed in developing ovules by *in situ* hybridisation (Hecht et al. 2001). In mature ovules, expression was restricted to the embryo sac where it was expressed in all cells. Following fertilization, *AtSERK1* was expressed in the endosperm and the zygote, and in embryos through the heart stage, at which time expression ceased. A low level of expression was also detected in adult vascular tissues.

AtSERK1 gene expression was also observed in the shoot apical meristem (SAM) and cotyledons of *Arabidopsis* seedlings treated with auxin. These are the sites at which embryogenic callus emerges in *Arabidopsis* (Mordhorst et al. 1998; von Recklinghausen et al. 2000). These observations indicated that *AtSERK1* expression was not restricted to embryogenic cells, but was characteristic of those cells capable of responding to hormone signals and competent to form somatic embryos or embryogenic cell cultures (Hecht et al. 2001). Ectopic expression of *AtSERK1* under control of the strong constitutive 35S promoter (35S::*AtSERK1*) showed that the frequency of the initiation of somatic embryos was increased by approximately 4-fold in transgenic seedlings (Hecht et al. 2001), implying that *AtSERK1* increases embryogenic competence.

Homologues of the *SERK* gene were also isolated from *Zea mays* (Baudino et al. 2001), *Poa pratensis* (Albertini et al. 2005), *Oryza sativa* (Hu et al. 2005), *Triticum aestivum* (Singla et al. 2008), *Musa acuminata* (Huang et al. 2009), *Brachiaria* spp (Koehler, 2010) and *Secale cereale* L.(Gruszczyńska et al., 2011).

Great success has been achieved in *B. distachyon* transformation studies, in which somatic embryogenesis is used for plant regeneration. However, although

important, the investigation of *SERK* gene expression as a potential marker for distinguishing competent cells to form somatic embryos *in vitro* has not been approached to study somatic embryogenesis in *B. distachyon*.

In this study, for the first time a *B. distachyon SERK* gene fragment (*SERK1*) was isolated and its expression in somatic embryogenesis induction was analyzed using *in situ* hybridization for monitoring the morphogenetic processes *in vitro*. The findings of this study will serve as a foundation for future research on the function of the *SERK* gene family in *B. distachyon*. These results also show that *B. distachyon* provides a useful model system for investigating the genetic regulation of somatic embryogenesis in grass species.

MATERIALS AND METHODS

Production of compact embryogenic callus (CEC) and histological sections for detailed observation of tissue development were obtained as described in the section Materials and Methods of Chapter 1.

Extraction of RNA from embryogenic callus

Total RNA was extracted from 6-week-old embryogenic callus culture (CEC) using the TRIZOL® Reagent (Invitrogen) according to the manufacturer's recommendations. The samples (500 mg) were macerated with 500 µL TRIZOL® in 1.5 mL Eppendorf tubes. The mixture of chloroform and isoamyl alcohol (24:1 v/v) was added to each microtube. Then, samples were homogenized in a vortex and incubated on ice for 5 min and centrifuged at 12,000 rpm for 15 min at 4 °C. After centrifugation, the aqueous phase was collected and placed into new tubes, an equal volume of isopropanol was added to precipitate RNA, and incubated for two hours at -20 °C. The material was centrifuged for 30 min at 13,000 rpm at 4 °C and the supernatant discarded, the pellet was washed in 500 uL of 70% ethanol (RNAse free) and placed to dry in a laminar flow hood. After drying the pellet was resuspended in 20 µL of water treated with diethyl pyrocarbonate (DEPC, Sigma).

Synthesis of single-stranded cDNA

For the synthesis of single stranded cDNA, it was used 3.0 mg of total RNA and 500 ng of oligodT added with 11 µL of DEPC-treated water 0.1%, incubated at 70 °C

for 5 min and then placed on ice for 2 min. The solution was added with 4 µL of buffer synthesis of the first DNA strand, 2 µL of dNTP mix and 1 ul (200 U) of enzyme reverse transcriptase (*SuperScript*™ *First-Strand Synthesis System*, Invitrogen™). The reaction was incubated at 42 °C for 1 h, then 15 min at 70 °C to inactivate the enzyme. The cDNA was stored at -20 °C.

Amplification of the *SERK* coding sequence

The cDNA from total RNA embryogenic callus was used as template for amplification of the coding sequence of *SERK* in *B. distachyon* with degenerate primers by Baudino et al. (2001). The combination of degenerate primers S1-S4 used was for amplification. The sequence of the primers and their positioning within the domains of the protein are shown in Table 1 and Figure 1.

Table 1. Degenerate primers used for amplification of *SERK* in *Brachipodium dystachyon* and their location in the protein (Baudino et al., 2001)

Primers	**Sequence**	**Estructural Domain**
S1	5'TGTHACRTGGGTRTCCTTGTARTCCAT3'	Kinase domain VII
S4	5'CCMTGYCCIGGATCTCCCCITTT3'	SPP

W = A or T; R = A or G; M = A or C; Y = C or T; H = A or C or T; S = C or G; S1 (*reverse primer*); S4 (*forward primer*).

The PCR reaction (25 µL) was performed in a solution containing 2.0 µL of cDNA, 2.5 µL of 10x buffer, 0.5 µL dNTPs , 0.75 µL of $MgCl_2$ (50 mM), 1 ul of each primer, 0.2 µL of Taq DNA polymerase (Platinum ®, Invitrogen). The thermocycler program was set to: denaturation at 95 °C for five minutes, followed by 35 cycles at 95 °C (1 minute), 50 °C (1 minute), 72 °C (1 minute) and a final extension at 72 °C for five minutes. The amplification products were analyzed by electrophoresis on 1% agarose gel.

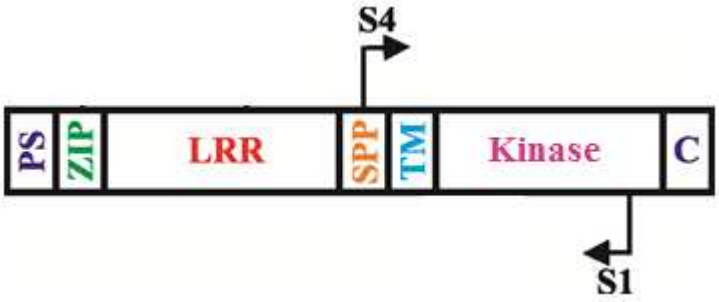

Figure 1. General Structure of *SERK* genes and degenerate primer position indicators used in the amplification. PS = signal peptide; = ZIP leucine zipper; LRR = leucine-rich repeats; = SPP region rich in proline, TM = transmembrane domain; Kinase domain; Region C = C terminal. Modified from Baudino et al. (2001).

Purification of DNA after electrophoresis and cloning of fragments

The amplified fragments were cut from the agarose gel and purified with the Kit Wizard® SV Gel and PCR Clean Up (Promega®) according to the manufacturer's instructions.

After quantification, the fragments were ligated into vector pGEM®-T Easy Vector Systems (Promega®), in a 3:1 ratio of insert:vector with the enzyme T4 DNA ligase (Promega®) following manufacturer's instructions. Transformation into *Escherichia coli* (XL1 blue competent cells) by thermal shock, was carried out using 2 uL of ligation (insert) and 40 µL of competent cells (1×10^8). After incubation at 37 °C for 1 hour, the cells were plated on selective LB solid medium (Sambrook and Russel, 2001) containing 100 µg/mL ampicillin, 20 µg/ml 5-bromo-4-chloro-3-indolyl -β-d-galactopyranoside (X-Gal) and then incubated at 37 °C for approximately 12 hours. To confirm the presence of the insert in the vector, plasmid DNA from white colonies was cleaved with the restriction enzyme EcoRI and fragments were separated by electrophoresis on 1% agarose gel.

Sequence analysis

A single positive clone was sequenced. After analysis of chromatogram and removal the edges of the vector the sequence obtained was compared with the sequences already deposited in the non-redundant database (NR) of NCBI using the BLAST software (Altschul et al. 1997). The software ORF Finder (http://www.ncbi.nlm.nih.gov/projects/gorf/) was used to identify the open reading frame.

The predicted amino acid sequence was aligned using the Clustal W software with other grass SERK proteins deposited in Genbank (http://www.ncbi.nih.nlm.gov), including a partial sequence of *B. distachyon*, for identification of structural domains. The phylogenetic tree was made using the aligned amino acid sequences to view the evolutionary relationships predicted from the multiple sequence alignment. The phylogenetic analysis was carried out using the *Molecular Evolutionary Genetics Analysis* software, MEGA version 4.0 (Tamura et al. 2007), available at http://www.megasoftware.net/mega4, using the Neighbor-Joining method (NJ) (Saitou and Nei, 1987). The reliability of the branching pattern of the tree was estimated using the bootstrap test (Felsenstein, 1985).

Collection and preparation of immature zygotic embryos and embryogenic calli for the analysis of *SERK* gene expression

Immature seeds 15 days post anthesis (Day 0) and embryogenic calli were collected from days 2, 6, 12, 14 and 21 of culture. The samples were immediately immersed in the fixative solution containing 4% paraformaldehyde and 0.25% glutaraldehyde in sodium phosphate buffer 0,01 M, pH 7.2. The samples were subjected to vacuum for 1 h at room temperature and then the fixative solution was immediately replaced and kept at 4 °C overnight. After this period the samples were rinsed in sodium phosphate buffer 0.01 M and dehydrated in an ethanol series (10, 30, 50, 70, 80, 85, 90, 95 and 100%) for 1 hour each. The samples were infiltrated in a series of ethanol: BMM (butyl-methyl-methacrylate, BMM) in the proportions 5:1, 5:2, 5:3, 5:4, 1:1, 1:2, 1:3, 1:4, 1:5 v/v and pure BMM (two changes), for at least 4 hours each step until the ratio 5:4, and for at least 24 hours in the following steps. The samples were placed in plastic capsules containing BMM, and polymerized for 48 hours at 4 °C under ultraviolet light 815 2537 A° (15 watts) and then stored at -20 °C.

Sections of 4 µm were cut in an automated advance rotary microtome (RM2155, Leica Microsystems Inc., USA) and placed in water droplets on glass slides treated with RNAse free DEPC Probe On Plus TM (Fisher Scientific Science). The sections were stretched with chloroform and the blades kept overnight in a heating plate at 60 °C. The slides were stored at 4 °C until use. Prior to hybridization, the BMM was removed in 100% acetone (two changes from 10 to 15 minutes), acetone: DEPC-treated water (1:1, v / v) for 10 minutes and twice in DEPC-treated water (10 minutes).

Production of antisense gene probe *SERK1*

A cloned fragment of 766 bp encoding a conserved region that extends from part of the transmembrane domain to approximately half of the kinase domain was used as template. The probe was labeled with digoxigenin (DIG-UTP), using the DIG RNA Labeling Kit (SP6/T7) according to manufacturer's (Roche Applied Science) recommendations. The probe concentration was examined by electrophoresis on agarose gel and marking confirmed by dot blot.

Hybridization reaction

Sixty ng of yeast tRNA (Gibco BRL®) and 60 ng probe were denatured at 80 °C for 5 minutes and added to 100 mL of hybridization buffer (10 mM Tris-HCl pH 7.5, 300 mM NaCl, formamide 50%, 1 mM EDTA pH 8.0, 1X Denhardt's solution). For hybridization, 100 µL of hybridization solution were placed on each slide and covered with Parafilm®. The slides were incubated in a moist chamber at 42 °C in the dark for a period of approximately 16 hours.

Reaction of post-hybridization and immunological detection

After hybridization the slides were washed in 4X, 2X, 0.5X and 1X SSC solution (20X SSC = 3 M NaCl, 0.3 M Na_3-citrate, pH 7.2), each solution for 30 minutes. The slides were maintained for 5 minutes in detection buffer 1 (0.1 M Tris HCl - pH 7.5, 0.15 M NaCl) and incubated for 30 minutes in blocking buffer. The sections were washed again in detection buffer sensing 1 for 5 minutes and incubated for 1 hour with the antibody anti-Digoxigenin AP Fab Fragments (Roche®) diluted 1:1000 in detection buffer 1. Following, two washes of 15 minutes each in detection buffer and one wash of 5 minutes in detection buffer 3 (0.1 M Tris HCl - pH 7.5, 0.1 M NaCl; 0.05 M MgCl2) were carried out. Sections were incubated in staining solution containing 4.5 µl of BCIP (5-bromo-4-chloro-3-indolyl-phosphate) (0.05 g / mL) and 4.5 µ of NBT (nitrobluetetrazolium) (0.05 g mL) in 1 ml of buffer 3 for 45 minutes in the dark. The sections were incubated in detection buffer 4 (0.01 M Tris HCl - pH 8.0, 1 mM EDTA) for 10 minutes to stop the reaction, and the slides were mounted in water.

Image capture was performed with an Olympus AX70TRF light microscope (Olympus Optical, Japan) with U-Photo system, coupled to a digital camera (AxioCam HR, Zeiss) and a microcomputer with the software for image capturing Spot Basic.

RESULTS

Analysis of the nucleotide sequence of the *B. distachyon SERK* fragment

Using the combination of degenerate primers S1/S4 designed to a conserved region of the *SERK* gene (Table 1), a 766 bp fragment was amplified by PCR from cDNA of embriogenic calli. A BLAST search with this fragment matched the (predicted) *Brachypodium distachyon* somatic embryogenesis receptor kinase 1-like (LOC100834508), accession no. XM_003571369.1 in the GenBank. The BLAST search of this nucleotide sequence resulted in several *SERK* similarity hits from other monocot species. The *B. distachyon SERK* fragment showed the highest identity (99%) with *SERK1* of *B. distachyon* and, between 89% and 93% (e-value 0.0), with *SERK* of wheat (*Triticum aestivum*), foxtail millet (*Setaria italica*) and rice (*Oryza sativa* - Japonica Group) (Table 2).

Table 2 - Comparison of the *SERK* nucleotide sequence resulting from a cDNA clone of embryogenic callus of *Brachypodium distachyon*, amplified with degenerate primers with sequences deposited in the non-redundant (NR) sequence database

Accession	Description	Database	Query cover (%)	E value	Max ident (%)
XM_003571369.1	*B. distachyon SERK1*	NCBI	61	0.0	99
AK333677.1	*T. aestivum SERK1*	NCBI	60	0.0	93
XM_004972669.1	*S. italica SERK 2*	NCBI	60	0.0	91
AB188247.1	*O. sativa SERK1*	NCBI	61	0.0	89

Analysis of the deduced amino acid sequences of *BdSERK*

The nucleotide sequence analysis of the software ORF Finder (Open Reading Frame Finder) (NCBI) confirmed the presence of an *Open reading frame (ORF)* of 639 bp in the *B. distachyon SERK* fragment. The multiple alignment of the deduced amino acid sequence (213 amino acids) with the sequences that showed high identities by BLASTp allowed the identification of highly conserved structural domains characteristic of the SERK protein that included part of the transmembrane domain and part of the kinase domain (Fig. 2).

Figure 2. Sequence alignments of SERK-like proteins of other monocot species with *B. distachyon* SERK, showing the high similarity of the SERK protein structural domains. The deduced amino acid sequences of SERK proteins were aligned, and amino acids differing from the consensus are colorless. Below the sequences, the protein domains are indicated by rectangles: SP = signal peptide; ZIP = leucine zipper; LRR = leucine-rich repeats; SPP = proline-rich region; TM = transmembrane domain; Kinase = protein-kinase domain; C = *C*-terminal domain. The accession numbers of the 7 other plant SERKs in the GenBank database include BdSERK1 (*Brachypodium distachyon* – XM_003571369.1), ZmSERK1 (*Zea mays* – AJ277702.1), ShSERK1 (*Saccharum* hybrid cv. CP88-1762 – ACT22809.1), SbSERK1 (*Sorghum bicolor* – XM_002447912.1), ZmSERK2 (*Zea mays* – AJ277703.1), SoSERK2 (*Saccharum officinarum* – TC79010) and SbSERK2 (*Sorghum bicolor* – XM_002454009.1). BdSERK LCT from the isolated *B. distachyon SERK* fragment .

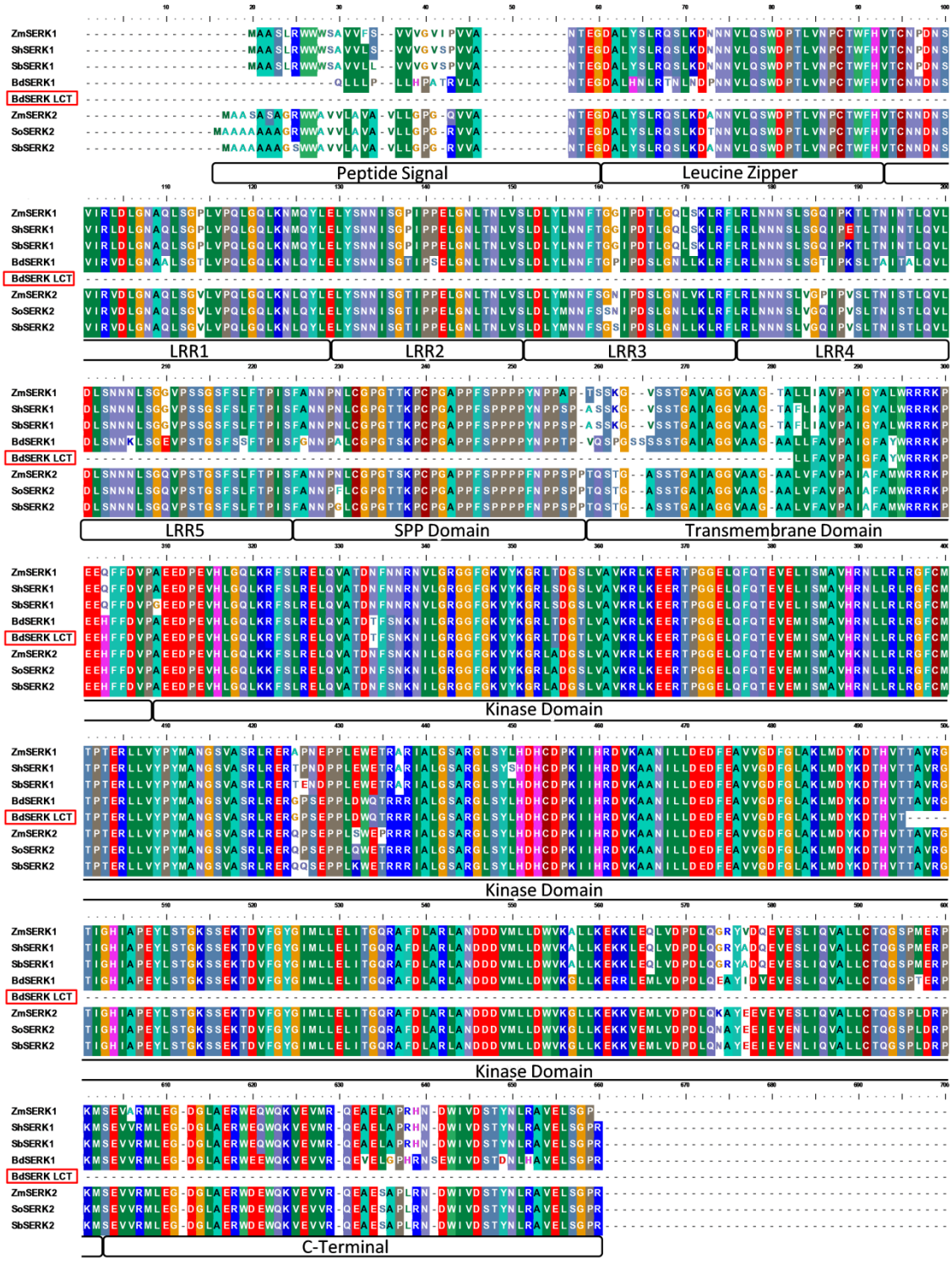
ZmSERK1
ShSERK1
SbSERK1
BdSERK1
BdSERK LCT
ZmSERK2
SoSERK2
SbSERK2
Peptide Signal
Leucine Zipper
LRR1
LRR2
LRR3
LRR4
LRR5
SPP Domain
Transmembrane Domain
Kinase Domain
Kinase Domain
Kinase Domain
C-Terminal

Phylogenetic analysis

The phylogenetic relationships between BdSERK and other SERK proteins were assessed through a phylogenetic tree reconstruction with deduced amino acid sequences that showed the highest similarities in Blast X. As shown in Fig. 4, two main branches were generated from the *SERK* gene family phylogenetic analysis, the branch containing the *B. distachyon SERK* fragment was only comprised of monocot sequences, which included *ZmSERK1*, *ShSERK1*, *SbSERK1* and *SoSERK2* and *SbSERK2*. Taken together, these alignments suggest that the cloned *B. distachyon* fragment is a *SERK1*-type gene.

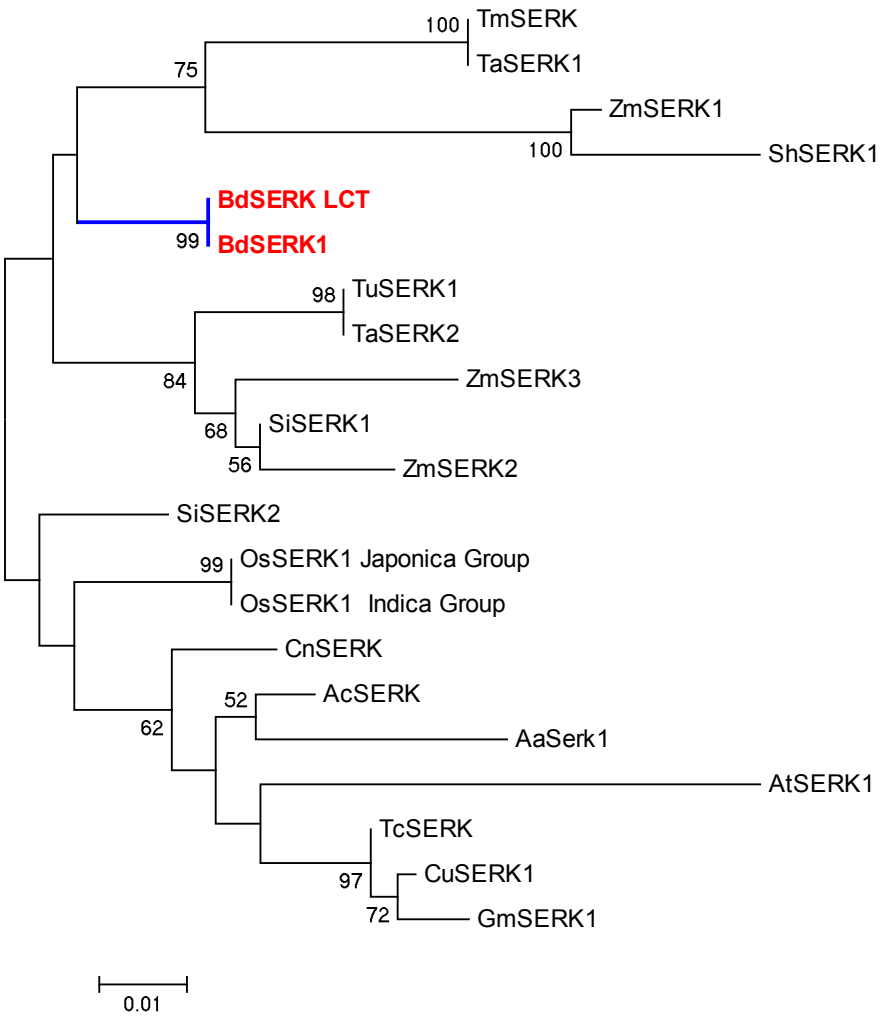

Figure 4. Phylogenetic relationship of SERK proteins. The phylogenetic tree was constructed using *MEGA version50*. Accession numbers of SERKs included in this analysis are as follows: *Ananas comosus* SERK, AEC46975.1; *Arabidopsis thaliana* SERK1, CAB38801.1; *Araucaria angustifolia* SERK1, ACY91853.1; *B. distachyon SERK1*, XP_003571417.1; *Citrus unshiu* SERK1, BAD32780.1; *Cocos nucifera* SERK, AAV58833.2; *Glycine max* SERK1, XP003556185.1; *Oryza sativa* Indica Group SERK1, AAR26543.1; *Oryza sativa* SERK1 (Japonica Group), AAU88198.1; *Saccharum* hybrid SERK1, ACT22809.1; *Setaria italica* SERK2,XP_004972726.1; *Setaria italica* SERK, XP_004952868.1; *Theobroma cacao* SERK, AAU03482.1; *Triticum urartu* SERK1, EMS66270.1; *Triticum aestivum* SERK1, AEP14551.1; *Triticum aestivum* SERK2, AEP14552.1; *Triticum monococcum* SERK1, AGH18696.1; *Zea mays* SERK1, NP 001105132.1; *Zea mays* SERK2, CAC37641.1; *Zea mays* SERK3, CAC37642.1.

Expression analysis of the *B. distachyon SERK* fragment

Immature zygotic embryos (Figs. 5A-C) dissected from seeds 15 days post anthesis (Day 0) were cultured on somatic embryogenesis induction medium and embryogenic calli were collected from days 2, 6, 12, 14 and 21 of culture for in situ hybridization analysis. Results showed that the immature zygotic embryo used as initial explant for somatic embryogenesis induction showed expression of the *B. distachyon SERK* in all its extension as well as in cells of the endosperm of the immature seed (Fig. 5B).

The blue-purple staining indicated that the *B. distachyon SERK* transcript was expressed during all the period of culture in somatic embryogenesis induction medium, at 2, 6, 12, 14 and 21 days after culture (DAC).

After 2 DAC in induction medium, explant tissues remained with strong hybridization signal in the embryo nodal region, where the scutellar parenchyma is continuous with the embryo mesocotyl internode, and in the epidermal cells of the scutellum, where mitotic divisions occurred (Figs. 5D-F). These divisions give rise to the proembryogenic masses.

After 6 DAC, the immature zygotic embryo showed strong expression of the *B. distachyon SERK* transcript in the embryo axis cells, nodal region, epidermal and subepidermal cells of the abaxial scutellum, as well as in cells of the vascular tissue in the scutellum and parenchyma cells adjacent to the vascular tissue (Figs. 5G-I). No expression signal was detected in non embryogenic cells that were developing into nonembryogenic callus.

After 12 DAC, results from in situ hybridization showed that spatial expression of *the B. distachyon SERK* occurred mainly in regions of the calli that contained meristematic zones (Figs. 6A, B). Histological sections stained with toluidine blue showed that these cells were small, isodiametric, non-vacuolated, and cytoplasm-rich, indicating a high metabolic activity (Figs. 6A, D). From 12 to 21 DAC, the proembryoid masses formed in the periphery of the callus were separated from the original explant. During this period, expression signals were also detected in embryoids at globular and scutellar stages. Globular and early-scutellar embryoids observed from 12 to 14 DAC in induction medium showed *SERK* expression in all cells (Fig. 6B), while further developed scutellar embryoids showed stronger signals localized in the peripheral cell layers of the newly formed scutellum (Fig. 6C). At 21 DAC, *B.*

distachyon SERK transcripts remained strongly present in the meristematic cells of the compact embryogenic calli and scutellar cells of the embryoids (Figs. 6E, F).

Figure 5. Spatial localization of *SERK* gene in *Brachypodium distachyon* line Bd21 during induction of somatic embryogenesis. (**A**) Immature zygotic embryo used as initial explant (15 d post anthesis); (**B)** Longitudinal section of immature embryo at 0 DAC stained with toluidine blue (TB) showing the nodal region (*asterik*), scutellum (*arrowhead*) and endosperm (En); (**C)** Embryo at 0 DAC with hybridization signal in all its extension and in cells of the endosperm (*arrow*) of the immature seed; (**D**) Explant at 2 DAC showing scutellum cells divinding into a continuous meristematic tissue densely stained with TB (*arrows*). Densely stained small cells appear at both sides of the embryo mesocotyl internode (*asterisk*); (**E**) Cells of the scutellum epidermis at 2 DAC com strong hybridization signal (*arrows*); (**F**) Strong hybridization signal appears in the region where the scutellar parenchyma is connected with the embryo mesocotyl internode; (**G**) Explant at 6 DAC showing initial embryogenic (Ec) and non-embryogenic (Nc) callus formation. Cl = coleoptile; (**H**) Strong signal appears in the embryo axis (Ea), nodal region (Nr), epidermal and subepidermal cells of the abaxial scutellum (arrow), cells of the vascular bundle and cells adjacent to the vascular tissue (Vb). (**I**) Explant section stained with TB showing densely stained small, cytoplasm-rich and prominent nuclei at 6 DAC (*arrow*). Meristematic cells in the ground tissue undergoing high division rate (*asterisk*).

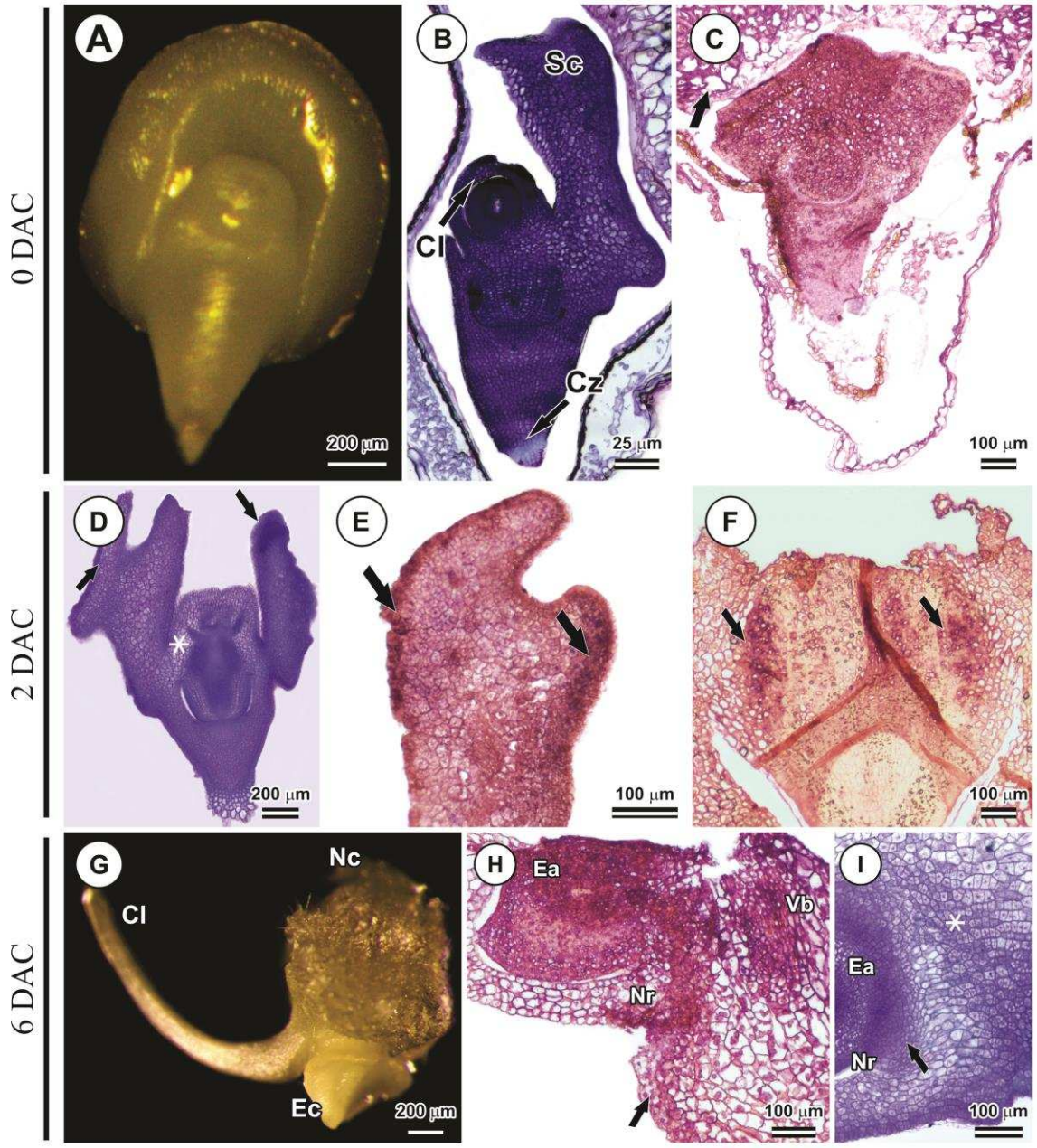
0 DAC
2 DAC
6 DAC
A
B
Sc
Cl
Cz
C
200 µm
25 µm
100 µm
D
E
F
200 µm
100 µm
100 µm
G
Nc
Cl
Ec
200 µm
H
Ea
Vb
Nr
100 µm
I
Ea
Nr
100 µm

Figure 6. Spatial localization of *SERK* gene in *Brachypodium distachyon* line Bd21 during induction of somatic embryogenesis. At 12 DAC: (**A**) Explant section showing zones of cytoplasm-rich cells densely stained with TB (*arrows*). (**B**) Embryoids at globular (*arrowhead*) and early-scutellar (*asterisk*) stages showing *SERK* expression in all cells. Note the transcript expression in a newly-formed proembryoid (*arrow*). At 14 DAC: (**C**) Section of embryogenic callus showing strong hybridization signal in meristematic zones (*arrows*). A strong signal in the periphery of the scutellum of the early-stage somatic embryos (*arrows*); (**D**) TB stained section showing zones of densely stained small meristematic cells (*arrows)* in embryoids at early scutellar stage. At 21 DAC: (**E**) Compact embryogenic callus subcultured on new induction medium; (**F**) Longitudinal section of compact callus showing strong hybridization signal in zones of meristematic cells (arrows).

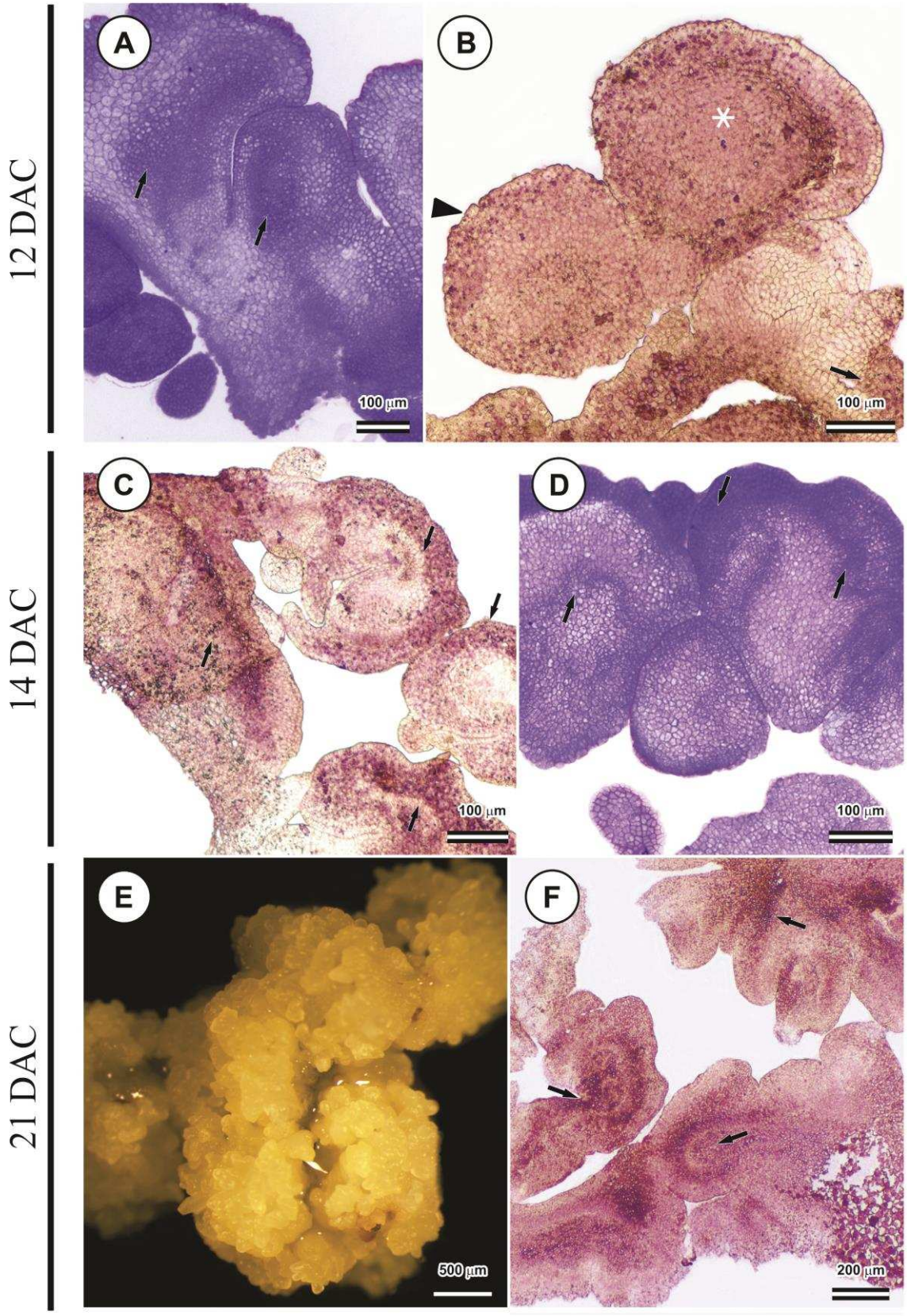
12 DAC
14 DAC
21 DAC
A
B
C
D
E
F
100 µm
100 µm
100 µm
100 µm
500 µm
200 µm

DISCUSSION

Somatic embryogenesis is considered a model system for the study of plant regeneration. It also has great potential for biotechnological applications especially in transgenic plants. Since the first report of *B. distachyon* somatic embryogenesis by Bablak et al. (1995), many protocols for transformation systems in *B. distachyon* via somatic embryogenesis have been described (Vogel and Hill, 2008; Alves et al., 2009). However, no reports on the molecular mechanisms of somatic embryogenesis in *B. distachyon* are available. An understanding of somatic embryogenesis regulation in *B. distachyon* during tissue culture will assist in the development of more effective regeneration protocols and also be useful as a model system for investigating the genetic regulation of somatic embryogenesis in other grass species.

The *SERK* gene encodes a leucine-rich repeat receptor kinase, a family of genes with roles in signal transduction pathways in plant development and metabolism. In this work using degenerate primers, a fragment correspondent of the *SERK* gene was amplified by PCR from cDNA of embryogenic culture of *B. distachyon*. Among the *SERK* genes reported to date, the amplified *SERK* fragment showed the highest nucleotide sequence identity with the predicted *B. distachyon SERK1*-like (99%, XM_003571369.1) and *Triticum aestivum SERK1* (93%, AK333677.1). The high sequence similarity found with other Poaceae species in amino acid sequence and protein structure indicates that the *B. distachyon SERK* gene can represent a possible ortholog. This is also supported by the relationships suggested by the phylogenetic analysis. The deduced ORF of 213 amino acids showed characteristic domains of the *SERK* gene, part of the transmembrane domain and part of the kinase domain, that are highly conserved in the SERK family. Although the forward primer (S4) is located at the SPP domain, the SPP motif is missing in the in the BLAST alignment of protein sequences with other species. The reason for this is that the longest reading frame obtained in the ORF finder program is located in the +2 frame and starts at nucleotide 128 not including the beginning of the sequence, whereas the other reading frame that includes the beginning of the sequence was detected at position -2, but in that position no conserved domain of the *SERK* gene was detected.

The *B. distachyon SERK* gene was expressed in the immature zygotic embryo (0.3–0.7 mm wide), which is the size commonly used to induce somatic embryos with a high efficiency in *B. distachyon* (Draper et al. 2001; Vogel and Hill, 2008). This size

corresponds to the early stages of zygotic embryo development in *B. distachyon* (Guillon et al., 2012). Expression of *SERK1* was also demonstrated in immature zygotic embryos of barrel medic (*Medicago truncatula*), maize (*Zea mays*), soybean (*Glycine max* (L.) Merr.) and rye (*Secale cereale* L.) by in situ RT-PCR analysis (Nolan et al., 2009; Zhang et al., 2011; Yang et al., 2011; Gruszczyńska et al., 2011). In the case of maize and soybean, the expression patterns of *ZmSERK1* and *GmSERK1* revealed a close relation to embryo size, in which as the size of the immature embryo increased, the expression of *SERK* decreased. In both species, immature embryos with a strong expression of the *SERK* genes were those suitable for embryogenesis (Zhang et al., 2011; Yang et al., 2011). Variations in the endogenous hormone levels in immature zygotic embryos used as initial explants may explain the difference in the ability to induce somatic embryogenesis (Jiménez, 2001). In maize, positive correlation was found between induction rate of embryogenic calli and content of abscisic acid and indole-3 acetic acid in immature embryos, while a negative correlation was found between increased level of gibberellin A3 and induction rate of embryogenic calli (Fu et al., 2006). Similarly, the expression of the *SERK* gene in the immature zygotic embryo indicates that the physiological condition and developmental stage of the zygotic embryo play an important role in somatic embryogenesis of *B. distachyon*.

The expression of the *B. distachyon SERK* gene was detected in the cellular endosperm of the immature *B. distachyon* seed. *SERK1* expression was also reported in the endosperm of *Arabidopsis* and *M. truncatula* (Hecht et al., 2001; Nolan et al., 2009). The process of endosperm cellularization is highly conserved in the dicot *Arabidopsis* and cereals at both the cytological and molecular levels (Olsen, 2004). Approximately 3% of the genes in angiosperm genomes that are transcribed during seed development are expressed exclusively in specific seed tissues and for about half of them, clear orthologs were found during seed development in both dicots (e.g. *Arabidopsis*) and monocots (e.g. barley) (Sreenivasulu and Wobus, 2013). Berger et al. (2006) suggested that as well as supplying nutrients to the developing seed, the endosperm functions as an integrator and mediator of signaling pathways and genetic programs that takes a central part in the control of seed growth and development. In *Arabidopsis*, two closely related LRR-RLKs were found expressing in the endosperm of seeds, HAIKU2 (IKU2) and EXTRA SPOROGENOUS CELLS (EXS), with role in controlling seed size (Canales et al., 2002; Luo et al., 2005). These findings led Nolan et al. (2009) to suggest that SERK1 may have a similar function of these LRR-RLKs in the control of seed

development in *M. truncatula*, which could also be the case of this study with the expression of SERK1 in the endosperm of the immature *B. distachyon* seed. Previous studies have shown that the *SERK* genes in different plant species have functions not only involved with somatic embryogenesis and are expressed at variable levels in different tissues. *ZmSERK1* in maize (Baudino et al. 2001), *MtSERK1* in *Medicago truncatula* (Nolan et al. 2003), *AtSERK1* in *Arabidopsis* (Colcombet et al. 2005; Kwaaitaal and de Vries, 2007), *PpSERK1* in *Poa pratensis* (Albertini et al. 2005), *TaSERK* in *T. aestivum* (Singla et al. 2008), *GhSERK1* in cotton (Shi et al., 2012) and *AcSERK1* in *Ananas comosus* (Ma et al., 2012) were expressed during induction of somatic embryogenesis as well as in somatic, zygotic and reproductive tissues. *OsSERK1* in rice (Hu et al. 2005; Song et al. 2008), *MaSERK1* in banana (Huang et al. 2010) and *GmSERK1* in soybean (Yang et al., 2011) were associated with somatic embryogenic competence and involved in disease resistance responses and mediating defense signal transduction.

In this study, expression of the *B. distachyon SERK* gene was analyzed during the *in vitro* culture of immature embryos for induction of somatic embryogenesis. According to the pattern of somatic embryos formation observed in *B. distachyon*, the meristematic tissues formed from scutellar epidermal cells expressing the *SERK* gene are the same which give rise to the nodular callus, indicating that the embryogenesis process takes place right at the beginning of culture on induction medium. Meristematic cells associated with the vascular bundle in the mesocotyl and cells of the zygotic embryo axis also showed expression signals, but somatic embryos of *B. distachyon* were obtained indirectly through the proliferation of meristematic cells present in the epidermis and nodal region of the immature embryo scutellum. Similarly, in *Arabidopsis*, *AtSerk1* was not only expressed in embryogenic cells, but was also found in cells capable of responding to hormone signals and competent to form somatic embryos or embryogenic cell cultures (Hecht et al. 2001).

The expression pattern of *B. distachyon SERK* gene detected in the regions of meristematic cells within the callus are consistent with previous studies in *Dactylis glomerata* (Somleva et al., 2000), *Triticum aestivum* (Singla et al., 2008), *Cocos nucifera* (Pérez-Núñez et al., 2009) and *Ananas comosus* (Ma et al., 2012), all monocotyledonous species, where high SERK1 expression signals were also detected in meristematic zones. In *B. distachyon* these cells formed proembryogenic structures and these structures eventually formed the somatic embryos.

During somatic embryogenesis induction, the *SERK* gene was detected in meristematic zones, globular and early scutellar embryoids, indicating that in this species this gene is expressed in embryogenically competent cells from the beginning of somatic embryo formation to beyond the globular stage. At 21 DAC, *SERK* mRNA still remained strongly present in cells of meristematic zones subtending the embryoids and in the peripheral cell layers of scutellar embryoids, indicating continuity of embryogenic competence in these cells. This pattern of *SERK* expression was also observed in other species. In the monocot *Dactylis glomerata, SERK* expression was observed in somatic embryos at different stages of development with continued expression in the apical meristem and transient expression in the protoderm, coleoptile and coleorhiza of somatic embryos (Somleva et al., 2000). *StSERK* expression in embryogenic cultures of *Solanum tuberosum* was detected during transition stages of embryos and fully-developed embryos (Sharma et al., 2008). In *M. truncatula*, somatic embryos exhibited strong expression of a *prSERK1::GUS* reporter construct from the early globular stage through to the cotyledonary stage of development (Nolan et al., 2009). In contrast, expression signals of *DcSERK* in *Daucus carota* (Schmidt et al., 1997) and *CnSERK* in *Cocos nucifera* (Pérez-Núñez et al., 2009) ceased after the globular stage.

The high sequence similarity of the predicted *B. distachyon* SERK amino acid sequences with those of other Poaceae species indicates that it could function as a LRR-RLK, and the histological results of this study suggest that the corresponding regions in BdSERK may play a functional role in somatic embryogenesis of *B. distachyon.*

Although further research is needed to provide a greater understanding of the molecular mechanisms controlling the tissue culture response of *B. distachyon,* the findings of his study are relevant information about the role of the *SERK* gene in the process of somatic embryogenesis.

Isolation and characterization of complete *B. distachyon SERK* sequences and expression analysis using Real-time RT-PCR on different tissues may provide fundamental information about these genes. Isolation and characterization of their promoters, the making of constructs (such as *BdSERK*-GUS) and overexpression and loss-of-function studies will be useful for better understanding the role of *SERK* genes in development and somatic embryogenesis of *B. distachyon* and its related cereal and biofuel grasses.

REFERENCES

ALVES S. C., WORLAND B., THOLE V., SNAPE J. W., BEVAN M. W., VAIN P. A protocol for *Agrobacterium*-mediated transformation of *Brachypodium distachyon* community standard line Bd21. **Nature Protocols**, v. 4, n. 5, p. 638-649, 2009.

ALBERTINI E., MARCONI G., REALE L., BARCACCIA G., PORCEDDU A., FERRANTI F., FALCINELLI M. *SERK* and *APOSTART*: candidate genes for apomixis in *Poa pratensis*. **Plant Physiology**, v. 138, p. 2185–2199, 2005.

ALTSCHUL S., MADDEN T., SCHAFFER A., ZHANG J., ZHANG Z., MILLER W., LIPMAN D. Gapped BLAST and PSI-BLAST: a new generation of protein database search programs. **Nucleic Acids Research**, v.25, p.3389-3402, 1997.

BABLAK P., DRAPER J., DAVEY M. R., LYNCH P. T. Plant regeneration and micropropagation of *Brachypodium distachyon*. **Plant Cell Tissue Organ Culture**, v. 42, p. 97–107, 1995.

BAUDINO S., HANSEN S., BRETTSCHNEIDER R., HECHT V. E. G., DRESSELHAUS T., LORZ H., DUMAS C., ROGOWSKY P. M. Molecular characterization of two novel maize LRR receptor-like kinases, which belong to the *SERK* gene family. **Planta**, v. 213, p. 1–10, 2001.

BERGER F, GRINI PE, SCHNITTGER A. Endosperm: an integrator of seed growth and development. **Current Opinion in Plant Biology**, v. 9, p. 664–670, 2006.

BEVAN M. W., GARVIN D. F., VOGEL J. P. *Brachypodium distachyon* genomics for sustainable food and fuel production. **Current Opinion in Biotechnology**, v. 21, p. 221-217, 2010.

BRKLJACIC J., GROTEWOLD E., SCHOLL R., MOCKLER T., GARVIN D.F., VAIN P., BRUTNELL T., SIBOUT R., BEVAN M., BUDAK H., CAICEDO A. L., GAO C., GU Y., HAZEN S.P., HOLT III B.F., HONG S.-Y., JORDAN M., MANZANEDA A.J., MITCHELL-OLDS T., MOCHIDA K., MUR L.A.J., PARK C.-

M., SEDBROOK J., WATT M., ZHENG S.J., VOGEL J.P. *Brachypodium* as a Model for the Grasses: Today and the Future **Plant Physiology**, v. 157, p. 3–13, 2011.

CANALES C., BHATT A. M., SCOTT R., DICKINSON H.. EXS, a putative LRR receptor kinase, regulates male germline cell number and tapetal identity and promotes seed development in *Arabidopsis*. **Current Biology**, v. 12, p. 1718–1727, 2002.

CATALÁN P., MÜLLER J., HASTEROK R., JENKINS G., MUR L. A. J. et al. Evolution and taxonomic split of the model grass *Brachypodium distachyon*. **Annals of Botany**, v. 109, p. 385–405, 2012.

COLCOMBET J., BOISSON-DERNIER A., ROS-PALAU R., VERA C. E., SCHROEDER J. I. ARABIDOPSIS SOMATIC EMBRYOGENESIS RECEPTOR KINASES 1 and 2 are essential for tapetum development and microspore maturation. **The Plant Cell**, v. 17, p. 3350-3361, 2005.

DRAPER J., MUR L. A. J., JENKINS G., GHOSH-BISWAS G. C., BABLAK P., HASTEROK R., ROUTLEDGE A. P. M. *Brachypodium distachyon*. A new model system for functional genomics in grasses. **Plant Physiology**, v. 127, p. 1539–1555, 2001.

FEHÉR A., PASTERNAK T. P., DUDITS D. Transition of somatic plant cells to an embryogenic state. **Plant Cell, Tissue and Organ Culture,** v. 74, p. 201–228, 2003.

FELSENSTEIN, J. Confidence limits on phylogenies: An approach using the bootstrap. **Evolution**, Rochester, v.39, p.783-791, 1985.

FU F. L., FENG Z. L., QU B. Y., LI W. C. Relationships between inducton rate of embryogenic callus and endogenous hormones content in maize. **Journal of Nuclear Agricultural Sciences**, v. 20, p. 10–14, 2006.

GUILLON F., LARRE C., PETIPAS F., BERGER A., MOUSSAWI J., ROGNIAUX H. A comprehensive overview of grain development in *Brachypodium distachyon* variety Bd21. **Journal of Experimental Botany**, v. 63, p. 739–755, 2012.

GRUSZCZYŃSKA A., RAKOCZY-TROJANOWSKA M., Expression analysis of somatic embryogenesis-related SERK, LEC1, VP1 and NiR ortologues in rye (Secale cereale L.). **Journal of Applied Genetics**, v. 52, p. 1–8, 2011.

HECHT V., VIELLE-CALZADA J. P., HARTOG M. V., SCHMIDT E. D., BOUTILIER K., GROSSNIKLAUS U. The *Arabidopsis* SOMATIC EMBRYOGENESIS RECEPTOR KINASE 1 gene is expressed in developing ovules and embryos and enhances embryogenic competence in culture. **Plant Physiology**, v. 127, p. 803–816, 2001.

HU H., XIONG L., YANG Y. Rice *SERK1* gene positively regulates somatic embryogenesis of cultured cell and host defense response against fungal infection. **Planta**, v. 222, n. 1, p. 107–117, 2005.

HUANG X., LU X. Y., ZHAO J. T., CHEN J. K., DAI X. M., XIAO W., CHEN Y. P., CHEN Y. F., HUANG X. L. *MaSERK1* gene expression associated with somatic embryogenic competence and disease resistance response in banana (*Musa* spp.). **Plant Molecular Biology Reports**, v. 28, p. 309–316, 2010.

IBI – THE INTERNATIONAL *BRACHYPODIUM* INITIATIVE. Genome sequencing and analysis of the model grass *Brachypodium distachyon*. **Nature**, v. 463, p. 763–768, 2010.

JIMÉNEZ V. M. Regulation of *in vitro* somatic embryogenesis with emphasis on to the role of endogenous hormones. **Revista Brasileira de Fisiologia Vegetal**, v.13, n.2, p. 196-223, 2001.

KOEHLER A. D. **Reprodução em *Brachiaria* spp.: *SERK* (*Somatic Embryogenesis Receptor-Like Kinase*) no desenvolvimento da antera, do ovário e na embriogênese.** Tese (Doutorado), CENA, USP. 2010, 108 P.

KWAAITAAL M. A. C. J., DE VRIES S. C. The *SERK1* gene is expressed in procambium and immature vascular cells. **Journal of Experimental Botany**, v. 58, n. 11, p. 2887–2896, 2007.

LUO M., DENNIS E. S., BERGER F., PEACOCK W. J., CHAUDHURY A. *MINISEED3* (*MINI3*), a *WRKY* family gene, and *HAIKU2* (*IKU2*), a leucine-rich repeat (*LRR*) *KINASE* gene, are regulators of seed size in *Arabidopsis*. **Proceedings of the National Academy of Sciences, USA**, v. 102, p. 17531–17536, 2005.

MA J., HE Y., WU C., LIU H., HU Z., SUN G. Cloning and Molecular Characterization of a SERK Gene Transcriptionally Induced During Somatic Embryogenesis in *Ananas comosus* cv. Shenwan. **Plant Molecular Biology Report**, v. 30, p. 195–203, 2012.

MORDHORST A. P., VOERMAN K. J., HARTOG M. V., MEIJER E. A., VAN WENT J., KOORNNEEF M., DE VRIES S. C. Somatic embryogenesis in *Arabidopsis thaliana* is facilitated by mutations in genes repressing meristematic cell divisions. **Genetics**, v. 149, p. 549–563, 1998.

MURASHIGE T., SKOOG F. A revised medium for rapid growth and bio assays with tobacco tissue cultures. **Physiologia Plantarum,** v. 15, p. 473–497, 1962.

NAMASIVAYAM, P., SKEPPER, J. HANKE, D. Identification of a potential structural marker for embryogenic competency in the *Brassica napus* ssp. *Oleifera* embryogenic tissue. **Plant Cell Reports**, v. 25, n. 9, p. 887-895, 2006.

NAMASIVAYAM, P. Acquisition of embryogenic competence during somatic embryogenesis. **Plant Cell, Tissue and Organ Culture**, v. 90, n. 1, p. 1-8, 2007.

NOLAN K. E., IRWANTO R. R., ROSE R. J. Auxin upregulates *MtSERK1* expression in both *Medicago truncatula* root-forming and embryogenic cultures. **Plant Physioology**, v. 133, p. 218–230, 2003.

NOLAN K. E., KURDYUKOV S., ROSE R. J. Expression of the *SOMATIC EMBRYOGENESIS RECEPTOR-LIKE KINASE1* (*SERK1*) gene is associated with developmental change in the life cycle of the model legume *Medicago truncatula*. **Journal of Experimental Botany**, v. 60, p.1759–1771, 2009.

OLSEN O. A. Nuclear endosperm development in cereals and *Arabidopsis thaliana*. **Plant Cell**, v. 16 (Suppl.), p. 214–227, 2004.

PÉREZ-NUÑÉZ, M.T., SOUZA, R., SÁENZ, L., CHAN, J.L., ZÚÑIGA-AGUILAR, J.J.. OROPEZA, C. Detection of a *SERK*-like gene in coconut and analysis of its expression during the formation of embryogenic callus and somatic embryos. **Plant Cell Reports**, v. 28, p. 11–19, 2009.

SAITOU, N., NEI, M. The neighbor-joining method: A new method for reconstructing phylogenetic trees. **Molecular Biology and Evolution**, Oxford, v.4, p.406-425, 1987.

SANTOS M. O., ROMANO E., YOTOKO K. S. C., TINOCO M. L. P., DIAS B. B. A., ARAGÃO F. J. L. Characterisation of the cacao somatic embryogenesis receptor-like kinase (*SERK*) gene expressed during somatic embryogenesis. **Plant Science**, v. 168, 723–729, 2005.

SCHMIDT E. D., GUZZO F., TOONEN M. A., DE VRIES S. C. A leucine-rich repeat containing receptor-like kinase marks somatic plant cells competent to form embryos. **Development**, v. 124, p. 2049–2062, 1997.

SHARMA S. K., MILLAM S., HEIN I., BRYAN G. J. Cloning and molecular characterization of a potato *SERK* gene transcriptionally induced during initiation of somatic embryogenesis. **Planta**, v. 228, p. 319–330, 2008.

SHI Y., ZHANG R., WU X., MENG Z., GUO S. Cloning and characterization of a somatic embryogenesis receptor-like kinase gene in cotton (*Gossypium hirsutum*). **Journal of Integrative Agriculture,** v. 11, n. 6, p. 898-909, 2012.

SINGLA B., KHURANA JP.., KHURANA P. Characterization of three somatic embryogenesis receptor kinase genes from wheat, *Triticum aestivum*. **Plant Cell Reports**, v. 27, p.833–843, 2008.

SOMLEVA M. N., SCHMIDT E. D. L., DE VRIES S. C. Embryogenic cells in *Dactylis glomerata* L. (Poaceae) explants identified by cell tracking and by *SERK* expression. **Plant Cell Reports**, v. 19, p.718–726, 2000.

SONG D., LI G., SONG F., ZHENG Z. Molecular characterization and expression analysis of *OsBISERK1*, a gene encoding a leucine-rich repeat receptor-like kinase, during disease resistance responses in rice. **Molecular Biology Reports**, v. 35, p. 275–283, 2008.

SREENIVASULU N., WOBUS U., Seed-Development Programs: A Systems Biology–Based Comparison Between Dicots and Monocots. **Annual Review of Plant Physiology**, v. 64, p. 189–217, 2013.

TAMURA, K., DUDLEY, J., NEI, M., KUMAR, S. MEGA4: Molecular evolutionary genetics analysis (MEGA) software version 4.0. **Molecular Biology and Evolution**, Oxford, v.24, n.8, p.1596-1599, 2007.

THOMAS C., MEYER D., HIMBER C., STEINMETZ A. Spatial expression of a sunflower *SERK* gene during induction of somatic embryogenesis and shoot organogenesis. **Plant Physiology and Biochemistry**, v. 42, p. 35–42, 2004.

VON RECKLINGHAUSEN I. R., IWANOWSKA A, KIEFT H., MORDHORST A. P., SCHEL J. H. N., VAN LAMMEREN A. A. M. Structure and development of somatic embryos formed in *Arabidopsis thaliana* pt callus cultures derived from seedlings. **Protoplasma**, **v.** 211, p. 217–224, 2000.

VOGEL J., BRAGG J. *Brachypodium distachyon*, a New Model for the Triticeae. **Genetics and Genomics of the Triticeae**, v. 7, p. 427-449, 2009.

VOGEL J., HILL, T. High-efficiency *Agrobacterium*-mediated transformation of *Brachypodium distachyon* inbred line Bd21–3. **Plant Cell Reports**, v. 27, p. 471–478, 2008.

YANG C., ZHAO T., YU D., GAI J. Isolation and Functional Characterization of a *SERK* Gene from Soybean (*Glycine max* (L.) Merr.). **Plant Molecular Biology Reporter**, v. 29, p. 334–344, 2011.

ZHANG S., LIU X., LIN Y., XIE G., FU F., LIU H., WANG J., GAO S., LAN H., RONG T. Characterization of a *ZmSERK* gene and its relationship to somatic embryogenesis in a maize culture. **Plant Cell Tissue Organ Culture**, v. 105, p. 29–37, 2011.

GENERAL CONCLUSIONS

Somatic embryos of *Brachypodium distachyon* arised from embryogenic callus formed from cells of the protodermis in the region of the scutellar node and extended to the periphery of immature zygotic embryos. This pattern of somatic embryogenesis can be considered indirect somatic embryogenesis, while the number of cells involved in embryoid formation and the broad multicellular base connecting somatic embryos and callus possibly indicate a multicellular origin of the somatic embryos. Somatic embryo differentiation followed the same morphological pattern of development of other members of the Poaceae. The pattern of accumulation and mobilization of storage reserves in somatic embryos was similar to that of zygotic embryos. Storage proteins and lipids were used up in the initial embryogenic process, supporting the idea that reserves are essential to morphogenetic processes. The high accumulation of starch in the first 2 days of culture followed by a decrease in number of granules and a late de novo accumulation in proembryonic masses suggest that starch is used both during embryogenic callus initiation and later in its development into proembryoids.

The *in silico* analysis confirmed the presence of characteristic SERK domains in the amplified *B. distachyon SERK* gene fragment, which can mean that the functions are conserved in *B. distachyon.* The *in situ* hybridization analysis showed that the *SERK* gene was present in embryogenic tissues before somatic embryo development and continued expressing through globular and scutellar stages, suggesting that the expression of the *B. distachyon SERK1* gene was associated with induction of somatic embryogenesis.

The results reported in this study convey important information about the morphogenetic events in the embryogenic pathway which has been lacking in *B. distachyon*. This study also demonstrates that *B. distachyon* provides a useful model system for investigating the genetic regulation of somatic embryogenesis in grass species.